

Diss. ETH No. 24838

Dynamics of gas transport in pore waters of lacustrine sediments

A dissertation submitted to
ETH ZURICH

for the degree of
DOCTOR OF SCIENCES

presented by
Lina Tyroller
Dipl.-Ing., Technische Universität Berlin (DE)
born 21.06.1982
citizen of Germany

accepted on the recommendation of
Prof. Dr. Rolf Kipfer, examiner
Dr. Matthias Brennwald, co-examiner
Prof. Dr. Bernhard Wehrli, co-examiner
Prof. Dr. Jens Greinert, co-examiner

2018

This thesis is dedicated to my father Dazi Tyroller and his ideals of free thinking and
limitless imagination.

Chapter 3 has been published as:

L. Tyroller; M. S. Brennwald; L. Mächler; D. M. Livingstone; R. Kipfer. Fractionation of Ne and Ar isotopes by molecular diffusion in water. *Geochimica et Cosmochimica Acta*, 136, 6066, (2014).

Chapter 4 has been published as:

L. Tyroller; M. S. Brennwald; H. Busemann; C. Maden; R. Kipfer. Negligible fractionation of Kr and Xe isotopes by molecular diffusion in water. *Earth and Planetary Science Letters*, 492, 73-78 (2018).

Chapter 5 has been published as:

L. Tyroller; Y. Tomonaga; M.S. Brennwald; C. Ndayisaba; S. Naehrer; C. Schubert; R. P. North, R. Kipfer. Improved method for the quantification of methane concentrations in unconsolidated lake sediments. *Environmental Science and Technology*, 50(13), 7047-7055 (2016).

Chapter 6 is to be published as:

L. Tyroller; Y. Tomonaga; M.S. Brennwald; R. Kipfer. Noble gases as tracer for the gas dynamics in methane supersaturated lacustrine sediments. *Environmental Science and Technology*.

Acknowledgements

First off, I would like to thank the referees of my dissertation Rolf Kipfer (alias RoKi), Matthias Brennwald, Bernhard Wehrli and Jens Greinert. Particularly, I want to thank Matthias and RoKi for their enthusiasm, commitment, and trust which was an important motivation and made my PhD-experience productive and inspiring. Further I am grateful for their time, ideas, extensive knowledge and constructive criticism which greatly helped to improve this thesis. They found the right balance in giving me intellectual freedom and support.

Eawag has been a source of friendships as well as of creative ideas, helpful advice and collaboration. Thanks to the former and present members of the Environmental Isotopes Group for their great support during the last few years and for the friendly atmosphere: Yama Tomonaga (for giving good advice and good coffee), David Livingstone (for sharing his life experience), Lars Mächler (for sharing his miniRUEDI expertise), Simon Figura (for sharing the office), Nadja Vogel, Stephan Huxol, Ryan North, Elaheh Ghadiri, Andrea Popp, Edith Horstmann, Alex Lightfoot and Jonas Zbinden. Thanks to the members of Surf department, in particular Carsten Schubert, Tonya del Sontro and Serge Robert. Special thanks are owed to the Eawag members from different departments for their friendship and the congenial environment: Anja, Anna, Bas, Benham, Caroline, Christian, Dirk, Elham, Jana, Joao, Joel, Kirstin, Michele, Numa, Tim and all the others that I cannot mention due to the limited space.

Furthermore I would like to acknowledge Halua Pinto de Magalhães whose work supports the findings of this thesis and Cyprien Ndayisaba who contributed with the results of his master thesis. Thanks to Stacey Priestly and Marianne Nuzzo for the good scientific cooperation and thanks to Hilmar Hofmann for borrowing his gas funnels. I also want to express my gratitude to the members of the noble gas laboratory at ETH Zurich. In particular, I thank Henner Busemann, Colin Maden, Urs Menet and Heiri Baur for their valuable support. Special thanks are due to Rafa Marcè, Joan Pere Casas and the other involved members of ICRA for the pleasant fieldwork at Lake Boadella. Furthermore I want to mention the Gemma (UPC Barcelona) with its creative research environment that was inspiring to do a PhD. Sincere thanks also to David Marks who checked the English in this thesis and to Aida Sadrossadat for contributing with her GIS expertise.

My deepest thanks go to my family, to my partner Navid and our son Yari, to my parents, Inge and Dazi, and to my sister Larissa, for supporting me all the way and for sharing the daily routine as well as the most fundamental moments in life.

Contents

1	Introduction	1
1.1	Noble gases as tracers for gas dynamics in lacustrine sediments	1
1.2	Outline	3
2	Concepts	5
2.1	Gases in the sediment pore water	6
2.1.1	Noble gases	7
2.1.2	Methane	10
2.2	Gas dynamics in lacustrine sediments and their impact on the noble gas composition	11
2.2.1	Pore water burial	11
2.2.2	Molecular diffusion	13
2.2.3	Secondary gas exchange with methane bubbles	14
3	Fractionation of Ne and Ar isotopes by molecular diffusion in water	17
3.1	Introduction	18
3.2	Material and methods	20
3.2.1	Experimental setup	20
3.2.2	Principles of the measuring method	22
3.3	Results and discussion	23
3.3.1	Experiment performance	23
3.3.2	Fractionation factors	24
3.4	Conclusions	26
4	Negligible fractionation of Kr and Xe isotopes by molecular diffusion in water	27
4.1	Introduction	27
4.2	Material and methods	28
4.2.1	Experimental setup	28
4.2.2	Determination of diffusion coefficients	31
4.2.3	Gas dilution	31
4.2.4	Analysis of noble gas isotopes	33
4.3	Results	33
4.4	Discussion	34
4.5	Conclusions	38

5	Improved method for the quantification of methane concentrations in unconsolidated lake sediments	39
5.1	Introduction	40
5.2	Experimental methods and procedures	42
5.2.1	Methods	42
5.2.2	Performance of the method	45
5.3	Results and Discussion	48
5.3.1	Performance of the copper tube headspace gas extraction (lab experiment)	48
5.3.2	Comparison of the performance of the two methods in sediments that have CH ₄ concentrations in the range of the expected methane saturation (Lake Lungern)	48
5.3.3	Performance of the two methods when sampling sediments with active bubble formation (Lake Rotsee)	50
5.4	Implications	52
6	Noble gases as tracer for the gas dynamics in methane supersaturated lacustrine sediments	55
6.1	Introduction	56
6.2	Study sites	57
6.3	Methods	59
6.4	Results and Discussion	59
6.4.1	Noble gas data from Lake Rotsee	59
6.4.2	Noble gas data from Lake Lungern	66
6.5	Conclusions	71
7	Pilot study: Noble gas concentrations in a deep clay sediment layer of Lake Zurich	73
7.1	Introduction	73
7.2	Study site	73
7.3	Methods	74
7.4	Results	74
7.5	Discussion	77
7.6	Conclusions	79
8	Conclusions and Outlook	81
8.1	Conclusions	81
8.2	Outlook	83

Summary

This work focuses on the dynamics of gases in lacustrine sediments. It emphasises the effects of transport processes on noble gases dissolved in the sediment pore water. In general, the noble gas concentrations in lacustrine sediments agree with the concentrations in the overlying lake water column. In turn, the noble gas concentrations in the overlying water column, i.e. air saturated water (ASW) concentrations, are determined by the partitioning between atmosphere and lake water. Due to their biogeochemical inertness, any deviation of noble gas concentrations in sediment pore water from ASW concentration is attributed to physical processes. Therefore, noble gases have been established as excellent tracers for the characterization of gas dynamics and transport processes in lacustrine sediments.

However, there are still open questions regarding the mechanism of the noble gas transport in the sediment pore water: (1) The behaviour of noble gas isotopes during molecular diffusion in water lacks of a sound physical basis. (2) The gas transport in lacustrine sediments varies extremely depending on the sediment properties. In three case studies noble gases were used to investigate on one hand the gas dynamics in supersaturated sediments (Lake Rotsee and Lake Lungern) and on the other hand the suppressed noble gas transport in highly compacted sediments (Lake Zurich).

The details, on how these questions were addressed, are explained in the following:

(1) Molecular diffusion is the key transport process for noble gases dissolved in the sediment pore water. Noble gas diffusion in water is commonly expected to cause a fractionation of noble gas isotopes in accordance with the square root relation, which describes the isotope fractionation to be inversely proportional to the square root of the ratio of their atomic mass. However recent studies challenge the applicability of the square root relation, derived from the kinetic theory of gases, to predict the fractionation of noble gas isotope by reason of molecular diffusion in water. Therefore the fractionation of the noble gas isotopes (Ne, Ar, Kr Xe) due to molecular diffusion in water was determined in a laboratory experiment. Surprisingly, only the fractionation of Ar isotopes can be adequately described by the square root relation. The fractionation of Ne, Kr and Xe isotopes was found to be much lower and even negligible. The results from the laboratory experiments provide a robust basis for studies that use the fractionation of the noble gas isotope ratios to assess molecular diffusion in water bodies, e.g. to investigate diffusive transport of noble gases dissolved in the pore water to gas bubbles formed in the sediment pore space.

(2) In sediments characterised by an active microbial gas production in their pore waters and hence supersaturated with reactive gases (e.g. CH_4), the transport of noble gases through the pore space is enhanced relative to the diffusion of noble gases in the pore water. The enhanced transport of noble gases results from their interaction with gas

bubbles that are formed in the sediment pore space and which are eventually released. Methods that are commonly used to determine CH_4 concentrations in the sediment pore water do not prevent gas exchange with the atmosphere during sampling and are therefore not suitable to quantify CH_4 in supersaturated sediments. To improve the accuracy of CH_4 measurements a new method for the analysis of CH_4 concentrations in sediment pore waters has been developed in the framework of this thesis.

This newly developed method was combined with noble gas analysis and applied to the sediments of two lakes, Lake Rotsee and Lake Lungern, which are characterised by an active bubble ebullition (mostly CH_4) from their sediments. The continuous CH_4 flux from the sediments of Lake Rotsee was determined using the noble gas concentration gradient, showing an increasing depletion relative to air saturated water (ASW) concentration with increasing sediment depth. The zone of active bubble ebullition from the sediment was indicated by the CH_4 concentration peak determined in the pore water, which exceeds the local saturation concentration by one order of magnitude.

Lake Lungern is subject to extreme water level variations, which induce bubble formation in the sediment pore water and emission of CH_4 together with the bubbles leaving the sediment. Furthermore, parts of the sediment fall dry during low water level. The noble gas excess relative to ASW determined in this zone was used to estimate the oxygen supply to the "dry falling" sediment.

In a pilot study on a glacial clay sediment of Lake Zurich a noble gas excess relative to ASW was determined as well. This excess might originate from inflowing glacial melt-water as a strong ^4He enrichment and the noble gas pattern in the pore water of the sediment are interpreted to indicate that noble gases have been quantitatively trapped in the clay for a period of several thousand years.

Overall the results of the laboratory experiments on noble gas isotope diffusion in water represent an important step towards establishing the ratio of $^{36}\text{Ar}/^{40}\text{Ar}$ as isotopic tracer for diffusive transport in unconsolidated sediments. Furthermore, this thesis gives a specific insight into the interaction of dissolved noble gases and reactive gas bubbles in the sediment pore water of gas supersaturated sediments, and the method developed for the determination of real in situ CH_4 concentrations contributes to the further investigation of such sediments. To summarize, this thesis illustrates that noble gases are ideal tracers for the gas dynamics in a wide range of lacustrine sediments, from gas supersaturated sediments to highly compacted clay sediments.

Zusammenfassung

Diese Arbeit befasst sich mit der Dynamik von Gasen in Seesedimenten. Der Schwerpunkt liegt auf den Transportprozessen in Seesedimenten und deren Auswirkungen auf die im Porenwasser gelösten Edelgase. Im Allgemeinen entsprechen die Konzentrationen der Edelgase im Porenwasser von Seesedimenten den Edelgaskonzentrationen in der darüberliegenden Seewassersäule. Die Edelgaskonzentrationen in der Wassersäule wiederum, die sogenannten atmosphärischen Gleichgewichtskonzentrationen (ASW), sind bestimmt durch den Gasaustausch zwischen atmosphärischer Luft und Wasser. Weil Edelgase biogeochemisch inert sind, kann jede Veränderung der Edelgaskonzentrationen im Porenwasser im Verhältnis zur ASW-Konzentration auf physikalische Prozesse zurückgeführt werden. Daher haben sich Edelgase als ideale Indikatoren für die Gasdynamik und die Transportprozesse von Gasen in Seesedimenten etabliert.

Trotzdem gibt es offene Fragen bezüglich der zugrundeliegenden Mechanismen des Transportes von Edelgasen in Seesedimenten: (1) Dem Verhalten von Edelgasen bei molekularer Diffusion durch Wasser liegt kein physikalisch akzeptables Erklärungsmodell zugrunde. (2) Der Gastransport in verschiedenen Seesedimenten variiert stark in Abhängigkeit von den Eigenschaften des Sediments. In drei Fallstudien wurden im Porenwasser gelöste Edelgaskonzentrationen benutzt, um einerseits die Gasdynamik in Seesedimenten, die mit Gasen übersättigt sind (Rotsee und Lungernsee) und andererseits den unterdrückten Gastransport in stark kompaktierten Sedimenten zu untersuchen (Zürichsee).

Im Folgenden wird im Detail dargelegt, wie diese Fragen angegangen wurden:

(1) Molekulare Diffusion ist der entscheidende Transportprozess für im Porenwasser gelöste Gase. Es wird im allgemeinen angenommen, dass Edelgasisotope durch molekulare Diffusion im Wasser fraktioniert werden, gemäss der „square root relation“ (Quadratwurzelformel), welche die Isotopen Fraktionierung als umgekehrt proportional zur Quadratwurzel des Verhältnisses ihrer molekularen Massen definiert. Neue Studien bestreiten allerdings, dass die Quadratwurzelformel, die vom kinetischen Gasgesetz hergeleitet wurde, die Fraktionierung von Edelgasisotopen durch molekulare Diffusion im Wasser korrekt beschreibt. Deshalb wurde die Fraktionierung von Edelgasisotopen (Ne, Ar, Kr, Xe) aufgrund von Diffusion durch Wasser in einem Laborexperiment bestimmt. Überraschenderweise kann nur die Fraktionierung von Ar Isotopen mit der Quadratwurzelformel beschrieben werden, während die Fraktionierung von Ne, Kr und Xe viel geringer oder sogar vernachlässigbar ist. Die Ergebnisse des Laborexperiments bilden eine gute Grundlage für Studien, in denen die Fraktionierung von Edelgasisotopen dazu verwendet wird, Diffusion im Wasser festzustellen, z.B. um den diffusiven Transport von gelösten Edelgasen zu Gasblasen, die im Sediment gebildet werden, zu untersuchen.

(2) In Seesedimenten in deren Porenwasser Gase von Mikroorganismen aktiv produziert werden und die deshalb übersättigt sind mit reaktiven Gasen (z.B. CH_4), ist der

Transport von Edelgasen beschleunigt im Verhältnis zum diffusiven Transport von Edelgasen durch das Porenwasser. Der Edelgastransport ist beschleunigt aufgrund der Wechselwirkungen mit den Gasblasen, die im Sediment entstehen und schliesslich freigesetzt werden. Methoden, die für gewöhnlich zur direkten Messung der Methankonzentration im Sediment verwendet werden, sind anfällig für einen Gasaustausch mit der Atmosphäre während der Probennahme und können daher nicht in gasübersättigten Sedimenten eingesetzt werden. Um eine höhere Genauigkeit der Methanmessung zu erreichen, wurde eine neue Methode zur Bestimmung von Methankonzentrationen im Porenwasser von Seesedimenten entwickelt. Diese Methode wurde mit Edelgasmessungen kombiniert und in zwei Seen angewendet (Rotsee, Lungernsee), die beide aktiv Gas (hauptsächlich CH_4) aus den Sedimenten freisetzen. Der kontinuierliche Methangasfluss aus den Sedimenten des Rotsees wurde mithilfe der Edelgaskonzentrationen quantifiziert, wobei die Edelgaskonzentrationen mit grösserer Sedimenttiefe abnehmen. Der Bereich der aktiven Gasblasenbildung im Sediment wurde anhand der Konzentrationsspitzen des Methans, welche die Sättigungskonzentration um eine Grössenordnung übersteigen, bestimmt.

Der Lungernsee ist von starken Wasserstandsschwankungen betroffen, die eine Bildung von Gasblasen im Sediment hervorrufen und eine Emission von Methan mit diesen Blasen bewirken. Ausserdem fallen während des Tiefststandes des Wasserpegels Teile des Sediments trocken. Der beobachtete Edelgasüberschuss im Verhältnis zu den ASW Konzentrationen wurde benutzt, um die Sauerstoffzufuhr in die zuvor trocken gefallen Sedimente zu berechnen.

In einer Pilotstudie an einem glazialen Ton des Zürichsees wurde ein Edelgasüberschuss relativ zu ASW gemessen. Diese Übersättigung könnte auf einen glazialen Schmelzwasserzufluss zurückzuführen sein, denn eine starke Übersättigung mit ^4He und die Zusammensetzung der Edelgase im Porenwasser des Sedimentes werden als Hinweis darauf interpretiert, dass die Edelgase in diesem Tonsediment über eine Zeitspanne von mehreren Tausend Jahren quantitativ eingeschlossen sind.

Die in dieser Doktorarbeit gewonnenen Erkenntnisse zum Verhalten von Edelgasisotopen bei Diffusion im Wasser sind ein wichtiger Schritt zur Etablierung des Argon Isotopenverhältnisses als Indikator für diffusive Gas-Transport-Prozesse in Seesedimenten. Desweiteren gibt diese Doktorarbeit Einblicke in die Interaktion von gelösten Edelgasen und reaktiven Gasblasen im Sedimentporenwasser von gasübersättigten Sedimenten. Die neu entwickelte Methode zur Messung von in situ Methankonzentrationen ist ein wichtiges Instrument für die genauere Erforschung solcher Sedimente. Insgesamt zeigt diese Arbeit, dass Edelgase ideale Indikatoren sind um die Gasdynamik in unterschiedlichsten Sedimenten - von gasübersättigten Sedimenten bis hin zu stark kompaktierten Tonsedimenten - zu untersuchen.

Chapter 1

Introduction

1.1 Noble gases as tracers for gas dynamics in lacustrine sediments

Lacustrine sediments contain matter in solid, liquid and gaseous states. The solid particles are quantitatively trapped in the pore space, whereas the extent of retention of the fluids in the pore space depends on the sediment characteristics. Under favourable conditions fluids can be trapped over large periods of time (Goldstein, 2001; Brennwald et al., 2004). Sediment records contain information reflecting temporal changes in the lake system and in the catchment basin, e.g. past climatic conditions and human influences (Perry and Taylor, 2009). In contrast to other environmental proxies present in lacustrine sediments, which only indirectly relate to environmental conditions (Zolitschka and Enters, 2009), noble gas concentrations in the sediment pore water are direct and straightforward proxies for past environmental conditions (for reviews see Kipfer et al., 2002; Schlosser and Winckler, 2002; Brennwald et al., 2013b). The noble gases in the sediment pore water are preset by the last gas exchange of the lake water and the atmosphere, i.e. air saturated water (ASW). ASW results from partitioning between air and water, i.e. air water exchange, which is well-defined by Henry's law and directly linked to water temperature and salinity as well as to the atmospheric pressure that prevailed during the gas exchange. This ASW - noble gas concentration is distributed within the whole lake by mixing processes and turbulent exchange and subsequently incorporated in the sediment. Thanks to advances in methodology (Brennwald et al., 2003; Tomonaga et al., 2011a) the noble gas concentrations in the pore water of lake sediments can be determined with high precision, and noble gases in the sediment pore water have been used to reconstruct paleotemperature and paleosalinity (Tomonaga et al., 2012, 2014, 2015) and to analyse transport processes and exchange of solutes and fluids in the sediment pore water (Brennwald et al., 2004, 2005; Chaduteau et al., 2007a,b; Pitre and Pinti, 2010; Tomonaga et al., 2011b). Although noble gases dissolved in lacustrine sediments have been successfully used to trace past environmental processes and conditions, not all underlying processes and mechanisms of noble gas transport in sediment pore water have been fully understood. An example for a process that lacks of a sound physical understanding is molecular diffusion of noble gas isotopes in pore water. Molecular diffusion is the main determinant of dissolved gases and solute transport through sediment pore water. In some sediments the diffusivity of noble gases in the sediment pore water is similar

to their molecular diffusivity in free water. In other sediments noble gases are quantitatively trapped in the sediment pore water and molecular diffusion is strongly suppressed so that it becomes virtually negligible (e.g. Brennwald et al., 2005; Pitre and Pinti, 2010; Tomonaga, 2010; Tomonaga et al., 2015).

The extent of the suppression of noble gas diffusion in sediment pore water can be detected using the observed isotope fractionation (Brennwald et al., 2005) and the isotopic difference in the noble gas diffusivities. In many studies the isotopic fractionation of noble gases due to molecular diffusion in water was assumed to be mass dependent and to be predicted by the inverse square root of the molecular masses, i.e. Graham's law (Graham, 1833; Richter et al., 2006). However Graham's law is derived from the kinetic theory of gases and has strictly speaking not been proven to be applicable for the diffusion of gas in water. Furthermore recent classical molecular dynamics simulation (Bourg and Sposito, 2008) challenged this commonly made assumption that the square root relation adequately describes the fractionation of noble gas isotopes due to molecular diffusion in water.

Another relevant application for noble gases dissolved in the sediment pore water is tracing secondary gas exchange with gas bubbles formed in the sediment. Noble gases dissolved in the sediment pore water have a great potential to depict the mechanisms underlying reactive gas bubble formation in the sediment and to study the bubble emission from the sediment. But so far only a single study on the interaction of noble gases and bubbles formed in the sediment pore water has been conducted (Brennwald et al., 2005). Carbon dioxide and methane are quantitatively the most important gases generated in lacustrine sediment. Carbon dioxide is characterized by a high solubility whereas methane is hardly soluble. Thus commonly methane is the quantitatively predominant gas in bubbles that can be formed in the sediment pore water when the total gas pressure exceeds the local hydrostatic pressure (Bastviken et al., 2011). In order to study the mechanisms of gas exchange of noble gases dissolved in the pore water with such gas bubbles present in the sediment, the methane concentration in the pore water of sediments needs to exceed the local saturation concentration. But the available methods for the direct determination of methane amounts in the pore water are often subject to gas loss (Adams, 1994) and therefore methane concentrations exceeding the local saturation concentration cannot be determined precisely, e.g. using a common method, in which a syringe is used for sampling, the sediment is exposed to the atmosphere for approximately two seconds (Hoehler et al., 1994). However the method for the analysis of noble gas concentrations in the pore water of lake sediments (Brennwald et al., 2003; Tomonaga et al., 2011a) has been proven to prevent any gas exchange with the atmosphere. In cases where methane concentrations in the pore water of sediments can be as adequately determined as the noble gas concentrations, the measurement of methane and noble gas concentrations in the sediment pore water is a promising tool to depict the gas dynamics in the pore waters of sediment characterized by methane gas over-saturation and related bubble formation.

On the base of the given analysis this thesis aims to study transport processes and gas dynamics in the sediment pore water to characterize the physical mechanisms that constrain the gas dynamics in sediment pore water as a necessary prerequisite for further establishing dissolved noble gases in sediment pore waters as proxies for past environmental conditions and processes. In particular this thesis focuses on:

- Building a robust basis for the interpretation of noble gas isotope ratios measured in the sediment pore water by conducting laboratory experiments to determine the effect of molecular diffusion in water on noble gas isotopes.
- Developing a new method for assessing the analysis of methane amounts in the sediment pore water to overcome the experimental limitations of commonly used methods.
- Investigating extreme cases, such as on one hand lake sediments with an enhanced noble gas transport through the sediment pore water, e.g. sediments characterized by strong microbial gas production and gas ebullition and on the other hand lake sediments where noble gas transport is almost negligible, such as highly compacted sediments. In glacial clays, for example, molecular diffusion is expected to be strongly suppressed and noble gas concentrations are expected to be preserved over a long period of time.

1.2 Outline

The thesis is structured in three parts: the analysis of molecular diffusion in water, the development of a method for the quantitative determination of methane, and an account of applications in the field. The first part (Chapt. 3 + 4) deals with isotopic fractionation of different noble gases due to molecular diffusion in water and presents the results of laboratory studies to determine the possible isotopic fractionation of noble gases as a result of molecular diffusion in water. The second part (Chapt. 5) introduces a new method for the determination of total methane in the pore water of lacustrine sediments. The third part (Chapt. 6 + 7) discusses results of noble gas studies in the unconsolidated sediments of three lakes. In the sediments of Lake Rotsee and Lake Lungern the gas dynamics related to bubble formation were investigated. The most recent results of noble gas concentrations in deep glacial clay sediment of Lake Zurich are presented as an prospect to future research.

Chapter 2: Concepts

This chapter provides the necessary background information on gases present in lacustrine sediments and on the gas dynamics and transport processes in the pore space of sediments. A special focus lies on molecular diffusion and on methane supersaturation causing a formation of gas bubbles in the sediment pore water. To understand how these two processes are affecting the noble gas concentrations is key for using noble gases as tracer for gas dynamics in lacustrine sediments.

Chapter 3: Fractionation of Ne and Ar isotopes by molecular diffusion in water

In this chapter the fractionation of Ne and Ar isotopes as a result of diffusive transport through water was determined experimentally in order to establish a robust basis to interpret dissolved noble gas concentrations as a measure for past environmental conditions in lakes and oceans. The presented results were obtained using a simple experimental set-up

consisting of a column containing immobilized water. Surprisingly a contrasting isotope fractionation was found for Ne and Ar although the relative difference of the mass of the isotopes of both elements is the same.

Chapter 4: Negligible fractionation of Kr and Xe isotopes by molecular diffusion in water

The different fractionation pattern of Ne and Ar isotopes upon molecular diffusion in water are the motivation for this chapter, which analyses the isotopic fractionation of Kr and Xe. Results were obtained using the same set-up and experimental principals as described in Chapt. 3. Both Kr and Xe were found to show a very low or even negligible isotopic fractionation that cannot be described by Graham's law at all.

Chapter 5: Improved method for the quantification of methane concentrations in unconsolidated lake sediments

Methods most commonly used to sample methane dissolved in pore water of lake sediments produce results that are subject to gas loss or to gas exchange with the atmosphere. To determine the true in situ amount of methane per unit mass of pore water in sediments, a new analytical method was developed and validated. The new method adapts techniques developed for noble gas analysis in pore waters to quantify the methane present in the pore space in dissolved and gaseous form.

Chapter 6: Noble gases as tracer for the gas dynamics in methane supersaturated lacustrine sediments

In eutrophic Lake Rotsee methane is produced biologically in the sediment. Methane ebullition from sediments was shown to cause a characteristic noble gas depletion in the pore water. This depletion pattern of the atmospheric noble gas concentrations and the peaks of supersaturation with methane in the sediment pore water were used to quantify methane emissions from the sediment pore water with a mass balance approach. The sediment of Lake Lungern is affected by strong lake level variations. The lake level lowering on one hand causes a release of the hydrostatic pressure acting on the sediment and therefore is expected to foster bubble formation in the sediment pore water containing methane concentrations close to saturation concentration. On the other hand parts of the sediment fall dry, which causes air to enter the sediment and excess-air, i.e. a surplus of atmospheric gases relative to ASW, to form when the lake level is rising again.

Chapter 7: Pilot study: Noble gas concentrations in a deep clay sediment layer of Lake Zurich

In Lake Zurich a highly compacted clay layer being exposed by a subaquatic landslide was sampled and was found to be strongly enriched in ^4He . The noble gas pattern in this clay layer were interpreted to indicate that molecular diffusion in the pore water is strongly suppressed. Hence noble gas concentrations determined in the sediment pore water might indicate past environmental conditions and processes during clay deposition, which according to the depositional environment and "U - Th - ^4He - age", took place during the last glaciation.

Chapter 2

Concepts

Noble gases are ubiquitously present in the terrestrial environment. As a result of their biogeochemical inertness, noble gas concentrations in the environment can only be altered by physical processes, and hence can be used to assess these processes. In meteoric waters the noble gas concentrations are a well-defined function of the water temperature and salinity as well as the atmospheric pressure that prevailed during gas exchange with the atmosphere. Noble gas concentrations in meteoric waters are therefore direct and straightforward proxies for reconstructing these environmental conditions and are applied successfully in aquatic systems (for a review, see Kipfer et al., 2002; Schlosser and Winckler, 2002; Aeschbach-Hertig and Solomon, 2013; Brennwald et al., 2013b).

In the past decade, research focused on lacustrine sediments, which build a natural archive for noble gases dissolved in their pore water (for a review see Brennwald et al., 2013b). Such noble gases were found to be excellent tracers for gas dynamics in lakes, e.g. transport and mixing processes, and have been successfully used to reconstruct past environmental conditions, e.g. the reconstruction of paleoclimate (Brennwald et al., 2004, 2005; Chaduteau et al., 2007a,b; Pitre and Pinti, 2010; Tomonaga et al., 2011b, 2015). The precise determination of noble gas concentrations dissolved in the pore water was possible thanks to a newly developed method (Brennwald et al., 2003; Tomonaga et al., 2011a). In sediments characterized by biological gas production the noble gas concentrations determined in the pore water have been used to trace the emission of such biologically produced gases. In the sediments of hypertrophic Lake Soppen (Switzerland), for example, a noble gas depletion relative to air saturated water was determined. By means of this depletion the past methane ebullition from the sediments of Lake Soppen were reconstructed (Brennwald et al., 2005). Other sediments are characterized by a diffusion suppression in their pore waters. In such sediments the composition of noble gases in the pore water may conserve information about past environmental conditions. In the sediments of Stockholm Archipelago (Sweden), for example, it could be shown that a noble gas supersaturation in the sediment pore water caused by a past sediment slide, i.e. mass movement, was trapped and conserved for more than a century (Tomonaga et al., 2015). The noble gas record determined in the pore water of deep drilling sediment cores in Lake Van (Turkey) made it possible to reconstruct past salinity in the lake over the last 250 kyr that is linked to the past water level in the lake (Tomonaga et al., 2014, 2017). In Lake Issyk-Kul (Kyrgystan) paleoenvironmental conditions dating back to the mid-Holocene were traced by means of the noble gas concentrations in the sediment pore

waters (Brennwald et al., 2004).

These studies make the case that noble gases dissolved in the sediment pore water are excellent tracers for the gas dynamics in lacustrine sediments. In this chapter an overview on the gas dynamics in lacustrine sediments is given. The relevant processes and mechanisms are discussed in more detail in Sect. 2.2. A special focus lies on molecular diffusion, which is introduced in the Sect. 2.2.2. Furthermore, this chapter gives a short overview of gases dissolved in the pore water of lacustrine sediments (see Sect. 2.1). Such gases are either autochthonously produced, e.g. by biological production (CH_4 , see Sect. 2.1.2) and by radioactive decay within the sediment matrix (^4He , see Sect. 2.1.1), or they are of allochthonous origin, e.g. atmospheric noble gases (see Tab. 2.1, Sect. 2.1.1). Commonly gases in the sediment are dissolved in the pore water, but in the case of supersaturation gas bubbles can be formed. Bubble formation and the interaction of dissolved noble gases with reactive gas bubbles (of mostly reactive gas species such as CH_4) is discussed in Sect. 2.2.

2.1 Gases in the sediment pore water

Gases in the sediment pore water are either the result of microbial production within the sediment (1), or they originate from the atmosphere (2) or from underlying (geogenic) sources (3).

(1) As a result of the decomposition and mineralization of the organic material in the sediments, gases are produced by micro-organism or by mineralisation processes in the sediments. The gas production is dependent mainly on the availability of electron acceptors, e.g. oxygen (O_2), nitrate (NO_3^-) and sulfate (SO_4^{2-}). Denitrification generates nitrogen gas (N_2), nitrous oxide (N_2O) and ammonia (NH_3 ; Liikanen et al., 2002). Under anaerobic or anoxic conditions fermentative processes and methanogenesis result in a production of carbon dioxide (CO_2) and methane (CH_4). In eutrophic lakes, characterized by O_2 depletion in the benthic zone CO_2 and CH_4 are usually quantitatively the most important gases produced in the sediment pore water. However, as CO_2 is characterized by a high solubility whereas CH_4 is hardly soluble (in the range of the solubility of argon) bubbles formed in the sediment pore water mainly contain CH_4 (e.g. in a study on a shallow eutrophic lake 80 - 90% of the emitted gas was CH_4 ; Martinez and Anderson, 2013). Other gases in the sediment pore water are present only in low concentrations or even as traces amounts, e.g. N_2O , NH_3 , hydrogen (H_2), carbon monoxide (CO) and sulphur dioxide (SO_2).

(2) Although N_2 is biologically produced as a result of denitrification, most of the N_2 in lakes and their sediments originates from the atmosphere, as do other non reactive trace gases present in the sediment pore water, such as the noble gases helium (He), neon (Ne), argon (Ar), krypton (Kr), xenon (Xe). Atmospheric gases exchange with the lake water at the lake surface. The equilibrium concentration which is established in the lake water during this gas exchange is referred to as air saturated water (ASW) (see Sect. 2.1.1). ASW is distributed throughout the lake by convection and turbulent transport and it is incorporated in the growing sediment at the lake bottom (Brennwald et al., 2013b).

(3) In fault zones CH_4 and CO_2 can seep through fractured rocks from deep hydrocarbon accumulations, e.g. an oil or gas reservoir, to the atmosphere and form mud volcanoes in aquatic environments (Etiope and Klusman, 2002). Reactive gases seeping

Table 2.1: Atmospheric composition (Ozima and Podosek, 2002)

Constituent	Volume ratio
Dry air	1
N ₂	7.81 10 ⁻¹
O ₂	2.09 10 ⁻¹
Ar	(9.34 ± 0.01) 10 ⁻³
CO ₂ *	** (3.905 ± 0.002) 10 ⁻⁴
Ne	(1.818 ± 0.004) 10 ⁻⁵
He	(5.24 ± 0.05) 10 ⁻⁶
CH ₄ *	** (1.803 ± 0.002) 10 ⁻⁶
Kr	(1.14 ± 0.01) 10 ⁻⁶
H ₂	4-10 10 ⁻⁷
N ₂ O*	** (3.242 ± 0.002) 10 ⁻⁷
CO	0.1-2 10 ⁻⁷
Xe	(8.7 ± 0.1) 10 ⁻⁸
*relatively variable gases	** IPCC report 2013

from a geogenic reservoir can be identified by their isotopic composition (e.g. biogenic $\delta^{13}C_{CH_4} \sim -60$ ‰ and thermogenic $\delta^{13}C_{CH_4} \sim -40$ ‰) and a characteristic noble gas pattern.

2.1.1 Noble gases

Atmospheric noble gases

The biggest reservoir for terrestrial noble gases is the atmosphere. However, with the exception of Ar the noble gas concentrations in the atmosphere are very low or even in the range of mere trace elements (Ozima and Podosek, 2002). The composition of noble gases and their isotopes in the Earth atmosphere is virtually stable in space and time (in the range of Myr). Therefore, air is commonly used as the noble gas standard and as the reference for discussion of noble gas data (see Tab. 2.1 and Tab. 2.2).

The atmosphere is also the most important source for noble gases dissolved in the sediment pore waters. Gases enter the lake through exchange at the lake surface during air water partitioning. This gas exchange happens fast relative to the mixing processes within the lake, and therefore the water at the lake surface is virtually in thermodynamical solubility equilibrium with the atmosphere (ASW). The equilibrium between gases in free gaseous phase and gases dissolved in water is given by Henry's law:

$$P_i = H_i(T,S)C_i \quad (2.1)$$

where P_i is the atmospheric partial pressure in the gas phase of a gas i , H_i is the Henry coefficient (see Tab. 2.3) depending on the temperature (T) and the salinity (S) of the water and C_i the equilibrium concentration of gas i in the water. The Henry coefficients in this work are calculated as recommended by Kipfer et al. (2002), and by using the

Table 2.2: The quantitatively most relevant noble gas isotopes and their relative molar abundances in atmospheric air (Ozima and Podosek, 2002)

Isotope	Molar abundance %
^3He	0.00014
^4He	100
^{20}Ne	90.50
^{22}Ne	9.23
^{36}Ar	0.3364
^{40}Ar	99.60
^{82}Kr	11.523
^{83}Kr	11.477
^{84}Kr	57.00
^{86}Kr	17.398
^{129}Xe	26.44
^{132}Xe	26.89
^{134}Xe	10.430
^{136}Xe	8.857

parametrizations of Weiss (1971b) for He and Ne, Weiss (1971a) for Ar, Weiss and Kyser (1978) for Kr, and Clever (1979) for Xe. Tab. 2.3 shows the Henry coefficients and molecular diffusivities of noble gases in water. Commonly the noble gas concentrations are denoted as $[\frac{\text{cm}^3(\text{STP})}{g}]$, i.e. the gas volume $[\text{cm}^3]$ at STP conditions, with temperature (0°C) and pressure (1 atm) per gram of water, and can be converted into molar units using:

$$\begin{aligned} 1 \text{ cm}^3(\text{STP}) &= 4.4615 \cdot 10^{-5} \text{ mol} \\ 1 \text{ mol} &= 22414 \text{ cm}^3(\text{STP}) \end{aligned} \tag{2.2}$$

The solubility of noble gases is temperature dependent (as is the case for gases in general) and increases with the atomic weight of the respective noble gas. The light noble gases He and Ne are hardly soluble, whereas the heavy noble gases Ar, Kr and Xe show higher solubilities. The light noble gases have larger diffusivities than the heavy noble gases, therefore often the light noble gases He and Ne show a different transport behaviour than the heavy noble gases Ar, Kr and Xe (see Tab. 2.3).

The water that attained ASW noble gas concentration at the lake surface is distributed throughout the whole lake by inherent mixing and convection. Therefore, commonly the noble gas concentrations dissolved in the lake water agree well with the expected ASW concentration calculated with Henry's law (Eq. 2.1).

Another way for atmospheric noble gases to enter the lake water is via dissolving air bubbles that originate from breaking waves at the lake surface (Craig and Weiss, 1971). If such bubbles dissolve several meters below lake surface under a higher hydrostatic pressure they can cause a noble gas excess relative to ASW noble gas concentration at the lake surface. However, this noble gas excess quickly re-equilibrates with the atmosphere and is not transported throughout the lake. Therefore, this process is commonly not relevant

Table 2.3: On the left: The Henry coefficients H_i in $[\text{bar}/(\text{cm}_{\text{STP}}^3/\text{g})]$ with $i = \text{He, Ne, Ar, Kr, Xe}$ at different water temperatures T and salinity $S = 0 \text{ g/kg}$ with STP referring to Standard Temperature ($T = 0^\circ\text{C}$) and Pressure ($P = 1 \text{ atm}$) (Kipfer et al., 2002). On the right: Molecular diffusivities of noble gases in water for different water temperatures (Jähne et al., 1987a; Klump, 2007).

T	0°C	5°C	10°C	15°C	20°C	0°C	5°C	10°C	15°C	20°C
	$H_i \left[\frac{\text{bar}}{\text{cm}_{\text{STP}}^3/\text{g}} \right]$					$D \left[10^{-9} \frac{\text{m}^2}{\text{s}} \right]$				
He	108.3	111.5	114.3	116.6	118.6	4.74	5.19	5.68	6.19	6.73
Ne	81.89	86.76	91.31	95.55	99.52	2.34	2.63	2.94	3.28	3.65
Ar	19.01	21.71	24.51	27.39	30.34	1.44	1.65	1.87	2.11	2.38
Kr	9.306	10.93	12.69	14.58	16.58	0.877	1.03	1.20	1.39	1.61
Xe	4.580	5.576	6.690	7.920	9.263	0.664	0.788	0.929	1.09	1.27

for the noble gas composition in the sediment.

Noble gas excess in pore water of oceans can also originate from melt water of ice containing entrapped air bubbles (Hohmann et al., 2002; Grundl et al., 2013). This path for atmospheric noble gases to enter the water body might also be relevant for lacustrine sediments, e.g. of lakes in polar regions or during periods of glaciation.

In contrast to open waters, groundwater is well known to show significant (atmospheric) noble gas excess, e.g. the commonly found noble gas concentrations determined in groundwater are significantly larger than ASW concentrations (for a review, see Aeschbach-Hertig and Solomon, 2013). This excess-air derives from the (partial) dissolution of air bubbles entrapped in the groundwater during infiltration.

Non atmospheric noble gases

Non atmospheric noble gases in the sediment pore water are produced by radioactive decay and/or emanate from geological strata. The sources and transport to the sediment for such non atmospheric noble gases are highly heterogeneous (e.g. diffusive transport from geochemical reservoirs, erosion of rocks, transport with the groundwater and volcanic discharge) and therefore can not easily be predicted. However, it is noted that only He (and in some rare cases Ar) is altered by non atmospheric noble gas sources. ^4He is produced by the alpha decay of uranium (U) and thorium (Th) series elements and ^3He from neutron (being the result of α particle interaction with light elements) induced decay of $^6\text{Li}(n,\alpha)^3\text{H}$ to ^3He (Tolstikhin et al., 1996). Due to the omnipresence of U and Th in sediments, the accumulation of ^4He in some sediments can be used to qualitatively scale the age of the sediment. If the ^4He concentration in the sediment pore water is assumed not to be affected by transport processes and if U and Th activity in the sediment is known, the age (t) can be calculated with the following equation (Geyh and Schleicher, 2012):

$$t = \frac{\text{He}}{1.19 * 10^{-13}(\text{U}) + 2.88 * 10^{-14}(\text{Th})} * \frac{q}{\rho} \quad (2.3)$$

where the He concentration is given in cc STP/g H₂O and has been corrected for atmospheric contribution, U and Th are given in g/g sediment, ρ is the density of the sediment and q the fractional porosity of the sediment (see Geyh and Schleicher, 2012). A typical time scale for the He chronometer to be applied is $> 10^2$ years.

In surface water ³He from radioactive decay of tritium, which has a half live of 4500 days, can be used for dating water on a short time scale, e.g. to asses groundwater recharge and the renewal time of surface water bodies (e.g. Schlosser, 1992; Hohmann et al., 1998; Beyerle et al., 2000; Solomon and Cook, 2000).

2.1.2 Methane

Methane, i.e. CH₄, is a poorly soluble gas that is produced biologically and is therefore abundant in many environmental systems on earth, e.g. in lakes and reservoirs. In particular, eutrophic lakes with a high primary production and a high sedimentation rate are characterized by sediment anoxia and methanogenesis (Lovley and Klug, 1982; Sobek et al., 2009). CH₄ in lacustrine sediment occurs in both dissolved and gaseous form, and is transported from the sediment into the overlying water column via molecular diffusion or it emanates as free gas via ebullition (Adams, 1994). Transport of gases by molecular diffusion is very slow. Therefore in sediments with a high CH₄ production ebullition often is the dominant transport process for CH₄ release (Bastviken et al., 2008; Del Sontro et al., 2010; Beaulieu et al., 2014). During bubble ascent CH₄ released from the sediment exchanges with the gas contained in the water column and therefore does not necessarily reach the atmosphere (Holzner et al., 2004; McGinnis et al., 2006). But in small, shallow lakes and in the littoral zone bubbles emerging from the sediment and containing CH₄ have the potential to reach the atmosphere and become relevant for the climate (Joyce and Jewell, 2003; Adams, 2005; McGinnis et al., 2006; Del Sontro et al., 2010).

Anthropogenically-induced eutrophication affects lakes, reservoirs, ponds and rivers on a global scale (Smith, 2003; Downing et al., 2008) and provokes an increasing CH₄ production in the anoxic sediments (Sobek et al., 2012). On the century scale, CH₄ has a global warming potential that is 24 times higher than CO₂ (Forster et al., 2007; Kirschke, 2013). Today, atmospheric CH₄ concentrations are rising, while mechanisms are still poorly understood (Nisbet et al., 2014). Atmospheric CH₄ contributes to climate change. Climate change has the potential to increase the trophic level of aquatic systems and may foster the CH₄ emission from such aquatic systems (Tranvik et al., 2009; Moss et al., 2011). Whereas for a long time CH₄ emissions from inland waters (lakes, reservoirs, ponds and rivers) have not been considered in the global CH₄ budgets (Forster et al., 2007), in the most recent IPCC report they have been accounted for as a significant source for atmospheric CH₄ (Flato et al., 2013). Other studies also emphasize the importance of inland freshwater as a source for atmospheric CH₄, estimating the CH₄ emission from inland freshwater to be in a range of 40 Tg CH₄/year (Bastviken et al., 2011; Kirschke, 2013), which is approximately 8 % of the total global methane emissions (Tsuruta et al., 2017). Furthermore, in recent studies that measure the CH₄ emissions from lakes and reservoirs using advanced techniques (Del Sontro et al., 2010; Grinham et al., 2011; Beaulieu et al., 2014) significantly higher CH₄ emissions were found than in preceding studies. Together with the fact that until the present CH₄ emissions from inland water, particularly rivers (Stanley et al., 2016), have not been adequately studied,

e.g. relevant regions are under-represented (Yang et al., 2011; Panneer Selvam et al., 2014; Sawakuchi et al., 2014), thus indicates that on a global scale CH_4 emissions from inland waters might still be underestimated (Cole et al., 2007; Downing, 2010; Ortiz-Llorente and Alvarez-Cobelas, 2012).

2.2 Gas dynamics in lacustrine sediments and their impact on the noble gas composition

As mentioned (Sect. 2.1.1) the quantitatively most important source for noble gases in the sediment pore water is the atmosphere (see Fig. 2.1 A. and Kipfer et al., 2002; Brennwald et al., 2013b). The concentrations in the sediment pore water are generally expected to correspond closely to the ASW concentration that prevailed in the bottom water of the lake during formation of the sediment (see Fig. 2.1 B. and Sect. 2.1.1). Due to their inertness noble gases are not affected by biological and chemical transformations, and any deviation of the noble gases dissolved in the sediment pore water from ASW is therefore interpreted to result from physical processes or from changes in the physical conditions prevailing in the respective water body (e.g. Brennwald et al., 2004, 2005; Strassmann et al., 2005).

2.2.1 Pore water burial

During sedimentation, part of the free open bottom water just above the sediment surface is incorporated into the sediment pore space. As the sediment grows, the lake water and the respective ASW noble gas concentrations are slowly separated from the lake water body and its mixing dynamics (Brennwald et al., 2013b). In relative terms the pore water is transported vertically from the water/sediment interface towards deeper sediment layers. This downward transport of the pore water is expressed as pore water burial velocity, i.e. the distance the pore water is transported away from the water/sediment interface in a given time. The burial velocity, or burial advection, is determined by sediment accumulation and the sediment compaction. The compaction of the sediment causes a vertical transport of sediment pore water relative to the sediment matrix. However, compaction is often assumed to be so small that it can be neglected. In this case, the pore water burial velocity (U) agrees with the growth rate of the sediment, i.e. the sedimentation rate. The sediments of oligo or mesotrophic lakes usually grow slowly (< 1 mm per year), and therefore a sediment core of a few meters can contain the sediments deposited during several hundred or even thousands of years (Litt et al., 2009; Tomonaga et al., 2012, 2014). In some sediments, diffusive transport of noble gases is suppressed to an extent that it is negligible compared to the transport due to sediment burial, i.e. advective transport. The Peclet number $\text{Pe} = U * L / D_i^0$ (with L referring to the characteristic length and D_i^0 to the effective diffusivity in accordance with Eq. 2.6, see e.g. Schwarzenbach et al., 2003; Brennwald et al., 2013b) serves to describe the fluid regime in the sediment pore water, e.g. if the diffusive transport of noble gases is suppressed compared to their advective transport the Peclet number is small, $\text{Pe} > 1$. In such sediments the noble gases carry information of the past environmental conditions. In other sediments the advective fluxes can be neglected in comparison to the diffusive flux ($\text{Pe} < 1$). In these sediments the

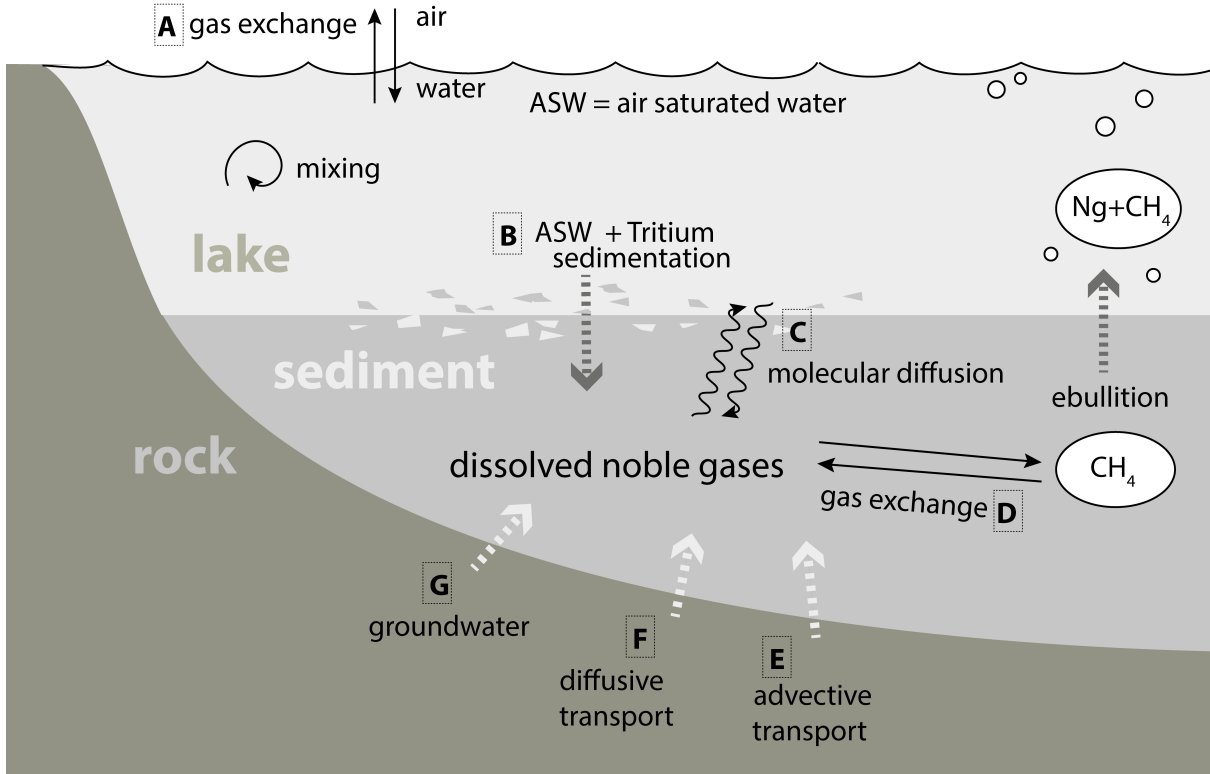


Figure 2.1: Chart illustrating the relevant sources (A,G,F,E) of noble gases in the sediment pore water and the physical processes (A,B,C,D) that have an impact on the noble gas composition in the sediment pore water. Noble gases in the sediment pore water are most commonly of atmospheric origin (A; see Sect. 2.1.1), whereby air saturated water at the lake surface is transported throughout the lake by mixing (B) and is subsequently incorporated in the growing sediment. But noble gases dissolved in the pore water can also derive from non atmospheric sources (see Sect. 2.1.1). It is mostly ^4He and ^3He that are produced in the sediment by radioactive decay or that emanate from the strata below, e.g. by advective transport with geogenic fluids (E), diffusing from the underlying rock (F) or (G) transported with the groundwater, which carries a mixture of atmospheric and non-atmospheric gases. The main physical processes that affect the noble gas concentration in the sediment pore water and that are discussed in this thesis are: (B) incorporation of noble gases dissolved in the lake water in the growing sediment (see Sect. 2.2.1), (C) the diffusive transport of noble gases dissolved in the sediment pore water (see Sect. 2.2.2), and (D) secondary gas exchange with reactive gases formed in the sediment pore water (see Sect. 2.2.3).

past ASW noble gas concentrations recorded in the pore water are affected by molecular diffusion, which results in a smoothing of the noble gas concentrations, i.e. resulting in a loss of information of past environmental conditions (Strassmann et al., 2005).

2.2.2 Molecular diffusion

As mentioned, molecular diffusion is the key transport process for dissolved gases and solutes in pore water. Molecular diffusion describes the transport of matter by random molecular motion (i.e. Brownian motion) and is the result of temperature, pressure or concentration gradients. In fluids, solutes move against a concentration gradient until a uniform concentration prevails in the fluid mass. In a one-dimensional system that consists of a binary mixture of species A and B the diffusive flux can be expressed with Fick's first law (Crank, 1975). If the concentration gradient is known, Fick's first law can be used to determine the diffusion coefficient of a solute in a solvent.

Molecular diffusion coefficients of gases in gas range between 10^{-6} to 10^{-5} [m²/s] while diffusion coefficients of gases and solutes in liquids are 3 to 4 orders of magnitude smaller in a range of 10^{-10} to 10^{-9} [m²/s] (Cussler, 2009). One approach to calculate D_i of a solute in a solvent is using the Stokes-Einstein equation, i.e. Brownian motion:

$$D_i = \frac{RT}{6\pi\eta_B r_A} \quad (2.4)$$

where R is the gas constant, T the temperature, η_B the viscosity of the solvent and r_A the radius of the solute. However, this equation can only be used if the size of the solute molecule is large relative to the size of the solvent molecule (Cussler, 2009). Jähne et al. (1987a) determined the elemental diffusion coefficients of noble gases in water with a diffusion cell containing immobilised water (see Tab. 2.3). Similar experiments were carried out as part of this thesis to determine a possible isotopic fractionation of noble gases upon molecular diffusion through water.

The diffusive transport in sediments, however, is restrained by the solid sediment particles and other factors. This matrix constraints can be expressed as follows (Berner, 1980):

$$F_A^{diff} = -\phi D_i^0 \frac{\Delta C_i}{\Delta x} \quad (2.5)$$

where F_A^{diff} is the diffusive flux, D_i^0 the effective diffusion coefficient of a substance i diffusing in water, C_i the concentration of the matter transported by diffusion and x the direction of the flux and ϕ is a factor that accounts for the transport assessable porosity.

The effective diffusivity is defined as:

$$D_i^0 = \frac{D_i}{a} \quad (2.6)$$

with a (≤ 1) being a factor that accounts for the tortuosity and other effects that inhibit molecular diffusion in the sediment pore water and D_i being the diffusion coefficient of a gas in free water. In the sediment, tortuosity is defined as the ratio of the effective distance that a solute travels in the pore water within the sediment matrix and the direct distance to the lower concentration (Berner, 1980; Maerki et al., 2004). It is expected that not only solid particles but also bubbles or gas voids present in the sediment pore

water can increase tortuosity and therefore reduce the diffusive exchange for dissolved solutes (Flury et al., 2015).

Previous research has established that in some sediments the diffusion of noble gases is suppressed to an extent that cannot be explained only by tortuosity effects (for a review, see Brennwald et al., 2013b). It was hypothesized that the pore diameter in such sediments might be extremely reduced as a result of the (diagenic) formation of minerals in the pore space or due to compaction. Another hypothesis assumes that pore space is composed of single, unconnected pores, so called "dead" pores, that do not allow diffusive exchange with the main pore space. Furthermore, it was hypothesized that microscopic bubbles present in the pore water might also lead to the fragmentation of the pore space, i.e. have similar properties to "dead" pores (Tomonaga, 2010; Brennwald et al., 2013b). Microbubbles can contain significant amounts of noble gases due to secondary gas exchange of the bubble with the noble gases dissolved in the surrounding pore water. Such trapped noble gases might be excluded from macroscopic diffusion through the pore space (Tomonaga, 2010; Brennwald et al., 2013b). In the following section bubble formation in the sediment and secondary gas exchange of dissolved gases with bubbles in the sediment pore water are discussed in more detail, as these processes are relevant for later chapters of this thesis.

2.2.3 Secondary gas exchange with methane bubbles

In sediments in which the sum of the partial pressures of all the gases dissolved in the pore water exceeds the total ambient pressure in the pore water, gas bubbles can form (see, e.g. Boudreau, 2012). The total ambient pressure in the sediment pore water or the in situ pressure in the pore water of a sediment is defined as the sum of the hydrostatic pressure (determined by the overlying water column) and the atmospheric pressure at the lake surface. In this thesis the term gas saturated pore water refers to sediment pore water where the partial pressure of the sum of all gases is equal to the total ambient pressure in the surrounding sediment. Similarly the term local saturation concentration refers to the partial pressure of a single gas being equivalent to the total ambient pressure in the sediment. The gas accumulation, i.e. bubble growth rate, in the sediment pore water and the shape of the gas voids in the sediment are highly dependent on the sediment properties. Lacustrine sediments often consist of fine-grained particles. In this case the bubbles formed in the pore water move the solid sediment matrix, thus creating gas voids that do not contain solid particles (Anderson et al., 1998). In muddy cohesive sediments bubbles are supposed to be eccentric oblate spheroid, i.e. disk - shaped. In soft and sandy sediments the bubbles tend to be more spherical (Boudreau et al., 2005). It is expected that bubbles near the water/sediment interface grow faster, in a few hours or days, whereas bubbles deeper in the sediment need a longer time to grow (Boudreau, 2012). When bubbles reach a critical size, which is determined by the sediment properties, the bubbles might ascend in the sediment and along preferential ways, i.e. cracks, channels and tubes. Finally such rising bubbles leave the sediment, i.e. a process called ebullition, which leads to degassing of the sediment (Holzner et al., 2004; McGinnis et al., 2006).

The causes of bubble formation and ebullition can be microbiological gas production, which can significantly increase the sum of the partial pressures of gases dissolved in the sediment pore water. Gas bubbles can also form in response to a changing in situ pressure

due to atmospheric and/or hydrostatic pressure drops, e.g. as result of lake level variation, or upon shear stress caused by benthic currents (Adams, 1994; Joyce and Jewell, 2003).

Gas bubbles formed in the sediment pore water consist of the gases that were present in the surrounding pore water during gas bubble formation (e.g. CH_4 , CO_2 and noble gases). The amount of a respective gas in the formed bubble depends on the partial pressure in the surrounding pore water and on the solubility of the respective dissolved gas. Thus when a gas bubble is formed in the sediment it causes a depletion of the sparingly soluble noble gases relative to their concentration prevailing in the sediment pore water before bubble formation. In sediments where methanogenesis results in a local CH_4 excess, which in turn causes gas bubbles to form, such newly formed bubbles (mainly) consist of the hardly soluble CH_4 gas (Chanton et al., 1989). These bubbles conceptually induce a diffusive transport of other gases (N_2 , CO_2 and noble gases) dissolved in the nearer pore water to these bubbles. The gas exchange between immobile bubble and surrounding pore water proceeds until the gas composition of the bubble attains equilibrium with the dissolved gases in the surrounding pore water. In the case of bubble ebullition or degassing, noble gases are stripped from the pore space together with the reactive gas. As a result the noble gas concentrations in the pore water of the sediment are depleted relative to the originally prevailing ASW concentrations (Brennwald et al., 2005; Holzner et al., 2008). A special case is fast ebullition by fast forming gas bubbles, which did not attain equilibrium before leaving the sediment. Here a fractionation of noble gas isotopes in the sediment pore water is expected, as molecular diffusion of noble gases in water is commonly assumed to fractionate the isotopic composition of noble gas species (Brennwald et al., 2005). This assumption of an isotopic fractionation of noble gas isotopes due to diffusion in pore water lacks a sound physical understanding, and hence was tested experimentally in the following two chapters (Chapt. 3 and Chapt. 4). The results of these laboratory experiments make a robust basis for studying the gas dynamics in lacustrine sediments, e.g. in sediments characterised by a methane bubble formation in their pore waters (see Chapt. 6). A prerequisite to investigating the interaction of gases dissolved in the sediment pore water with the methane bubbles formed in the pore space was the ability to measure methane concentrations in the sediment pore water with more precision. This was achieved by developing a new method for the analysis of methane concentrations in the sediment pore water (see Chapt. 5).

Chapter 3

Fractionation of Ne and Ar isotopes by molecular diffusion in water

Chapt. 3 has been published as:

L. Tyroller; M. S. Brennwald; L. Mächler; D. M. Livingstone; R. Kipfer. Fractionation of Ne and Ar isotopes by molecular diffusion in water. *Geochimica et Cosmochimica Acta*, 136, 6066, (2014). ¹

Abstract Molecular diffusion in water is a physical transport mechanism that plays an important role in many environmental processes. As the abundances of the chemically inert noble gases and their isotopes are controlled only by physical processes, they are ideal tracers for gas transfer processes in aquatic systems. Molecular diffusion in water is often thought to cause the mass-dependent fractionation of noble gas isotope ratios, e.g. $^{20}\text{Ne}/^{22}\text{Ne}$ and $^{36}\text{Ar}/^{40}\text{Ar}$, under the assumption that the isotopic fractionation of gases in water can be adequately described in terms of a "square root relation", i.e. in terms of the reciprocal of the square root of the ratio of their atomic masses. To quantify reliably the fractionation of $^{20}\text{Ne}/^{22}\text{Ne}$ and $^{36}\text{Ar}/^{40}\text{Ar}$ we determined the change in the isotope ratios of Ne and Ar after they had diffused through immobilised water. The Ne isotope fractionation factor, expressed as the ratio of the diffusion coefficients of ^{20}Ne and ^{22}Ne , was found to be $D_{^{20}\text{Ne}}/D_{^{22}\text{Ne}} = 1.010 \pm 0.003$, which is considerably lower than that predicted from the square root relation, but close to results obtained from recent molecular dynamics calculations. In contrast to this, the Ar isotopic fractionation factor was found to be $D_{^{36}\text{Ar}}/D_{^{40}\text{Ar}} = 1.055 \pm 0.004$, agreeing with that predicted from the square root relation. Thus, neither the square root relation nor calculations based on molecular dynamics are capable of giving a general explanation of the isotopic fractionation of both Ne and Ar that results when these gases undergo molecular diffusion through water. Our experimental results do not rely on a theoretical model and are considered to provide an accurate and robust quantification of the isotopic fractionation of Ne and Ar isotopes induced by molecular diffusion through water.

¹This work was financed by the Swiss National Science Foundation (SNF-project 200020 – 132155). We thank Frank Richter and an anonymous reviewer for their helpful criticism, which greatly helped in improving the manuscript.

3.1 Introduction

Noble gases and their isotopes are used as environmental tracers in aquatic systems because of their sensitivity to the transport and exchange of solutes and fluids. Noble gas concentration patterns in natural water bodies have been successfully used to reconstruct palaeoclimates, to analyse circulation and mixing within water bodies, to quantify water residence times and to study the geochemical origin of fluids injected into water bodies (for reviews see Kipfer et al., 2002; Schlosser and Winckler, 2002; Aeschbach-Hertig and Solomon, 2013; Brennwald et al., 2013b)

Molecular diffusion in water is commonly expected to result in the elemental fractionation of noble gases and in the fractionation of the ratios of noble gas isotopes owing to systematic differences in their diffusion coefficients (e.g. Ozima and Podosek, 2002). The fractionation of the isotope ratios of noble gases dissolved in water (e.g. $^{20}\text{Ne}/^{22}\text{Ne}$ and $^{36}\text{Ar}/^{40}\text{Ar}$) has been used to assess the importance of molecular diffusion for various environmental processes, such as: (I) transport in pore water; (II) degassing in supersaturated pore water; and (III) the dynamics of excess air in groundwater.

- I. If the transport of noble gases in pore water (e.g. in lake sediments) is controlled by molecular diffusion, the noble gas isotope ratios in the pore water would be expected to be fractionated relative to the noble gas isotope ratios found in air-saturated water. If the transport of noble gases in the sediment is dominated by advection, however, no fractionation would be expected.
- II. Bubble formation and degassing generally results when the partial pressure of dissolved gases in the pore water exceeds the in situ pressure. In environmental systems such as lake sediments (Brennwald et al., 2003, 2005, 2013b) and groundwater (for a review see Aeschbach-Hertig et al., 2008), patterns in the concentrations of dissolved noble gases are used to trace the formation of bubbles generated by biological processes (e.g. the production of CO_2 or CH_4). The difference of the partial pressure of the gases in the bubble and in the surrounding water results in the diffusion of noble gases from the water into the bubbles. If the bubbles remain in the water until gas exchange between the bubbles and the surrounding water reaches steady state, the gas partitioning is controlled by the solubilities of the gases. This results in the elemental fractionation of the noble gases in the surrounding water, but in virtually no isotopic fractionation. If the bubbles leave the water before steady state is attained, the noble gas isotope ratios are assumed to be fractionated relative to air-saturated water (Lippmann et al., 2003; Brennwald et al., 2005; Zhou et al., 2005; Klump et al., 2006; Visser et al., 2007).
- III. Excess air results from the entrapment of air bubbles in groundwater. Owing to the increasing hydrostatic pressure during groundwater recharge, the entrapped bubbles dissolve, leading to the higher noble gas concentrations (relative to air-saturated water) that are characteristic of groundwater. The formation of excess air has been explained using various different conceptual models (for a review see Schlosser and Winckler, 2002; Aeschbach-Hertig and Solomon, 2013). Molecular diffusion plays a role in models that describe the partial re-equilibration of excess air in groundwater with the atmosphere. Part of the excess air diffuses through the groundwater body and to the soil gas of the unsaturated zone. The isotope ratios $^{20}\text{Ne}/^{22}\text{Ne}$ and ^{36}Ar

^{40}Ar have therefore been suggested as tools to determine which of the different conceptual models for excess-air formation is likely to be most correct (Holocher et al., 2002; Kipfer et al., 2002; Peeters et al., 2002a; Aeschbach-Hertig and Solomon, 2013). This is important because these conceptual models are necessary when using noble gas concentrations to reconstruct the environmental conditions that prevailed during groundwater recharge.

All the above-mentioned applications of noble gas isotope ratios in aquatic systems to interpret noble gas concentration patterns in terms of physical gas transport processes rely on a parameterisation of the diffusion rates in terms of the reciprocal of the square root of the atomic mass of the gas. This "square root relation" is implicitly derived from Graham's Law (Graham, 1833), which describes the fractionation of two gas species undergoing diffusion in a gaseous matrix for the case where collisions between different gas molecules are rare and pressure is constant (Schwarzenbach et al., 2003; Cussler, 2009). Because Graham's Law and the square root relation derived from it are both ultimately based on kinetic gas theory (Moore, 1999), they lack the theoretical basis that would allow their application to the diffusion of solutes through water. The square root relation can be stated in the following form (e.g. Richter et al., 2006) :

$$\frac{D_i}{D_j} = \sqrt{\frac{M_j}{M_i}} \quad (3.1)$$

where D_i and D_j are the diffusion coefficients of the diffusing gases i and j , and M_i and M_j are their molecular masses. If gas-gas collisions are more frequent, however, the square root relation is modified by introducing the reduced masses μ_i and μ_j of the diffusing gases (e.g. Craig and Gordon, 1965; Richter et al., 2006):

$$\frac{D_i}{D_j} = \sqrt{\frac{\mu_j}{\mu_i}} \quad \text{with } \mu_i = \frac{M_i M_{\text{ma}}}{M_i + M_{\text{ma}}} \text{ and } \mu_j = \frac{M_j M_{\text{ma}}}{M_j + M_{\text{ma}}} \quad (3.2)$$

where M_{ma} is the molecular mass of the matrix gas through which comparatively low concentrations of gases i and j with molecular masses M_i and M_j , respectively, are diffusing.

Recent molecular dynamics calculations (Bourg and Sposito, 2008) have challenged the applicability of the square root relation for characterizing the isotopic fractionation of dissolved noble gas isotopes by molecular diffusion in water. Bourg and Sposito (2008) simulated the diffusion of different noble gases and their isotopes in water on an atomic scale, predicting their behaviour by assuming theoretical intermolecular potential functions. Their results suggest a more general power-law form of Eq. 3.1:

$$\frac{D_i}{D_j} = \left(\frac{M_j}{M_i} \right)^\beta \quad (3.3)$$

in which $0 < \beta < 0.2$ rather than the expected value of $\beta = 0.5$.

Experimental data on the fractionation of noble gases by molecular diffusion in water are scarce. Jähne et al. (1987a) measured the elemental diffusivities of He, Ne, Kr, Xe and Rn in water and found them to be consistent with the square root relation (Eq. 3.1). In their experiments, gas diffuses from a gas-filled chamber through a diffusion cell containing immobilised water into another chamber. The advantage of this experimental approach is

that the system can be described with a single diffusion equation (Schwarzenbach et al., 2003; Cussler, 2009) that can be fitted to the experimental data. However this approach has not yet been used to determine the fractionation of the isotopes of a single noble gas species.

To date the only experimental data available on the kinetic isotopic fractionation of noble gas isotopes in water have been based on air/water gas exchange models, where mass transfer at the gas/water interface is related to diffusion (for a review see Cussler, 2009). Jähne et al. (1987a) studied gas/water mass transfer in an evasion experiment with a circular wind-wave facility and concluded that the isotopic fractionation of He was consistent with the square root relation. A recent study (Tempest and Emerson, 2013) determined gas/water mass transfer for Ne and Ar in a system in which the gas headspace was connected to degassed water. In this experiment, the isotopic fractionation observed was weaker than that predicted by the square root relation, but similar to that predicted by the molecular dynamics model of Bourg and Sposito (2008). However, the setup used in these studies was designed to study the transfer of gases across the thin boundary layers of the air/water interface in natural surface waters, and this is affected by large-scale mixing on both sides of the interface (Jähne et al., 1987b). The quantitative relationship between the gas-exchange rates obtained in such mass-transfer experiments and the diffusion coefficients of the gases involved depends on the choice of a suitable gas-exchange model (Schwarzenbach et al., 2003; Cussler, 2009). Combining an empirical gas-exchange model for natural waters with gas-transfer rates obtained in an artificial laboratory experiment with considerably different turbulence levels in the boundary layers does not provide a direct measurement of the isotopic fractionation resulting from molecular diffusion in water.

Instead of a "mass transfer approach", in this study a "diffusion approach" is used in which the diffusive transport of gases through immobilised water can be expressed by a single diffusion equation. To our knowledge this is the first time that the isotopic fractionation of noble gases has been measured based on a diffusion approach using an experimental setup similar to the modified Barrer method used by Jähne et al. (1987a). We determined directly the fractionation of $^{20}\text{Ne}/^{22}\text{Ne}$ and $^{36}\text{Ar}/^{40}\text{Ar}$ resulting from molecular diffusion in bulk water and measured the relative differences of the isotope fluxes through a diffusion column containing immobilised water. We compare our experimentally measured isotopic fractionation with the two versions of the square root relation (Eqs. 3.1, 3.2) and molecular dynamics calculations (Eq. 3.3) to evaluate the applicability of each.

3.2 Material and methods

3.2.1 Experimental setup

Our setup (Fig. 3.1) consisted of a diffusion column comprising two gas-filled chambers, A and B, separated by a diffusion cell. Before the start of the experiment, both chambers were flushed with carrier gas (N_2 of 99.999% purity, Carbagas, Switzerland) to remove residuals of other gases from the apparatus. During the experiment, chamber A was continuously flushed with one of the test gases (Ne or Ar of 99.999% purity, Carbagas, Switzerland; gas flow: $8 \text{ cm}^3_{\text{STP}}/\text{min}$) and chamber B with the carrier gas (N_2 gas flow: $4 \text{ cm}^3_{\text{STP}}/\text{min}$). The difference in the partial pressure of the test gas between A ($\sim 1 \text{ atm}$)

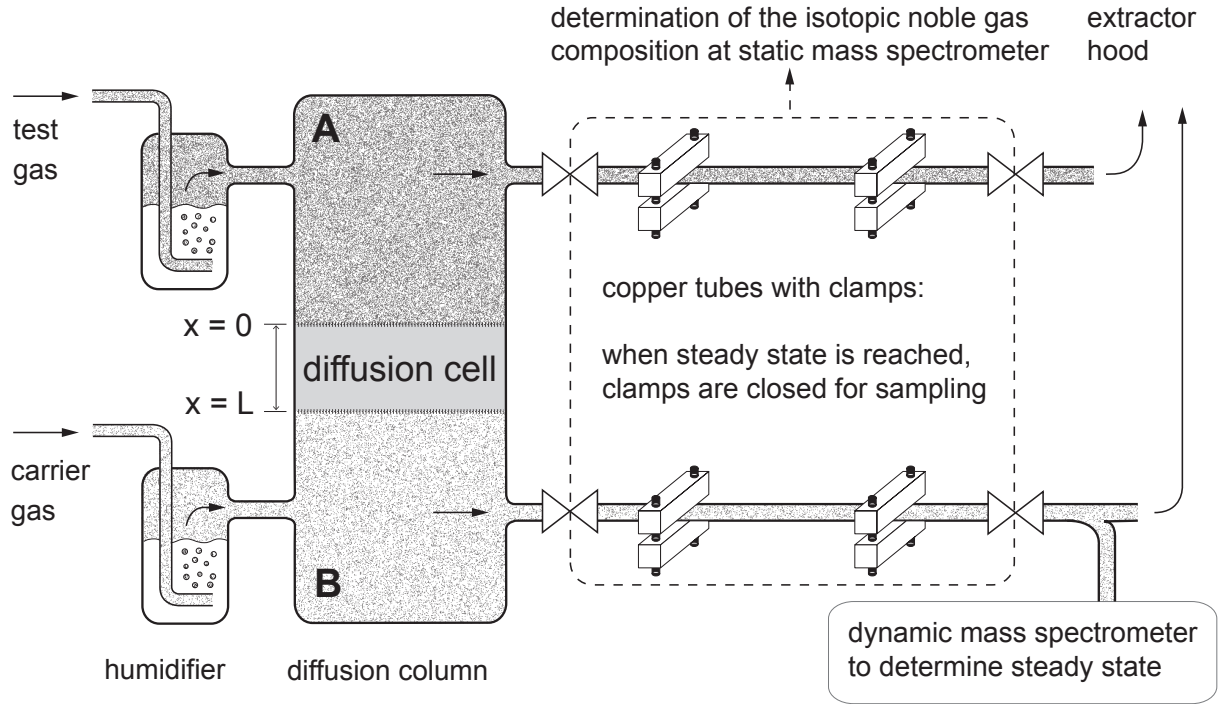


Figure 3.1: Experimental setup. During the experiment both temperature and pressure were kept constant. A test gas and a carrier gas are flushed continuously through two chambers (A and B, respectively) separated by a diffusion cell containing an agar-water gel. All fittings, valves and connection tubes are gas-tight and made of stainless steel or copper. Desiccation of the agar-water gel in the diffusion cell, which might result in cracks, is prevented by bubbling the gases through pure water in humidifiers to saturate them with water vapour before they are injected into the gas-filled chambers. Bacterial growth in the diffusion cell is inhibited by adding 0.01% NaN_3 to the gel. The outflowing gases are discharged into an extractor hood. The gas-carrying outlet tubes are always open to ambient air at local atmospheric pressure.

and B (~ 0 atm) meant that some of the test gas diffused through the diffusion cell from chamber A to chamber B. The test gas reaching chamber B was flushed out together with the carrier gas. To prevent turbulent transport within the diffusion cell, the water in the diffusion cell was immobilised by adding 0.5% agar (porosity 99%) as recommended by Jähne et al. (1987a). The agar-water gel lay on a glass frit (porosity 42%). Repeated experiments were carried out using different gel thicknesses ($L = 1.7\text{--}2.0$ cm, see Tab. 3.1). Turbulent mixing can be assumed to result in homogeneously mixed gases in chambers A and B, making additional mechanical homogenisation unnecessary.

The carrier gas flowing out of chamber B was continuously analysed and monitored with a quadrupole mass spectrometer operated in dynamic mode (Mächler et al., 2012) to assess the performance of the experimental apparatus and to determine when the gas flux through the diffusion cell had attained steady state. These measurements were not used to determine the $^{20}\text{Ne}/^{22}\text{Ne}$ and $^{36}\text{Ar}/^{40}\text{Ar}$ ratios because of interference resulting from doubly charged ions and matrix effects, which strongly limits the precision of the noble gas analysis (see Mächler et al., 2012). When the continuous measurements indicated that the test-gas flux through the diffusion cell had attained steady state, samples of the gases

flowing out of chambers A and B were taken in copper tubes for isotope-ratio analysis by static mass spectrometry (Beyerle et al., 2000). In brief, the gas samples were separated into a He-Ne fraction and an Ar-Kr-Xe fraction using a series of cryogenic traps. These gas fractions were then purified using additional cryogenic traps, zeolite traps and getter traps, which removed any reactive gases. The purified noble gases were then analysed in a custom-built, sector-field mass spectrometer by peak-height comparison relative to an air standard processed using exactly the same procedure as that used for the sample gas.

3.2.2 Principles of the measuring method

After switching on the flow of test gas through chamber A, the test gas starts to diffuse through the diffusion cell. In an initial, non-steady-state phase, the test-gas flux through the diffusion cell increases until it eventually attains steady state.

Non-steady state

By differentiating Eq. 4.24a of Crank (1975) with respect to time, the time-dependent diffusive flux $F_i(t)$ of the test-gas species i from the diffusion cell into chamber B can be calculated as follows:

$$F_i(t) = \frac{D_i C_i(0)}{L} \left(1 + 2 \sum_{n=1}^{\infty} (-1)^n \exp \left(-D_i n^2 \pi^2 \frac{t}{L^2} \right) \right) \quad (3.4)$$

where t is time ($t = 0$ at the start of the experiment, when chamber A is completely flushed by the flow of test gas); D_i is the diffusion coefficient of species i in the diffusion cell; and $C_i(x)$ is the concentration of species i in the diffusion cell at position x ($x = 0$ at the top of the diffusion cell and $x = L$ at the bottom; see Fig. 3.1). The assumptions underlying Eq. 3.4 are that $C_i(0 \leq x \leq L) = 0$ for $t < 0$; that $C_i(0) > 0$ and is time-independent for $t \geq 0$, and that $C_i(L) \ll C_i(0)$ for $t \geq 0$. The breakthrough time T (the characteristic time required for F_i to undergo a substantial increase) is given by Eq. 4.26 of Crank (1975):

$$T = \frac{L^2}{6D_i} \quad (3.5)$$

Steady state

The gas flux $F_i(t)$ from the diffusion cell into chamber B is considered to have attained steady state when $t \sim 3T$ (Daynes, 1920; Crank, 1975). Eq. 3.4 can then be simplified to:

$$F_i = D_i \frac{C_i(0)}{L} \quad (3.6)$$

The isotopic fractionation factor for two different species i and j – i.e. the ratio of their diffusion rates or, equivalently, of their diffusion coefficients – can be obtained from the concentration ratio $R_{i,j}^0 = C_i(0)/C_j(0)$ at the upper interface of the diffusion cell and

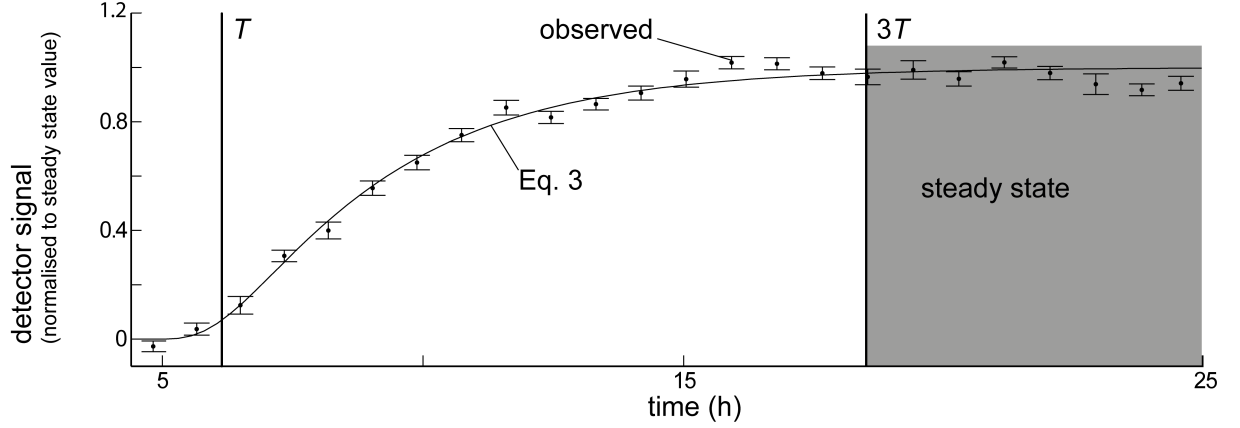


Figure 3.2: Breakthrough curves of ^{20}Ne . Dots indicate "observed" data, measured in the outlet of chamber B with a quadrupole mass spectrometer (error bars indicate standard errors). The curve shown is the theoretical breakthrough curve, calculated from Eq. 3.4 with $D_{^{20}\text{Ne}} = 3.0 \cdot 10^{-9} \text{ m}^2/\text{s}$ (Wise and Houghton, 1968) and $L = 2.0 \text{ cm}$. The breakthrough time $T = 6.2 \text{ h}$ was calculated from Eq. 3.5 based on the same values for $D_{^{20}\text{Ne}}$ and L . Steady state is considered to be attained at time $3T$ (Daynes, 1920; Crank, 1975).

the flux ratio $R_{i,j}^L = C_i(L)/C_j(L) = F_i/F_j$ at the lower interface of the diffusion cell, according to Eq. 3.6:

$$\frac{R_{i,j}^L}{R_{i,j}^0} = \frac{F_i/F_j}{C_i(0)/C_j(0)} = \frac{D_i}{D_j} \quad (3.7)$$

Note that the isotopic fractionation of Ne and Ar at solubility equilibrium in water is very small (see Beyerle et al., 2000). If i and j are two isotopes of the same element, $R_{i,j}^0$ can therefore be assumed to be identical to the isotope concentration ratio in the pure test gas flowing through chamber A, and $R_{i,j}^L$ can be assumed to be identical to the concentration ratio of the two isotopes in the carrier gas leaving the system via chamber B. We were therefore able to determine the isotope fractionation factor from Eq. 3.7 simply by measuring the isotope ratios in chambers A and B using static mass spectrometry. The advantage of this approach is that quantification of the fractionation factor is virtually independent of the geometry of the diffusion column, as it relies only on the isotope concentration ratios in chambers A and B, which can be measured precisely and straightforwardly using a standard noble gas analysis protocol (Beyerle et al., 2000).

3.3 Results and discussion

3.3.1 Experiment performance

Fig. 3.2 shows the observed and theoretical breakthrough curves calculated using Eq. 3.4. The curves are in excellent agreement, as are the breakthrough times, indicating that the experiment performs exactly as would be expected based on the description given above (Sect. 3.2.2). By inserting the isotope ratios measured in chambers A and B into Eq. 3.7, an accurate quantification of the isotopic fractionation resulting from diffusive transport through the diffusion cell can therefore be obtained.

Table 3.1: $^{20}\text{Ne}/^{22}\text{Ne}$ and $^{36}\text{Ar}/^{40}\text{Ar}$ ratios and their standard errors measured in chambers A and B at steady-state conditions in different experimental runs (2 runs with Ne, 4 runs with Ar) using diffusion cells with different thicknesses L .

	$^{20}\text{Ne}/^{22}\text{Ne}$	$^{36}\text{Ar}/^{40}\text{Ar} \cdot 10^{-3}$
Chamber A ($R_{i,j}^0$)		
Test gas (dry):	9.76 ± 0.02	3.36 ± 0.01
Test gas (humidified):	9.76 ± 0.02	3.36 ± 0.01
Mean, error of the mean:	9.76 ± 0.02	3.36 ± 0.01
Chamber B ($R_{i,j}^L$)		
$L = 1.7$ cm	9.86 ± 0.02	3.54 ± 0.01
$L = 1.7$ cm	—	3.54 ± 0.01
$L = 2.0$ cm	9.86 ± 0.02	3.54 ± 0.01
$L = 2.5$ cm	—	3.56 ± 0.01
Mean, error of the mean:	9.86 ± 0.02	3.545 ± 0.006

3.3.2 Fractionation factors

The flux of the test gas through the diffusion cell attained steady state approximately 18 h after the start of the experiment ($3T$ in Fig. 3.2). $^{20}\text{Ne}/^{22}\text{Ne}$ and $^{36}\text{Ar}/^{40}\text{Ar}$ ratios measured in the test gas leaving chamber A were equal to the ratios measured in the test gas before it passed through the humidifier. The results of different replicate experiments are given in Tab. 3.1. $^{20}\text{Ne}/^{22}\text{Ne}$ and $^{36}\text{Ar}/^{40}\text{Ar}$ ratios were measured at steady state in chambers A and B. For the Ne test gas in chamber A the measured isotope ratio was slightly lower than in air ($^{20}\text{Ne}/^{22}\text{Ne} = 9.80$; Ozima and Podosek, 2002), which is consistent with the findings of Pavese et al. (2005) that purified atmospheric Ne from different commercial sources tends to be enriched in ^{22}Ne . The $^{36}\text{Ar}/^{40}\text{Ar}$ ratio in the test gas in chamber A showed no fractionation relative to the $^{36}\text{Ar}/^{40}\text{Ar}$ ratio of air ($^{36}\text{Ar}/^{40}\text{Ar} = 3.384 \cdot 10^{-3}$; Ozima and Podosek, 2002). Note that for consistency with previous data measured in our noble gas laboratory we used the $^{36}\text{Ar}/^{40}\text{Ar}$ value of Ozima and Podosek (2002) (as recommended by the IUGS Subcommittee on Geochronology) rather than the more recent values reported by Lee et al. (2006) and Mark et al. (2011).

For both the $^{20}\text{Ne}/^{22}\text{Ne}$ and $^{36}\text{Ar}/^{40}\text{Ar}$ ratios the results obtained from the individual replicate gas samples agreed to within their respective standard errors. In agreement with the theory, the ratios determined were found to be independent of the thickness of the diffusive layer (Tab. 3.1). Diffusion through the diffusion cell resulted in increases of $1.0 \pm 0.3\%$ and $5.5 \pm 0.4\%$, respectively, in the experimentally observed $^{20}\text{Ne}/^{22}\text{Ne}$ and $^{36}\text{Ar}/^{40}\text{Ar}$ ratios.

Tab. 3.2 lists the fractionation factors calculated from Eq. 3.7 using the mean values of the $^{20}\text{Ne}/^{22}\text{Ne}$ and $^{36}\text{Ar}/^{40}\text{Ar}$ ratios measured in chambers A and B (Tab. 3.1) and compares the experimentally determined isotopic fractionation with the isotopic fractionation predicted by the square root relation (Eq. 3.1), by the modified square root relation

Table 3.2: Comparison of fractionation factors determined experimentally in this study with fractionation factors determined from the square root relation or molecular dynamics calculations (including standard errors; the 2σ errors reported by Bourg and Sposito (2008) were converted to 1σ errors) and from the square root relation*, treating water as if it were a gas of molecular weight 18.

	$D_{20\text{Ne}}/D_{22\text{Ne}}$	$D_{36\text{Ar}}/D_{40\text{Ar}}$
This study (from means in Tab. 1)	1.010 ± 0.003	1.055 ± 0.004
Square root relation (Eq. 3.1)	1.049	1.054
Modified square root relation* (Eq. 3.2)	1.022	1.017
Molecular dynamics (Bourg and Sposito, 2008) (Eq. 3.3)	1.014 ± 0.001	1.008 ± 0.002

(Eq. 3.2) and by the results of the molecular dynamics simulation of Bourg and Sposito (2008), see Eq. 3.3. Our experimentally determined $^{20}\text{Ne}/^{22}\text{Ne}$ fractionation factor is significantly smaller than that calculated from the square root relation (Eq. 3.1), but agrees with the predictions based on the molecular dynamics calculations (Bourg and Sposito, 2008, Eq. 3.3). In contrast to this, our experimentally determined $^{36}\text{Ar}/^{40}\text{Ar}$ fractionation factor agrees with that calculated from the square root relation (Eq. 3.1), but *not* with that based on the molecular dynamics calculations. The $^{20}\text{Ne}/^{22}\text{Ne}$ and $^{36}\text{Ar}/^{40}\text{Ar}$ fractionation factors predicted by the modified square root relation (Eq. 3.2) are inconsistent with all our experimental results.

Note that the $^{20}\text{Ne}/^{22}\text{Ne}$ and $^{36}\text{Ar}/^{40}\text{Ar}$ fractionation factors inferred from the square root relation (Eq. 3.1) are very similar, because the mass ratios of the two isotope pairs are almost the same ($20/22 \approx 0.909$ and $36/40 \approx 0.900$). This close agreement is in contrast to the difference in the fractionation behaviour of the Ne and Ar isotopes observed in our experiments. It is possible that this discrepancy results from the fact that square root relation is based on the kinetics of diffusion in gases rather than in water. We also note that for Ar, the results of the molecular dynamics calculations of Bourg and Sposito (2008) are not consistent with the experimental results of our study. As pointed out by the authors, the accuracy of the molecular dynamics calculations is limited by our knowledge of the intermolecular potential functions used in the model.

Therefore, and because the results obtained from the modified square root relation (Eq. 3.2) are also inconsistent with the experimental results, neither of the forms of the square root relation nor the molecular dynamics simulation would seem to provide an adequate, generally valid, physically sound description of the isotopic fractionation of both Ne and Ar that results from molecular diffusion in water. However, our results do provide clear evidence that the square root relation is able to describe adequately the isotopic fractionation of $^{36}\text{Ar}/^{40}\text{Ar}$. Arguments on the transport of dissolved substances in water by molecular diffusion that are based primarily on the $^{36}\text{Ar}/^{40}\text{Ar}$ ratio (e.g. Peeters et al., 2002a; Brennwald et al., 2005) therefore remain valid and can still be used to determine whether molecular diffusion controls noble gas abundances in natural water, as the assumed behaviour of the Ar isotopes is consistent with our newly determined isotopic fractionation factor.

We hypothesize that different intermolecular forces between noble gases and dipole

water molecules might explain our experimental findings. This hypothesis is supported by quantum-chemical calculations supplemented by structural parameters describing the geometry of noble gas-water complexes in liquid water (Bagno, 1998; Sun et al., 2013), with water molecules clustering around dissolved noble gases as a result of intermolecular interactions (Ludwig, 2001). Bagno (1998) found the intermolecular force between Ne and liquid water to be 40–60% lower than that between Ar and liquid water. A recent study by Sun et al. (2013) found the geometry of the Ne-(liquid)water complex to differ from the geometry of the Ar-(liquid)water, Kr-(liquid)water and Xe-(liquid)water complexes. In Ne-(liquid)water complexes, Ne is orientated away from the hydrogen bonds, implying that the internal rotation of the H₂O molecule is hindered less than in the case of Ar, Kr and Xe, which are orientated towards the hydrogen bonds. Sun et al. (2013) also found that the prevailing geometry of Ne-water complexes was almost the same for ²⁰Ne and ²²Ne, and concluded therefore that the isotopic effect on the structures of the Ne-water complex was small. These findings might establish a conceptual framework for understanding why diffusive transport through water fractionates Ne and Ar isotopes differently.

3.4 Conclusions

We empirically quantified the fractionation of ²⁰Ne/²²Ne and ³⁶Ar/⁴⁰Ar ratios in response to the molecular diffusion of Ne and Ar in water. For ²⁰Ne/²²Ne the experimentally determined fractionation factor ($D_{20\text{Ne}}/D_{22\text{Ne}} = 1.010 \pm 0.003$) agrees well with the results of the molecular dynamics calculations of Bourg and Sposito (2008) ($D_{20\text{Ne}}/D_{22\text{Ne}} = 1.014 \pm 0.001$). However, it is significantly lower than that predicted either by the square root relation, Eq. 3.1 ($D_{20\text{Ne}}/D_{22\text{Ne}} = 1.049$) or the modified square root relation with reduced masses, Eq. 3.2 ($D_{20\text{Ne}}/D_{22\text{Ne}} = 1.022$). By contrast, for ³⁶Ar/⁴⁰Ar, the experimentally determined fractionation factor ($D_{36\text{Ar}}/D_{40\text{Ar}} = 1.055 \pm 0.004$) agrees well with that predicted by the square root relation ($D_{36\text{Ar}}/D_{40\text{Ar}} = 1.054$) (implying that models relying on this relationship remain valid). However, it is significantly higher than that predicted either by the modified square root relation ($D_{36\text{Ar}}/D_{40\text{Ar}} = 1.017$) or by the molecular dynamics calculations of Bourg and Sposito (2008; $D_{36\text{Ar}}/D_{40\text{Ar}} = 1.008 \pm 0.003$).

Thus, neither the square root relation nor the molecular dynamics approach of Bourg and Sposito (2008) is capable of giving a general explanation of our experimental results for the fractionation of both ²⁰Ne/²²Ne and ³⁶Ar/⁴⁰Ar. We speculate that the different fractionation behaviour of ²⁰Ne/²²Ne and ³⁶Ar/⁴⁰Ar in water is related to intermolecular interactions between water molecules in the liquid phase and dissolved noble gases (Bagno, 1998; Sun et al., 2013). To expand our knowledge of the molecular diffusion of noble gas isotopes, we suggest measuring the isotopic fractionation resulting from diffusion for all noble gases and their isotopes in water and in other liquids with different physico-chemical properties (e.g. oils or alcohols). Despite the lack of a theoretical model that is able to explain quantitatively the fractionation factors determined in our experiments, we consider that our direct measurements provide a robust basis for studies that use the fractionation of the noble gas isotope ratios ²⁰Ne/²²Ne and ³⁶Ar/⁴⁰Ar to assess molecular diffusion in water bodies.

Chapter 4

Negligible fractionation of Kr and Xe isotopes by molecular diffusion in water

Chapt. 4 has been published as:

L. Tyroller; M. S. Brennwald; H. Busemann; C. Maden; R. Kipfer. Negligible fractionation of Kr and Xe isotopes by molecular diffusion in water. *Earth and Planetary Science Letters*, 492, 73-78 (2018). ²

Abstract Molecular diffusion is a key transport process for noble gases in water. Such diffusive transport is often thought to cause a mass-dependent fractionation of noble gas isotopes that is inversely proportional to the square root of the ratio of their atomic mass, referred to as the square root relation. Previous studies, challenged the commonly held assumption that the square root relation adequately describes the behaviour of noble gas isotopes diffusing through water. However, the effect of diffusion on noble gas isotopes has only been determined experimentally for He, Ne and Ar to date, whereas the extent of fractionation of Kr and Xe has not been measured. In the present study the fractionation of Kr and Xe isotopes diffusing through water immobilised by adding agar was quantified through measuring the respective isotope ratio after diffusing through the immobilised water. No fractionation of Kr and Xe isotopes was observed, even using high-precision noble gas analytics. These results complement our current understanding on isotopic fractionation of noble gases diffusing through water. Therefore this complete data set builds a robust basis to describe molecular diffusion of noble gases in water in a physical sound manner which is fundamental to assess the physical aspects of gas dynamics in aquatic systems.

4.1 Introduction

The inert noble gases and their isotopes have been established to trace physical processes in aquatic systems, e.g. the transport and exchange of solutes and fluids (Brennwald

²Acknowledgements: We thank Nadia Vogel for her introduction to the magnet sector field noble gas mass spectrometer built in-house at the noble gas laboratory at ETH Zürich. This work was financed by the Swiss National Science Foundation (SNF-project 200020 – 132155).

et al., 2013b). Molecular diffusion in water is a key transport mechanism that plays an important role in aquatic systems and in particular in the sediments of lakes, rivers and oceans. Despite the great potential of noble gases and their isotopes to analyse diffusive transport in lacustrine sediments, the isotopic fractionation of noble gas diffusing through water has only been studied for He, Ne and Ar (Jähne et al., 1987a; Tyroller et al., 2014). As a follow-up to our recent work on the diffusion of Ne and Ar isotopes in water (Tyroller et al., 2014), this paper assesses the possible fractionation of Kr and Xe isotopes by molecular diffusion in water. In general, the study used the same experimental set-up, analytical techniques, principles and equations as presented by Tyroller et al. (2014). The present study is motivated by the unexpected results of a computational simulation (Bourg and Sposito, 2008) and the aforementioned experimental study (Tyroller et al., 2014), both of which challenged the commonly held assumption that molecular diffusion in water results in a fractionation of noble gas isotope ratios according to the square root relation, that is also referred to as Graham’s Law (Graham, 1833). This relation is derived from the kinetic theory of gases (Moore, 1999) and can be written as (e.g. Richter et al., 2006):

$$\frac{D_i}{D_j} = \left(\frac{M_j}{M_i} \right)^\beta \quad (4.1)$$

where D_i and D_j are the diffusion coefficients of the diffusing gases i and j , with their molecular mass M_i and M_j , respectively, and $\beta = 0.5$.

However, our previous study (Tyroller et al., 2014) found a different fractionation behaviour of Ne isotopes during molecular diffusion in water. Ar isotopes do fractionate as predicted by the square root relation, in contrast to Ne isotope fractionation, which was found to be much lower and which agreed to a reasonable extent with the results from molecular dynamics calculations (Bourg and Sposito, 2008). These molecular dynamics calculations simulate the diffusion of different noble gases and their isotopes in water on an atomic scale by applying a combination of chemical theories and classical, non-quantum-mechanical theories.

In order to explain the different behaviour of Ne and Ar isotope fractionation and to understand the fractionation behaviour of other noble gas isotopes as a result of molecular diffusion in water, this study aims to complete the experimental dataset on noble gases by assessing the fractionation behaviour of Kr and Xe. The fractionation of Kr (^{82}Kr , ^{83}Kr , ^{84}Kr , ^{86}Kr) and Xe (^{129}Xe , ^{132}Xe , ^{134}Xe , ^{136}Xe) isotopes was determined by directly measuring the relative differences of fluxes of isotopes through a diffusion column containing immobilised water. In addition, the elemental diffusion coefficients of Kr and Xe were determined with the same set-up in order to confirm the correct operation of the experiment.

4.2 Material and methods

4.2.1 Experimental setup

The method used to determine the fractionation of Kr and Xe isotopes closely follows the method described in our earlier work measuring the fractionation of Ne and Ar isotopes undergoing molecular diffusion in water (Jähne et al., 1987a; Tyroller et al., 2014). In

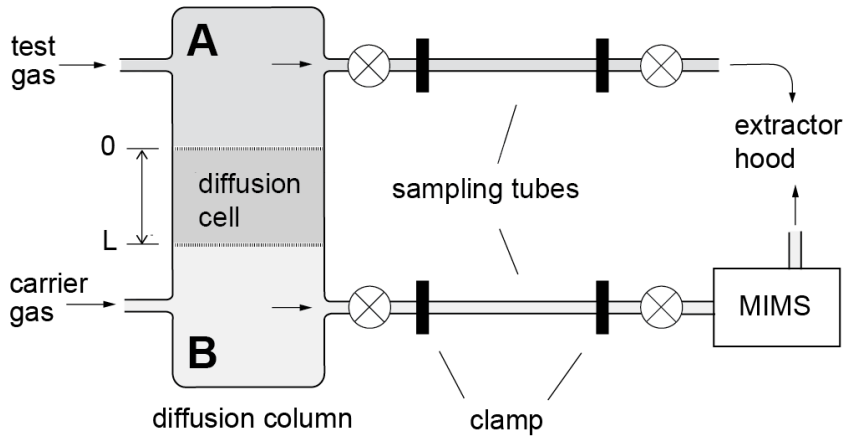


Figure 4.1: Drawing of the experimental set-up (adopted from Tyroller et al., 2014). Experimental conditions are presented in Tab. 4.1. The test gas, made up of Kr and Xe, was flushed through chamber A, while the carrier gas, pure N_2 was flushed through chamber B. After the system attained steady state, samples of both test gas and carrier gas were taken by closing the sampling copper tubes connected downstream with gas-tight clamps. As shown for Ne and Ar (Tyroller et al., 2014), the dissolved gas concentration at the gas/water interfaces can be assumed to be in solubility equilibrium.

general, the same experimental set-up, analytical techniques, principles and equations were used, with the exception of a modification in sample processing which is discussed below in some detail.

The key constituent of the experimental set-up, the diffusion column, was composed of two continuously flushed gas chambers, A and B, which were separated by a diffusion cell (Fig. 4.1). This diffusion cell consisted of an approximately 1.4 cm thick water layer which was immobilised by adding agar (1%) to suppress turbulent transport within the liquid thus guaranteeing that the gas was transported purely by molecular diffusion as in free water (Jähne et al., 1987a; Cussler, 2009). The agar-water-gel lay on a glass frit (porosity 42%).

In an initial phase, the two gas-filled chambers, A and B were both flushed with carrier gas (N_2 of 99.999% purity, Carbagas, Switzerland). Samples were taken from chambers A and B during this initial phase, and no noble gases were detected in them, even when analysing on a low-blank system (Busemann et al., 2000; Heber, 2002). The experiment was initiated by flushing chamber A with noble gas bearing test gas (consisting of 30% Kr and 30% Xe and 40% pure N_2 gas), while chamber B was still flushed with the pure, i.e. noble gas free, carrier gas. Both the test and the carrier gas were saturated with water vapour before being flushed through chambers A and B, respectively, to prevent drying of the diffusion layer. Diffusion of the test gas through the diffusion cell from chamber A to chamber B was forced by the difference in the noble gas partial pressure between A (~ 0.3 bar) and B (~ 0 bar).

The experiment consisted of two sequences with different flow regimes:

1. Non-steady state: Initially the flow regime was in non-steady state. The test-gas flux diffusing from chamber A through the water cell was carried by the nitrogen

Table 4.1: Experimental parameters and their estimated uncertainties defining the set-up of the diffusion cell. Note that the uncertainties of these parameters did not affect the measurement of isotope fractionation because the isotope ratios were determined at steady state conditions, which were independent of the experimental conditions (Tyroller et al., 2014). However, the determination of the elemental diffusion coefficients was affected by the experimental design of our diffusion experiment. Thus, the uncertainty of the elemental diffusion coefficients was constrained mainly by the errors of the design of the diffusion cell.

Experimental parameter	Range	Absolute uncertainty
Thickness of the diffusion cell with agar-water-gel [cm]	1.4	0.1
Agar-water-gel/gas interface area [cm ²]	28.3	0.1
Temperature [K]	296.0	0.5
Flow rate, carrier gas [ml/min]	2.5	0.1
Kr concentration in the agar-water-gel [$\times 10^{-2} \frac{cc}{g}$]	1.62	
Xe concentration in the agar-water-gel [$\times 10^{-2} \frac{cc}{g}$]	2.83	

gas flushed through chamber B to a quadrupole mass spectrometer operated in dynamic mode (miniRUEDI, Gasometrix GmbH, Mächler et al., 2012; Brennwald et al., 2016). The miniRUEDI measurements allowed the gas flow to be continuously monitored (measuring He, Ar, Kr, Xe, N₂ and O₂ concentrations; with mass/charge ratio 84 m/z for Kr and 130 for Xe) to assess the performance of the experimental apparatus. The measurements also determined the time when the gas flux through the diffusion cell attained steady state. This gas specific breakthrough curves were also used to determine the elemental diffusion coefficients of Kr and Xe.

2. Steady state: When the gas composition of the outflow from chamber B became constant, the flow regime was in a steady state. This steady state flow was reached after waiting for at least three times the typical breakthrough time, T , of the respective gas (see Sect. 4.3). In steady state the isotopic fractionation factor for two isotopes i and j can be expressed as the ratio of their diffusion rates or as the ratio of their diffusion coefficients (i.e. D_i and D_j) and can be determined by applying the following formula:

$$\frac{R_{i,j}^L}{R_{i,j}^0} = \frac{F_i/F_j}{C_i(0)/C_j(0)} = \frac{D_i}{D_j} \quad (4.2)$$

Where $R_{i,j}^0 = C_i(0)/C_j(0)$ is the concentration ratio at the upper interface of the diffusion cell ($x = 0$) with $C_i(0)$ and $C_j(0)$ being the concentrations of the isotopes i and j respectively, measured in the outflow of chamber A. And $R_{i,j}^L = C_i(L)/C_j(L) = F_i/F_j$ is the flux ratio at the lower interface of the diffusion cell ($x = L$) with $C_i(L)$ and $C_j(L)$ being the isotope concentrations measured in the outflow of chamber B. Once the experiment was operating in steady state gas, samples were taken from the outflow of chamber A and B respectively and stored in copper tubes for later analysis of noble gas isotopes with noble gas mass spectrometry. For further details on the set-up, the experimental principles and

the applied mathematics used to calculate isotopic fractionation refer to the previous work on Ne and Ar fractionation (Tyroller et al., 2014).

For the analysis of Kr and Xe isotopes, unlike the study on Ne and Ar isotope fractionation, the final sample of gas taken and stored in copper tubes had to be diluted by several orders of magnitude because the final isotope analysis was carried out with a mass spectrometer designed for high accuracy and high-sensitivity analysis of Kr and Xe isotopes. This was operated in static mode at very low pressures ($< 10^{-9}$ mbar; Busemann et al., 2000; Heber, 2002). Dilution was carried out with a gas calibration apparatus designed to reach exact concentrations even when diluting noble gases over several orders of magnitude down to a pressure range that allowed analysis with the highly-sensitive, static noble gas mass spectrometer. The dilution procedure and dilution apparatus are described in Sect. 4.2.3.

4.2.2 Determination of diffusion coefficients

In principle, the set-up of the diffusion column can be used to determine diffusion coefficients in a quantitative manner (Saltzman et al., 1993). Here, the target of the experiments was to make specific determinations of the fractionation behaviour of Kr and Xe isotopes. Thus, the experiment was not designed to obtain elemental diffusion coefficients, but to identify possible isotopic fractionation within a single experiment (see Tab. 4.1). As a result, it was decided to use normalised noble gas breakthrough curves (see Fig. 4.3), obtained in order to evaluate when the flow regime in the diffusion cell was in the steady state. As a by-product of this procedure the elemental diffusion coefficients were determined, but not in a rigorously quantitative manner. A theoretical breakthrough curve for this experimental set-up was calculated (Tyroller et al., 2014) and was fitted to the observed breakthrough curve by using the respective diffusion coefficient as fit parameter.

4.2.3 Gas dilution

For gas dilution, a gas-calibration apparatus built in-house at the noble gas laboratory at ETH Zürich was used. This special gas line was designed to prepare precisely known noble gas mixtures as standards in order to normalise noble gas mass spectrometry. It is also possible to determine the exact volumes of reservoirs and pipettes on it. The partial pressure of the test gas in the copper tube samples taken during the diffusion experiment were reasonably well known (chamber A: 0.3 bar Kr and Xe according manufacturer’s instructions; chamber B: in the range of 10^{-6} bar according to miniRUEDI analysis). For the high-precision Kr and Xe analysis using static noble gas mass spectrometry, the gas partial pressures had to be reduced to minimum 10^{-12} bar. Samples were diluted according to a systematic dilution plan to reach the predefined gas pressure needed for the final analysis. The dilution plan defines the sequence of steps needed to expand the initial quantity of gas into the dilution volumes based on the initial partial pressure of gas in the precisely calibrated volume P_g (see Fig. 4.2). In the final step, the sample reservoir, V_R , was filled. Later an adequate gas aliquot could be taken from this reservoir using the pipette P_x . Each sample was treated according its specific dilution plan. The gas-filled copper tube from the diffusion experiment was connected to the dilution gas line (initial valve setting: T1-T5, T7-T9, T11, R1, R2 open, T6, T10 closed) and the gas

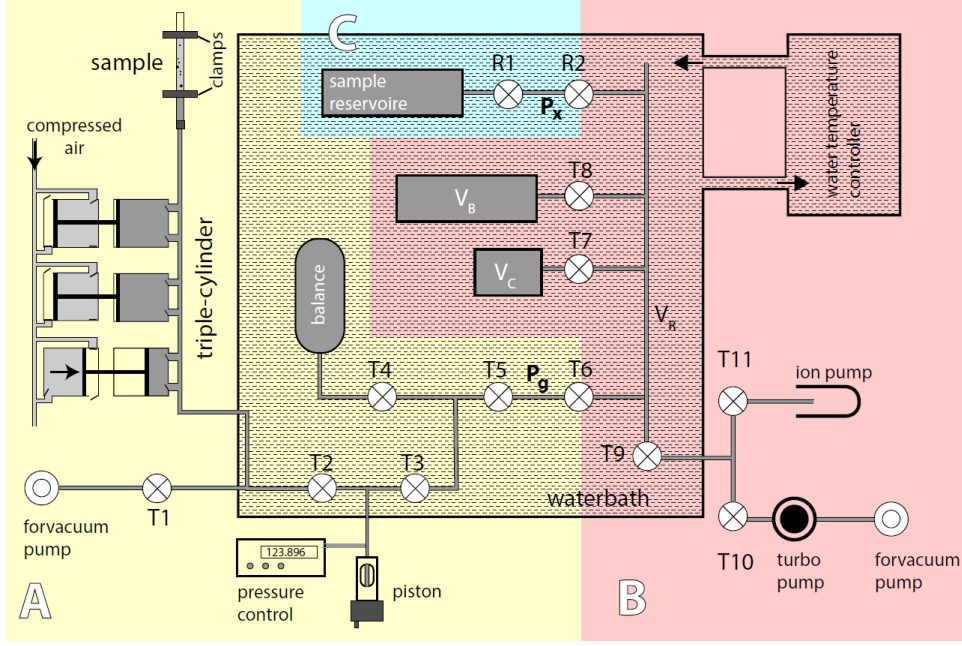


Figure 4.2: An apparatus designed to prepare noble gas standards at the ETH noble gas laboratory was used to dilute the gas. It consisted of three parts: A, B and C. **A. The gas line (yellow) was used to fill a defined gas amount into pipette P_g with an exactly known volume.** This part consisted of an adaptor for copper tube samples (swagelok fitting), a roughing pump, to evacuate the gas line to $\sim 5 \times 10^{-3}$ mbar before the gas inlet, a piston for fine adjustment of the pressure, a balance volume and a triple cylinder. This triple cylinder system was made of three segments each consisting of a double-actuation compressed air piston connected at the left to the end of flexi-bellows. By opening or closing the respective valves of the piston, the volume within the flexi-bellow could be changed. By moving the pistons of the triple cylinder in combination, gas could be compressed and expanded, thus enabling the pressure in the line to be adjusted. The triple cylinder was used to reach a defined pressure (measured by a calibrated, high precision manometer) in the gas line and volume P_g . Volume P_g (0.957845 ± 0.000811 cm³) was the inlet to the dilution line. **B. The dilution line (red) was used to dilute the defined gas amount in P_g by several orders of magnitude.** The dilution line consisted of a roughing pump, a turbo pump and an ion getter pump. These pumps evacuated the dilution compartments, the tubing V_T (59.331 cm³), the dilution volumes V_C (384.11 cm³), V_B (2006.776 cm³) and the reservoir, V_R , to a pressure of $\sim 10^{-7}$ mbar before noble gas dilution. Dilution factors were calculated from the known volumes of the dilution compartments. **C. The reservoir (blue) was filled with the diluted gas from the gas line.** For each sample to be diluted, a new reservoir with pipette was attached and pumped prior to being filled with gas. After being filled with the gas at low pressure the reservoir and its pipette, P_x , were disconnected from the dilution apparatus and connected to a mass spectrometer for the isotope ratio analysis. The volume of the pipette, P_x , was very small relative to the sample reservoir. As a result, the pipette could be filled repeatedly with the gas from the reservoir, i.e. gas aliquots could be taken from the reservoir, with virtually no effect on the amount of gas contained in the reservoir. All fittings, valves and tubing were ultra high vacuum-tight and made of stainless steel. Parts of the gas line, the dilution line and the reservoir are submerged in a water bath to keep the temperature and pressure constant and uniformly distributed during dilution.

filling apparatus was pumped in order to reach a pressure in the range of 10^{-3} to 10^{-4} mbar in the gas line and a pressure of approximately 10^{-7} mbar within the dilution line. After evacuation, the gas dilution line was set for the sample gas inlet (T1-T11 closed) and the copper tube sample containing the gas from the diffusion experiment was opened. The sample gas was then expanded to the inlet of the gas dilution line by means of the triple cylinders. These triple cylinders were manipulated until the pre-set pressure in the inlet pipette, P_g , was reached. The gas was left for 30 minutes to equilibrate within the line. P_g was then disconnected from the inlet line by closing valve T5 and the amount of gas in P_g was subsequently expanded into the dilution line (valve T6 open) and diluted according the dilution plan. Each dilution step consisted of opening the valve of the respective dilution volumes (V_B , V_C) and waiting for approximately 30 minutes to allow the pressure in the respective volumes to equilibrate. The respective dilution reservoir was then closed and the residual gas was pumped out from the dilution line. In the last dilution step, the remaining gas was allowed to expand into the gas reservoir, V_R , and was separated by closing the valves of its pipette, P_x (R1, R2 closed).

The closed reservoir, V_R , and its pipette, P_x , were detached from the gas dilution line and connected to the noble gas spectrometer for final isotope analysis. In this way, V_R was used as a gas reservoir from which precise gas aliquots could be taken through the gas pipette, P_x , allowing multiple measurements of the isotopic composition of Kr and Xe from the sample gas.

4.2.4 Analysis of noble gas isotopes

The measurements of Kr and Xe isotopes from the gas sample in the reservoir were carried out on a magnet sector field noble gas mass spectrometer built in-house at the noble gas laboratory at ETH Zürich (e.g. Busemann et al., 2000; Heber, 2002). The mass spectrometer was equipped with a Baur-Signer ion source, a Faraday cup and a secondary electron multiplier (operated in counting mode). Kr and Xe were ionised with 100 eV electrons, whereby isotopes were easily separated by the achievable mass resolution of about 100 ($M/\Delta M$) (Busemann et al., 2000; Heber, 2002).

4.3 Results

Fig. 4.3 shows the observed and the theoretical breakthrough curves of the test gas diffusing through the water cell (see Sect. 4.2.2) normalised to the steady state concentration of Kr and Xe. The observed and the fitted breakthrough curves agree with each other. As a by-product of the measurements, the elemental diffusion coefficients of Kr and Xe were estimated.

Tab. 4.2 summarises the results of the different replicate gas dilution experiments and analyses to determine the relative isotopic fractionation of Kr and Xe due to diffusion in water. Note that the replicated experiments comprise four independent diffusion experiments that were carried out under the same conditions and using the same experimental set-up and experimental parameters. Each independent experiment included a renewal of the dilution cell, the flushing of the system with carrier gas before starting the experiment and observation of the breakthrough curve until steady state was achieved. Thus, the diffusion experiments were repeated four times. The isotopic compositions of

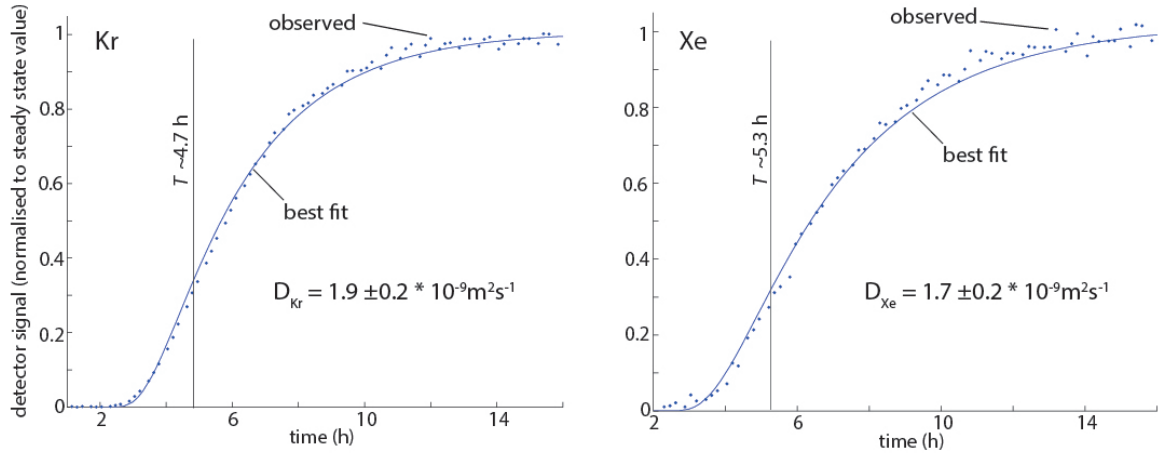


Figure 4.3: Breakthrough curves of Kr and Xe measured with miniRUEDI, uncalibrated raw data normalised to the steady state value obtained towards the end of the experiment. Dots indicate "observed" data, measured in the outlet of chamber B with a quadrupole mass spectrometer. The blue curve shown is the theoretical breakthrough curve fitted by adjusting the diffusion coefficient. The breakthrough time T was defined as $T = \frac{L^2}{6D_i}$ (Crank, 1975) where L indicates the thickness of the diffusion cell and D_i the diffusion coefficient of the respective gas species i .

Kr and Xe (i.e. the respective isotope ratios in chambers A and B) were measured in gas samples taken after the steady state was attained in chambers A and B. Note also that under such steady state conditions the relative isotopic fraction due to molecular diffusion can simply be calculated from the ratio of the respective isotope ratios in chamber A ("unfractionated") and chamber B ("fractionated"; see also the experimental set-up Fig. 4.1).

4.4 Discussion

The good agreement of the observed and the fitted breakthrough curves of Kr and Xe (see Fig. 4.3) suggests that our diffusion experiment performed well. Furthermore, the calculated elemental diffusion coefficients for Kr and Xe agree with some of the previous results to a reasonable extent (see Tab. 4.3).

Our experimental data (Tab. 4.2) make the case that Kr and Xe isotopes do not significantly fractionate during molecular diffusion through liquid water. In addition our results reject the hypothesis that Kr and Xe isotopes fractionate according to the square root relation (continuous line in Fig. 4.4). The results show that the isotope fractionation for Kr and Xe was much smaller than predicted by the square root relation. In contrast, these results are consistent with the assumption of negligible fractionation, i.e. molecular diffusion in water virtually does not fractionate either the Kr or Xe isotopes. To determine conclusively whether Kr and Xe isotopes do slightly fractionate when diffusing through water, additional experiments are needed achieving a much better experimental precision than our experiment.

As with earlier studies (Bourg and Sposito, 2008; Tyroller et al., 2014) this work

Table 4.2: Four independent experiments were carried out to determine the possible fractionation of Kr and Xe isotopes due to molecular diffusion in water. The ratios of Kr and Xe isotopes were determined 5 to 7 times for each sample from a corresponding experiment (typical errors of the measured ratios were in a range of 0.3 - 0.5 %). The fractionation factors were determined by dividing the isotope ratio of the "fractionated" sample through the ratio of the "unfractionated" sample, see text.

	$\frac{D_{86\text{Kr}}}{D_{84\text{Kr}}}$	$\frac{D_{83\text{Kr}}}{D_{84\text{Kr}}}$	$\frac{D_{82\text{Kr}}}{D_{84\text{Kr}}}$	
exp. 1	0.9950	0.9997	1.0000	
exp. 2	0.9949	1.0028	0.9979	
exp. 3	1.0040	1.0159	1.0035	
exp. 4	0.9920	0.9913	1.0006	
Mean, error of the mean:	0.9965 ± 0.0026	1.0024 ± 0.0051	1.0005 ± 0.0012	

	$\frac{D_{136\text{Xe}}}{D_{132\text{Xe}}}$	$\frac{D_{134\text{Xe}}}{D_{132\text{Xe}}}$	$\frac{D_{131\text{Xe}}}{D_{132\text{Xe}}}$	$\frac{D_{129\text{Xe}}}{D_{132\text{Xe}}}$
exp. 1	1.0008	1.0031	1.0018	0.9953
exp. 2	1.0001	1.0002	0.9997	0.9982
exp. 3	0.9999	1.0028	0.9989	1.0015
exp. 4	0.9964	0.9995	1.0006	0.9990
Mean, error of the mean:	0.9993 ± 0.0010	1.0014 ± 0.0009	1.0003 ± 0.0006	0.9985 ± 0.0013

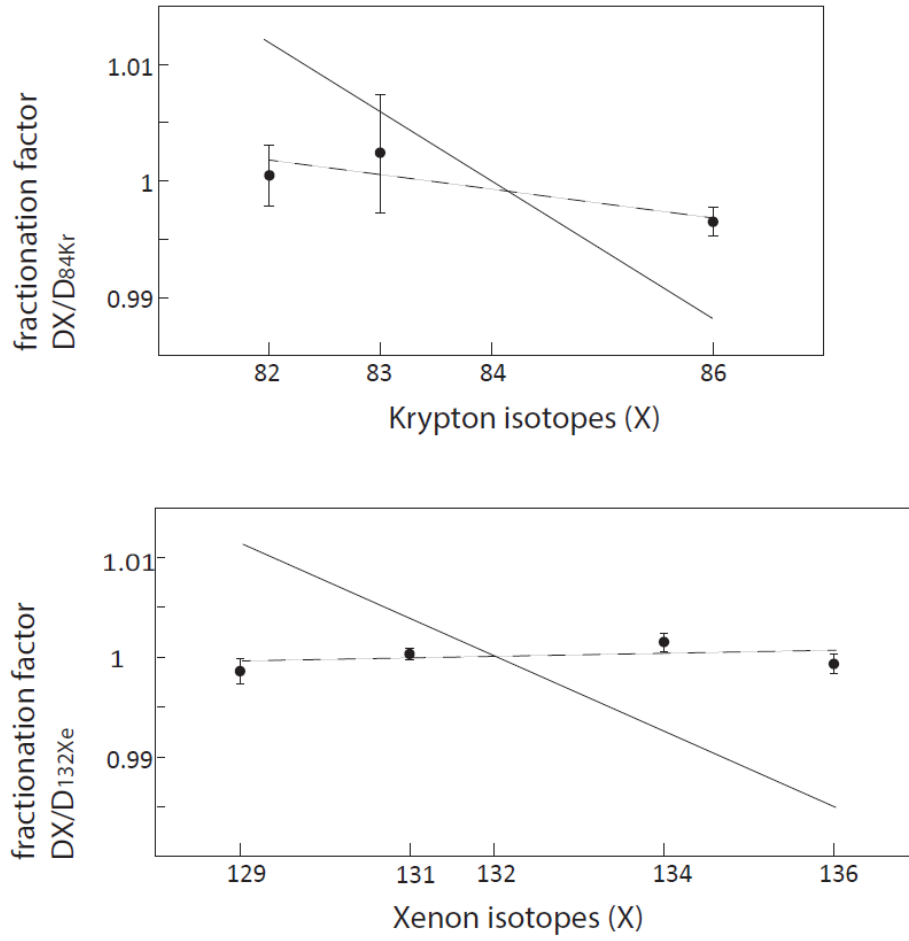


Figure 4.4: Experimentally determined fractionation of Kr and Xe isotopes (normalised to ^{84}Kr and ^{132}Xe , respectively) due to molecular diffusion in water. The continuous line reflects the expected fractionation according to the square root relation. The dashed line reflects the linear least squares regression through the experimental data.

Table 4.3: Comparison of literature values for the diffusion coefficients of Kr and Xe in water and results of this study. The diffusion coefficients of Kr and Xe determined in this study are the mean value of the diffusion coefficients determined with the best fit to the observed breakthrough curve of two experiments (see Fig. 4.3), the errors are given at the 1 sigma level. The breakthrough curves of the other experiments were not suitable for such fitting because recording of the data started later approximately at half time of the breakthrough of the gas. We note that in the light of our results the higher diffusion coefficients of Kr and Xe reported in literature seem to be more robust.

Experimental determination				MD simulation	This study
Wise and Houghton (1968)	Boerboom and Kleyn (1969)	Jähne et al. (1987a) (0.5% agar)		Bourg and Sposito (2008)	(1% agar)
D_i [$10^{-9}m^2s^{-1}$], (T = 298 K)					
D_{Kr}	1.93 *	0.803	1.84	1.97 ± 0.13	1.9 ± 0.2
D_{Xe}	0.6 *	0.827	1.47	1.57 ± 0.11	1.7 ± 0.2

*scaled to 25°C temperature

also challenges the applicability of the square root relation to scale the fractionation of noble gas isotopes undergoing molecular diffusion in water. For Ne, Kr and Xe, the fractionation of their isotopes as a result of molecular diffusion was found to be much smaller than predicted by the square root relation, whereas Ar was shown to fractionate according to the square root relation.

Currently, we do not have a clear explanation for the different isotopic fractionation patterns of atmospheric noble gases (Ne - Xe) diffusing in water. We hypothesise that factors other than molecular mass, such as the interaction of noble gas isotopes with the microstructure of liquid water, may constrain the different fractionation patterns of noble gas isotopes undergoing molecular diffusion in water.

A recent study on isotopic fractionation, using ab initio molecular dynamics (AIMD) to simulate dissolved gas species and the surrounding liquid, supports this hypothesis by showing the importance of configurational effects on isotopic fractionation (de Magalhães et al., 2017). This study shows that noble gases interact with the water molecules during diffusion, which results in different diffusion regimes. For small particles (Ne) inter-cavity hopping is the dominant transport mechanism, whereas for large particles (Kr, Xe) the transport is dominated by mass-independent viscous friction (see de Magalhães et al., 2017). Over long enough time scales neither transport mechanisms lead to a fractionation of the isotope ratio. However, Ar falls in between these two diffusion regimes, where the molecular collision with the surrounding water molecules prevails. This may explain the different isotope fractionation of Ar due to molecular diffusion in water.

4.5 Conclusions

We empirically quantified the elemental diffusion coefficients of Kr and Xe isotopes in water as well as the respective isotope fractionation in response to molecular diffusion in water. The estimated elemental diffusion coefficients of Kr ($D_{Kr} = 1.9 \pm 0.2 \times 10^{-9} m^2 s^{-1}$) and Xe ($D_{Xe} = 1.7 \pm 0.2 \times 10^{-9} m^2 s^{-1}$) in water agree reasonably well with preceding studies. This suggests that our diffusion experiment using a diffusive layer of immobilised water performed well.

Kr and Xe isotopes were found to only negligibly fractionate within the precision of our measurements. The determined fractionation was much smaller than the fractionation predicted by the square root relation for Kr and Xe isotopes diffusing through water. Thus, our results clearly contradict the commonly held assumption that the fractionation of Kr and Xe isotopes due to molecular diffusion in water can be approximated by the square root relation. These findings were confirmed by recent AIMD simulations where the fractionation of Kr and Xe isotopes as a result of molecular diffusion in water was also found to be negligible. This was attributed to a hydrodynamically controlled diffusion regime (Brownian motion, see de Magalhães et al., 2017).

To gain a conceptual understanding of the mechanism behind diffusive transport through water we suggest using different experimental approaches to measure the isotopic fractionation of all noble gases undergoing molecular diffusion in water. We expect that AIMD calculations accounting for the quantum-mechanical interactions of the electronic structure of the noble gases and the water molecules may reveal the fundamental mechanisms behind the fractionation behaviour of noble gas isotopes due to molecular diffusion in water. In addition we suggest to measure the isotopic fractionation of oxygen isotopes in water, because oxygen is of a similar size as Ar and therefore may also be fractionated due to molecular diffusion in water.

Chapter 5

Improved method for the quantification of methane concentrations in unconsolidated lake sediments

Chapt. 5 has been published as:

L. Tyroller; Y. Tomonaga; M.S. Brennwald; C. Ndayisaba; S. Naehrer; C. Schubert; R. P. North and R. Kipfer. Improved method for the quantification of methane concentrations in unconsolidated lake sediments. *Environmental Science and Technology*, 50(13), 7047-7055 (2016). ³

Abstract There is conclusive evidence that the methods most commonly used to sample methane (CH_4) dissolved in pore water of lake sediments produce results that are likely to be affected by gas loss or gas exchange with the atmosphere. To determine the in situ amount of CH_4 per unit mass of pore water in sediments, we developed and validated a new method, that combines techniques developed for noble gas analysis in pore waters with a standard headspace technique to quantify the CH_4 present in the pore space in dissolved and gaseous form. The method was tested at two sites: Lake Lungern, where CH_4 concentrations were close to saturation; and Lake Rotsee, where CH_4 concentrations are known to exceed saturation, and where CH_4 bubble formation and gas ebullition are commonly observed. We demonstrate that the new method, in contrast to the available methods, more reliably captures the total amount of CH_4 per unit mass of pore water consisting of both dissolved and free CH_4 (i.e. gas bubbles) in the pore space of the sediment.

³Acknowledgements: We would like to thank Alfred Lück for determining the sedimentation rate in Lake Rotsee and Serge Robert for contributing the SSM results for 2014. This study is dedicated to the memory of Gijs Nobbe who helped to run the first analysis in 2011 with great dedication. We also appreciate the constructive input of three anonymous reviewers, which greatly helped to improve our manuscript. The study was mainly funded by the Swiss National Science Foundation (SNF Grants 200020-132155 and 200021-124981). Further funding was provided by the European Union project Hypox - In situ monitoring of oxygen depletion in hypoxic ecosystems of coastal and open seas and land-locked water bodies (EC Grant 226213), a Marie Curie International Outgoing Fellowship (Contract No. PIOF-GA-2012-332404, Project NoGOS), and the European Cooperation in the Field of Scientific and Technical Research (COST) Actions ES0902 (Swiss State Secretariat for Education and Research, Project SBF C11.0029) and ES1301 and by Eawag, the Swiss Federal Institute of Aquatic Science and Technology.

5.1 Introduction

Methane (CH_4) in the atmosphere acts as a potent greenhouse gas (Forster et al., 2007). Inland waters (Kirschke, 2013) are one of its many sources, particularly microbiological production in eutrophic lakes (Lovley and Klug, 1982; Sobek et al., 2009). Anthropogenically induced eutrophication currently affects inland waters (lakes, reservoirs, ponds and rivers) on a global scale (Smith, 2003; Søndergaard et al., 2007; Downing et al., 2008), together with increasing CH_4 production (Sobek et al., 2012), which has recently been identified as relevant for the global carbon budget (Cole et al., 2007; Battin et al., 2009; Downing, 2010; Ortiz-Llorente and Alvarez-Cobelas, 2012). Taking into account that sediments are the main zone of CH_4 production in lakes and rivers (Bastviken et al., 2008), quantifying the real amount present in sediment pore water is vital for an understanding of its impact on aquatic systems and its relevance for climate change (Bastviken et al., 2004, 2008).

A method that can accurately determine the spatial and temporal distribution of CH_4 amounts in the sediment pore space is required in order to quantify the CH_4 budget in lake sediments. The central experimental challenge, applying commonly used methods for the analysis of CH_4 concentrations in the pore water of (lacustrine) sediments, is that CH_4 occurs in both dissolved and free gaseous form (e.g. as bubbles, Adams, 1994). In this paper, we refer to the sum of both the in situ dissolved CH_4 concentration plus the amount of CH_4 present in gaseous form as the total amount of CH_4 per unit mass of pore water (i.e. “ CH_4 -TAMP”). CH_4 bubbles are formed in the lacustrine sediment when methane concentrations exceed the CH_4 in situ saturation concentration (i.e. supersaturation) in the pore water (Boudreau et al., 2005). Causes for this CH_4 supersaturation are CH_4 production by microorganisms within the sediment and hydrostatic pressure decrease during reservoir drawdown (Joyce and Jewell, 2003).

In aquatic systems characterised by active bubble emission from the sediments, CH_4 amounts are expected to exceed the in situ saturation concentration in the pore water. However, conventional methods for CH_4 analysis are often subject to gas loss and fail to adequately determine CH_4 -TAMP expected in such systems (Del Sontro et al., 2010; Sobek et al., 2012; Corella et al., 2014). Using conventional methods attempting to determine CH_4 -TAMP in lacustrine sediments (for a review see Adams, 1994), samples are collected either (1) from the recovered cores or (2) by in situ devices (Adams, 1994), as discussed below.

1. In recovered sediment cores, CH_4 -TAMP is usually determined by using a tipless syringe to sub-core the sediment core at previously-defined sampling ports along the core liner (syringe standard method “SSM”). The extracted bulk sediment is transferred by the tipless syringe into a glass vial, which is closed with a septum for subsequent headspace analysis (Adams, 1994; Hoehler et al., 1994; Popp et al., 1995; Jørgensen et al., 2001; Schubert et al., 2010; Sobek et al., 2012; Sollberger et al., 2014). During this transfer, the sediment is normally exposed to air for about two seconds, resulting in secondary gas exchange, i.e. CH_4 loss from the sample (Hoehler et al., 1994). Such CH_4 loss is estimated to range from 2 to 31% during transfer of the sediment from the core to a sample vial by a syringe, when applying the SSM method to bulk sediment containing numerous bubbles (Adams, 1994). Although being known to be subject to gas loss, the SSM method is commonly used to quan-

tify CH₄ concentrations in the sediment pore water of lakes and oceans (Adams, 1994; Hoehler et al., 1994; Popp et al., 1995; Jørgensen et al., 2001; Schubert et al., 2010; Sobek et al., 2012; Sollberger et al., 2014). As a result, the concentrations reported in such studies are conceived to be biased. For example, sediment samples from a study using the SSM method at Lake Wohlen, where an active CH₄ bubble emission to the atmosphere was demonstrated (Del Sontro et al., 2010), showed CH₄ concentrations that were significantly lower than respective in situ saturation concentration (Sobek et al., 2012). Another example is the application of the SSM method at Lake Geneva at locations where bubbles were abundant and visible in the sediment core (Corella et al., 2014): “Ebullition was observed at several [...] coring locations but supersaturation of CH₄, which is needed for bubble formation (Boudreau et al., 2005), was not reached in most of the cores [...]” (Sollberger et al., 2014). While the authors suggest that this undersaturation is explained by the heterogeneity of the sediment, we hypothesize that it might be the result of gas loss during the sampling procedure. The amounts of CH₄ in the pore water of Lake Rotsee have been investigated in studies applying different methods, one study applied the dialyzer method (see below), whereas the others applied the SSM method (Falz et al., 1999; Schubert et al., 2010; Naecher et al., 2012, 2014). The results determined by the SSM method (0.7 - 5.9 mM CH₄) always showed concentrations lower than in situ saturation concentration and were an order of magnitude lower than the CH₄-TAMP determined by the dialyzer method (20 - 40 mM CH₄) (Falz et al., 1999). To conclude, in productive sediments with obvious CH₄ supersaturation, the concentrations determined by the SSM method are severely biased toward lower concentrations. This is mainly explained by secondary gas exchange during SSM sampling, resulting in gas loss. Therefore, the SSM method is not an appropriate method to quantify the true CH₄-TAMP in unconsolidated sediments of lakes (and oceans). Nevertheless the SSM method is frequently applied (Adams, 1994; Hoehler et al., 1994; Popp et al., 1995; Jørgensen et al., 2001; Schubert et al., 2010; Sobek et al., 2012; Sollberger et al., 2014).

2. Another method commonly applied for in situ sampling is the peeper or dialyzer method (Dyck and Da Silva, 1981; Adams, 1994; Stephenson et al., 1994). According to this method, a plexiglas plate with water-filled chambers covered by a dialysis membrane (Adams, 1994) is inserted into the sediment. The plate is left in the sediment for 1 - 3 weeks until the equilibrium between the pore water and the water in the chambers is attained. After the plate has been retrieved, the water in the chambers is sampled by piercing the membrane with a syringe. Diffusion of gases through the membrane during retrieval of the dialyzer plate and gas exchange with the atmosphere when piercing the membrane of the dialyzer compartments can result in gas loss (Adams, 1994). In addition, the method is time consuming and the degree of equilibration is often uncertain, as it depends on the sediment porosity, which may not be known. And again, the determined CH₄-TAMPs tend to be biased toward lower values (Adams, 1994). Peeper methods appear to be inappropriate for quantitatively capturing poorly soluble species, as indicated by the comparison of CH₄-TAMPs obtained from peepers and squeezing technique for the determination of total methane in the sediment (Adams and Van Eck, 1988). Further disadvantages are the high expenses and high amounts of work associated

with setting and collecting of the dialyzer plates. If dialyzer plates are used to sample gas-rich sediments at great depths, the membranes can break as a result of degassing during retrieval (Stephenson et al., 1994).

In order to reliably quantify the real, in-situ CH_4 -TAMP in lacustrine sediments, we propose an adaptation of a method that has been developed to sample and analyse noble gases in the pore water of unconsolidated sediments (Brennwald et al., 2003; Tomonaga et al., 2011a). Noble gas concentrations in the sediment pore water provide information on transport and gas exchange processes within the sediment and were used to reconstruct past climatic conditions and to quantify CH_4 ebullition (Kipfer et al., 2002; Brennwald et al., 2005, 2013b). The method for noble gas analysis in lacustrine sediments has been shown to prevent degassing and atmospheric contamination artefacts during sampling (Brennwald et al., 2003; Tomonaga et al., 2011a; Brennwald et al., 2013b) and thus might allow the unbiased assessment of the CH_4 -TAMP of unconsolidated sediments in rivers, lakes and oceans. We tested the new method in a laboratory experiment and at two Swiss lakes: (1) Lake Lungern, where CH_4 -TAMPs throughout the sediment core are expected to agree with the in situ saturation concentration; and (2) Lake Rotsee, where the pore water of the sediment is significantly supersaturated with CH_4 and where bubbles are visible in sediment cores.

5.2 Experimental methods and procedures

5.2.1 Methods

To determine CH_4 concentrations in the pore water of sediments, the sampling method commonly used for the measurement of noble gases in the pore water of unconsolidated sediments (Brennwald et al., 2003; Tomonaga et al., 2011a) was combined with a standard headspace technique (Kampbell et al., 1989). Important features of this combined method, the copper tube centrifugation (“CTC”) method include the separation of pore fluids from the sediment by centrifugation and storage of the pore water in a copper tube, prior to analysis.

Copper tube centrifugation method

Pore water samples for CH_4 analysis were acquired according to the sampling protocol developed and optimised for noble gas analysis in lacustrine sediments (Brennwald et al., 2003; Tomonaga et al., 2011a). The sediment cores were collected using a gravity corer and a plastic liner, where holes (or sampling ports) were drilled along the liner. Threads were carved in these sampling ports allowing the later connection to modified Swagelok-fittings (SS-600-1-6BT). Prior to coring the sampling ports were sealed by adhesive tape. Immediately after core retrieval (within a few to 30 min after core retrieval), each sediment core was placed in a horizontal position to prevent the vertical migration and loss of bubbles formed in the core during sampling. Copper tubes (30 cm length, ≈ 1 cm diameter) with modified Swagelok-fittings were then attached to the pre-drilled sample ports of the liner by piercing the adhesive tape. For more details regarding sediment core retrieval and sampling refer to Brennwald et al. (2003). Subsequently, the sediment in the liner was pressurised by two pistons inserted into each end of the core. Such pressurising

minimises and counteracts the bubble formation that arises from degassing as a result of increased temperatures and the equilibration of the core with ambient pressure. The pistons were pushed into the liner to increase the pressure acting on the sediment within the liner. Pressure is augmented until pushing the bulk sediment through the ports into the attached sample containers, i.e. copper tubes. This squeezing results in a displacement of the sediment in the liner, which reduces the spatial resolution of the sampling depth. After adequate flushing and optical observation that sediments was pushed through the copper tube, the copper tubes were made airtight using two stainless steel pinch-off clamps (see Fig. 5.1, Panel A), the same as those used for sampling noble gases dissolved in lake and groundwater (Kipfer, 1991; Beyerle et al., 2000). We note that sandy or other coarse sediments where grain size is similar with the diameter of the copper tube, severely constrains sampling. Subsequently the closed copper tubes were split into two aliquots by adding and closing additional pinch-off clamps. The two aliquots of each sample were centrifuged. The first aliquot was used to determine the geometrical position of the sediment/water interface within the copper tube. According to this position (~ 3 cm next to the pinch-off clamp in the up position during centrifugation), an additional pinch-off clamp was placed on the remaining aliquot to separate the pure pore water from the compressed sediment matrix (Tomonaga et al., 2011a).

While the previously described steps of sample processing are the same as in case of processing sediment samples for noble gas analysis (for details see Tomonaga et al., 2011a), in the following the processing of the sediment samples for methane analysis differs to the processing of sediment samples for noble gas analysis (Beyerle et al., 2000; Brennwald et al., 2003; Tomonaga et al., 2011a). The aliquot samples were treated twice in an ultrasonic bath for 15 minutes each time (i.e. before centrifugation and after separation of the pure pore water). Treatment in the ultrasonic bath has two purposes: it loosens the sediment matrix (e.g. improves the compressibility of the sediment) and suppresses bacterial activity (Ince and Belen, 2001) in the water phase (refer to Fig. 5.1, Panel B, step 1). The storage of the pore water in the copper tube constrains bacterial growth (Sarsan, 2013). To further reduce bacterial activity, the samples were kept at $+3$ °C and were processed immediately after sediment sampling. If analysis could not be carried out within a few days after sampling, the samples were frozen and stored at -20 °C to inhibit biological activity.

For the final gas chromatographic (GC) analysis, the gas content within the sample was extracted using a common headspace technique. For this purpose, an additional copper tube segment with a septum was attached to build a headspace of about 8 mL. One end of this additional copper tube segment was connected to the pore water sample using a Swagelok SS-600-6 fitting (Fig. 5.1, Panel B, step 2). The other end was sealed airtight with a Swagelok SS-8-VCO-6-600 fitting and a Swagelok SS-8-VCO-4 female nut holding a 3.4-mm-thick PTFE septum (Infochroma G074-SK32FW02) tailored to fit into the connector. The headspace was filled with pure nitrogen (N_2) before opening the sample towards the headspace. To this end, the copper tube segment (headspace) was evacuated and flushed with pure N_2 three times (Fig. 5.1, Panel B, steps 3 and 4) and finally left filled with N_2 at atmospheric pressure. The pinch-off clamp separating the pore water sample from the headspace was then opened. To equilibrate the headspace with the pore water, the sample was shaken for 3 minutes by hand (Fig. 5.1, Panel B, step 5). The sample gas was extracted from the headspace (Fig. 5.1, Panel B, step



B

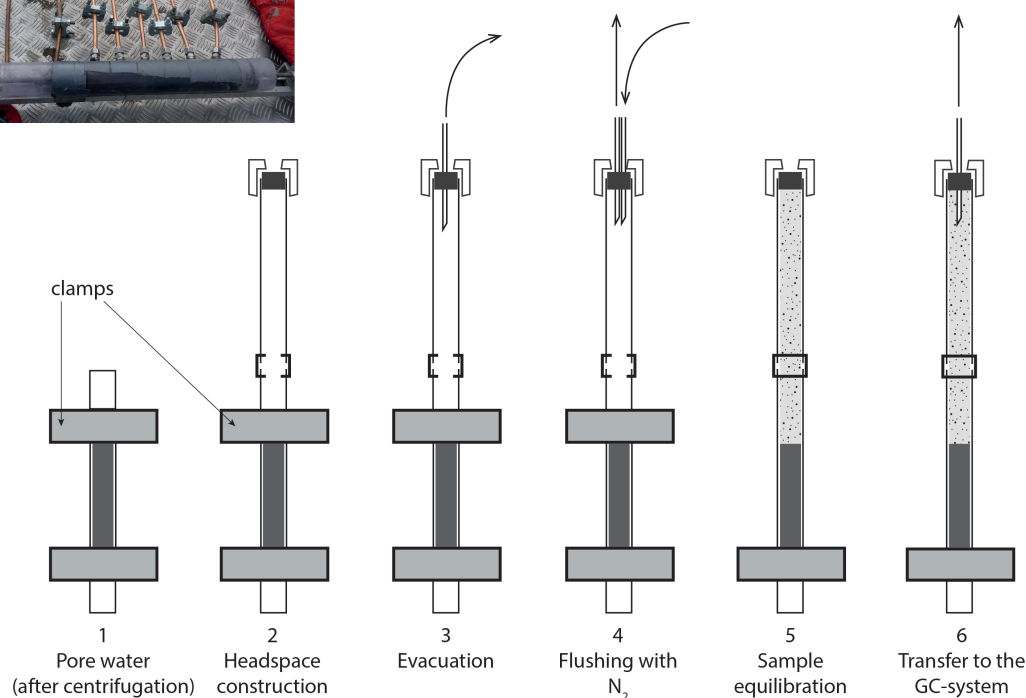


Figure 5.1: **A.** Experimental set-up: The photo was taken after sampling the sediment and after closing copper tubes airtight with pinch-off clamps. The core liner is mounted in the squeezer and copper tubes with fittings are attached to the sampling ports. **B.** Preparation of the samples headspace for the subsequent gas/methane analysis by gas chromatography (GC). 1) Pure pore water sample separated from the sediment matrix by centrifugation (Tomonaga et al., 2011). 2) Headspace construction by mounting an additional copper tube segment with Swagelok fittings. 3) Headspace evacuation and 4) flushing the headspace with nitrogen at atmospheric pressure (steps 3 and 4 are repeated three times). 5) Opening and shaking of the water sample 3 times for 60 seconds to reach gas equilibrium with the headspace (the gas mixture from the head space and from the water sample are shown in the graph as grey and dotted area). 6) Gas injection into the GC for final CH_4 quantification.

6) and injected to a GC for final CH₄ analysis by an gas tight injector, i.e. a needle connected to a metal tube coupled with a 24-port valve (VICI). To control the stability of the analysis a standard with a known methane concentration was measured alternating with the samples. The oven of the GC-FID (flame ionisation detector made up of Agilent HP6890GC, with a 30 m Supelco Carboxen 1010 column x 530 μ m inner diameter x 3 μ m film thickness, and a carrier gas He) was programmed to run at 100 °C for 4 minutes. Subsequently, the temperature was increased by 20 °C per minute up to 130 °C and kept at that temperature for another 3.5 minutes. The detector signal was converted into CH₄ amounts by calibration against gas standards with known CH₄ concentrations. The used calibration fully covered the range of methane concentrations in the samples. The pore water mass of each sample was determined by the difference in weight between the pore water-sample container (copper tube with N₂-headspace and pore water sample prior to analysis) and the empty sample container (empty copper tube, clean and dry after analysis). In addition, the volume of the headspace was determined for each sample by filling the total volume of the sample container with water (copper tube completely filled with water). The headspace volume was then calculated by the difference in the weight of the total volume of the sample container and the weight of the pore water-sample container (copper tube with N₂ filled headspace and pore water sample prior to analysis). The total volume of the sample container was determined for each copper tube by refilling the empty sample container with water and measuring the quantity. The CH₄-TAMP in the pore water was calculated using Bunsen solubility (Colt, 2012) for CH₄ at the given equilibration temperature in the headspace.

Syringe standard method

For the CH₄ analysis by the SSM method (Adams, 1994; Hoehler et al., 1994; Popp et al., 1995; Jørgensen et al., 2001; Schubert et al., 2010; Sobek et al., 2012; Sollberger et al., 2014) sediment cores were collected in the same manner as for the CTC method (see Brennwald et al., 2003). After core retrieval at each sampling port, 2.0 ± 0.2 cm³ of the sediment were extracted with a tipless 5 mL syringe. Sediments in the syringe were transferred to 25 mL glass vials. At the same time, 5 mL of 25% sodium hydroxide solution were added to prevent bacterial activity. The headspace gas contains ambient air ($\approx 1,75$ ppm methane). The vials were sealed with a butyl stopper, crimped with an aluminium cap. The samples were equilibrated overnight in a water bath at a constant temperature. Subsequently, the headspace gas content was analysed using the GC-FID described above and the methane concentrations from the whole sediment were corrected to pore water concentration by accounting the sediment porosity.

5.2.2 Performance of the method

We tested the performance of the CTC method in comparison with the SSM method in three steps: i. Assessment of the efficiency of the copper-tube headspace gas extraction; ii. Comparison of the performance of the CTC and SSM methods in the sediment pore water with CH₄-TAMP in the range of CH₄ in situ saturation concentration (Lake Lungern); and iii. Comparison of the performance of the CTC and SSM methods for sediments from Lake Rotsee that were obviously heavily supersaturated in CH₄.

i. *Assessment of the efficiency of the copper-tube headspace gas extraction*

Water with a virtually constant CH_4 concentration was generated by pumping pure CH_4 gas through a diffuser at the bottom of a 10 L container filled with tap water. Small CH_4 bubbles were generated by the diffuser and, during their rise in the water column, the initially-dissolved gases were replaced by CH_4 . The oxygen concentration in the tap water was continuously controlled by an O_2 sensor (WTW Multi 340i-electrode CelloX 325). When oxygen concentration in the water became zero, the water was assumed to have reached CH_4 saturation and bubbling was stopped. Subsequently, water samples were taken and analysed by means of a standard technique (using 117 mL glass vials and N_2 to create a headspace, see Kampbell et al., 1989) for the analysis of dissolved methane and the copper tube headspace extraction (see Sect. 5.2.1). Samples were taken consecutively through a plastic tube connected to an outlet at the bottom of the water container. Sampling time between consecutive samples was kept short to minimise the effect of gas loss from the tank being covered with a cap.

For the CH_4 analysis by the copper tube headspace technique, a copper tube was flushed with the CH_4 -loaded water. A sample of approximately 2 cm^3 was sealed airtight by closing two pinch-off clamps. The volume taken was similar to the amount of pore water extracted by the centrifugation of a typical lacustrine sediment sample. This volume is about 6 times smaller than the sample in the glass vial (12 cm^3). Results for the copper tube sample were therefore more likely to be affected by weighing errors and errors in determining the headspace volume. As a result, the overall analytical uncertainties are considerably larger than those for the analysis using glass vials. A better analytical precision for the CTC method can be achieved by optimising the sample inlet to the GC, e.g. by extracting the dissolved gases from pore water directly into a pre-evacuated extraction line (Brennwald et al., 2013a). Nevertheless, the advantage of using the copper tube headspace for CH_4 extraction is that samples can be readily analysed by most GCs without any modifications.

ii. *Comparison of the performance of the CTC and SSM methods in the sediment pore water where CH_4 -TAMP is known to be in the range of CH_4 in situ saturation concentration (Lake Lungern)*

Lake Lungern, a reservoir situated in Canton Obwalden (Switzerland), is used for hydropower production and is therefore subject to high, artificially-induced water level variations. The lake level fluctuates between approximately 650 and 690 m.a.s.l. with low levels in winter and high levels in summer. Most of the littoral sediments originate from cropland that was flooded when the lake was dammed. The organic and mineral load of two inflowing rivers contributes to sediment formation in the littoral zone. High CH_4 concentrations were reported in the water column of Lake Lungern (Diem et al., 2012). CH_4 emissions in the form of small bubbles visible at the water surface have also been reported in the littoral area (Ostrovsky, 2009). During field sampling in March 2013, two sediment cores were taken at the same location within a radius of less than 1 m, from a site which had shown active CH_4 bubble release in the previous summer when the lake was at its highest level. When sampling the sediment, the water level was at its lowest and had been virtually stable throughout the preceding month. The difference between the lake level at its lowest

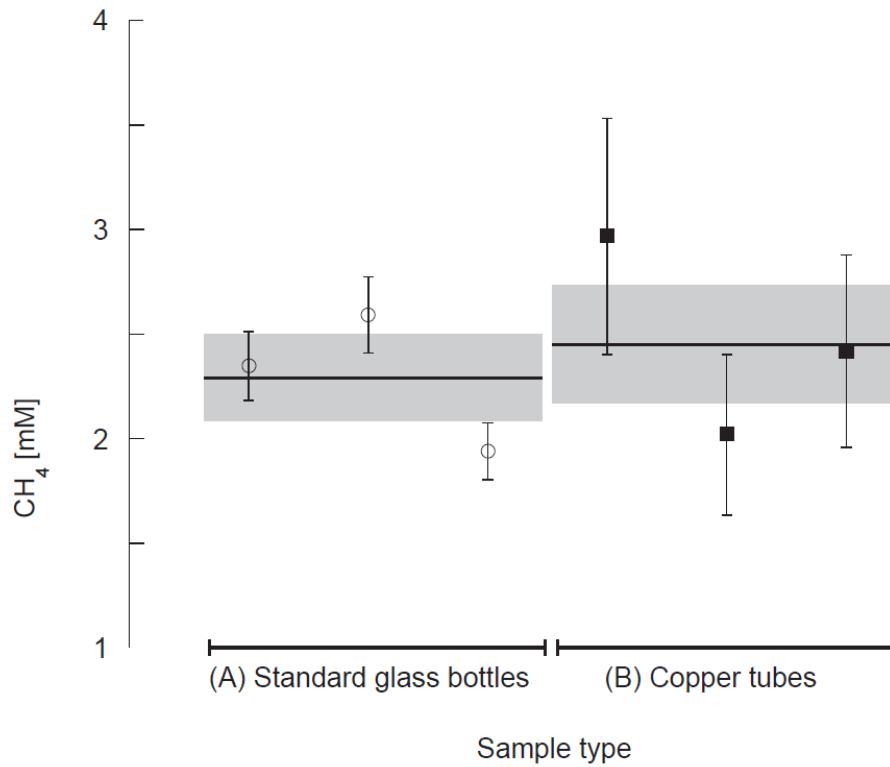


Figure 5.2: Comparison of the CH₄ concentrations determined in artificially CH₄-supersaturated water samples by (A) standard technique (Kampbell et al., 1989) in glass bottles (open circles) and (B) with the new copper tube headspace technique (black squares). The mean CH₄ concentration (continuous black lines) determined with both sampling methods (A) and (B) agrees in terms of experimental errors (grey areas represent the error of the mean). The determined concentrations exceed the expected CH₄ saturation concentration most likely due to microbubbles formation (McGinnis et al., 2015), which is often found in aquatic systems that are artificially aerated (Holzner et al., 2012).

in the winter and its maximum level in the summer was 20 m. This lowering of the lake level caused a strong pressure release in the sediment and fostered degassing and bubble formation as the overlying water column decreased. Depleted dissolved gas concentrations (i.e. He, Ne, Ar, Kr, Xe) in the pore water of these sediments, with regard to the expected air-saturated water concentrations, were found in an earlier study and were interpreted as resulting from gas stripping by CH₄ bubbles formed in and released from the sediment (Tyroller et al., 2013). Due to low air and water temperatures during sampling (between + 4 and - 5 °C), biological activity in the sediment was most likely very low or even non-existent (Duc et al., 2010). In order to avoid the effect of pressure release and degassing during sediment core retrieval, the cores were taken from a site with a water depth of only 5 cm. For these reasons (namely, low hydraulic pressure, limited biological activity, and stable lake levels over a long period), we assume that CH₄ concentrations in the pore water of the sediments are close or equal to the expected saturation concentration.

iii. *Comparison of the performance of the CTC and SSM methods for sediments supersaturated in methane (Lake Rotsee)*

Lake Rotsee ⁴ is a small eutrophic pre-Alpine lake, close to the city of Lucerne (Switzerland). Due to its wind shielded location Lake Rotsee only mixes once a year in early spring and has a stable stratified water column and an anoxic hypolimnion for the rest of the year (Schubert et al., 2010). The sediments of Lake Rotsee are known to emit CH₄ (Schubert et al., 2010; Naeher et al., 2012, 2014). The CH₄-TAMP of the sediments had been determined previously by the SSM and dialyzer methods (Falz et al., 1999; Schubert et al., 2010; Naeher et al., 2012, 2014). The sediments of Lake Rotsee were sampled towards the end of September 2011, 2013 and 2014. At each campaign, 2 to 4 sediment cores were taken within a radius of circa 15 m from the same location at a water depth of 15 - 16 m. Because of the stable conditions in Lake Rotsee and because samples were always taken in the same month and at virtually the same location similar methane amounts were expected in the different years. Cores taken in 2011 and 2013 were processed with the CTC method (see Sect. 5.2.1). However, the sediment core from 2014 was processed differently. In 2014, the holes for the ports to connect the copper tubes to sample the sediment were drilled after retrieval of the sediment core. This procedure allows the ports to be set in ideal positions with regard to the retrieved sediment core. We note, however, that post-retrieval drilling induces vibration and prolongs sampling time. Both actions foster bubble movement within the sediment core and subsequent bubble loss.

5.3 Results and Discussion

5.3.1 Performance of the copper tube headspace gas extraction (lab experiment)

Methane concentrations of CH₄-enriched water determined using a standard technique (Kampbell et al., 1989) and copper tube headspace technique agree within experimental errors (see Fig. 5.2), both were in a range of 2 - 3 mM CH₄. Thus, the performance of the copper tube headspace method for CH₄ analysis is at the same level as that of the accepted standard method.

5.3.2 Comparison of the performance of the two methods in sediments that have CH₄ concentrations in the range of the expected methane saturation (Lake Lungern)

SSM method: The CH₄-TAMPs determined with the SSM method in the pore water of Lake Lungern ranged between 0.5 and 1.7 mM (see Fig. 5.3) and were always lower than in situ saturation concentrations for CH₄.

⁴The term Lake Rotsee used in Chapt. 5, Chapt. 6 and in the publication (Tyroller et al., 2016) is incorrect, but the lake should be referred to as Rotsee or Lake Rot. However, the term Lake Rotsee has been commonly used in previous studies (e.g. Ammann and Lotter, 1989; Müller et al., 1998; Naeher et al., 2012) and hence was chosen for a better recognition.

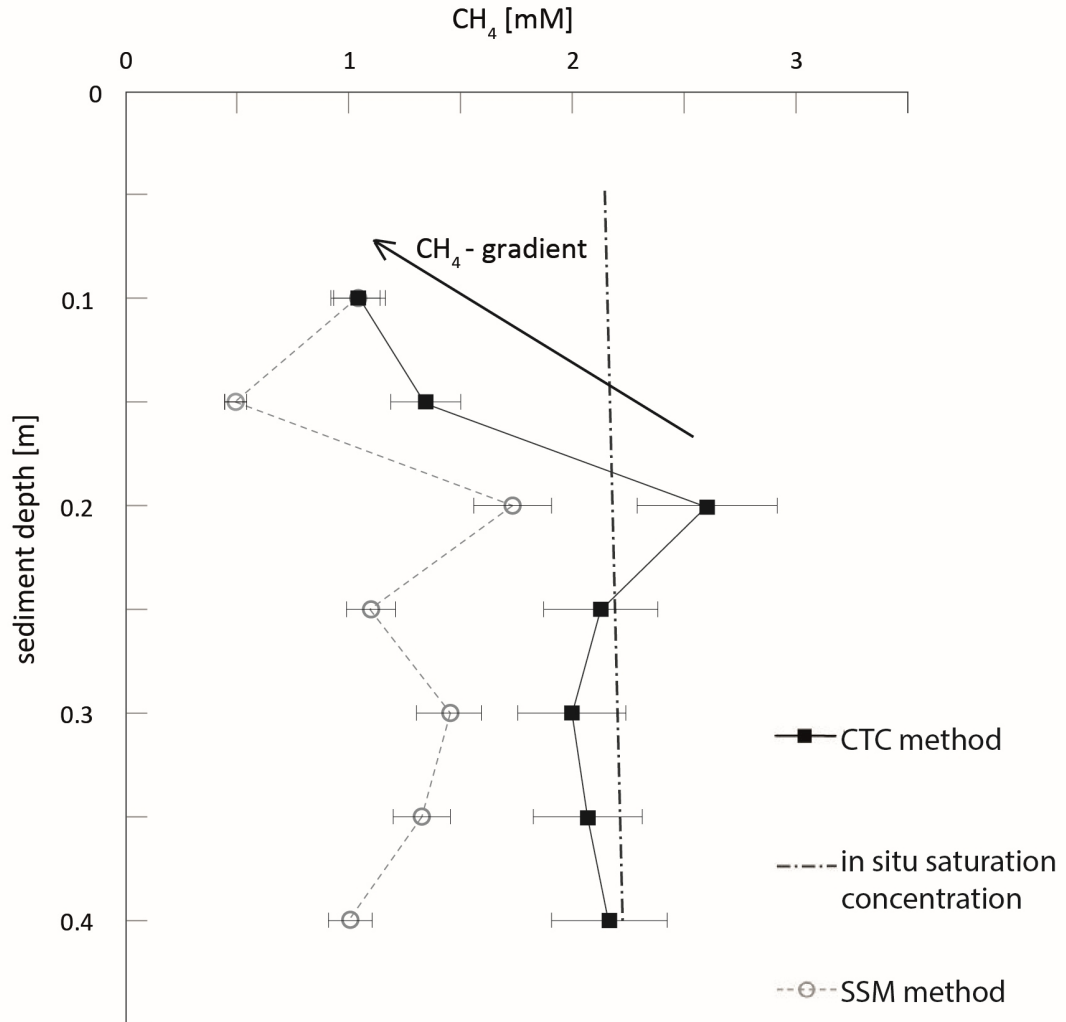


Figure 5.3: Comparison of the CH_4 concentration profiles determined with SSM and CTC method in the pore water in Lake Lungern in the winter of 2012 at low water level and hence with a very low overlying water column (5 cm). We note that CH_4 in situ saturation concentration was calculated with Henrys law (Sander, 1999), assuming a pure CH_4 gas phase. Spatial error on the sediment depth varies between 1 cm for the SSM method and 2.5 cm for the CTC method. Due to displacement of the sediment during squeezing the error on the vertical localisation of samples taken with CTC method is higher. In the upper 20 cm of the sediment, CH_4 concentrations are characterised by a strong gradient decreasing towards the sediment/water interface.

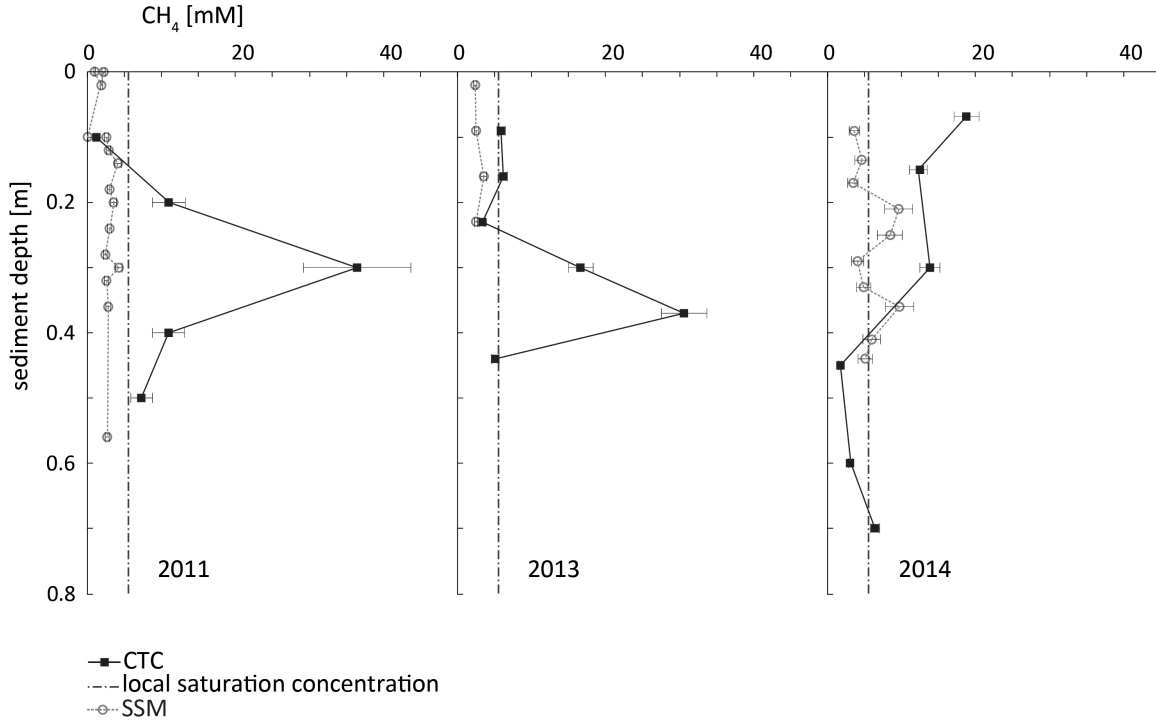


Figure 5.4: Comparison of the CH_4 concentration profiles measured in the pore water of Lake Rotsee in 2011, 2013 and 2014 at a water depth of about 16 m: SSM; CTC method; and in situ saturation concentration of CH_4 calculated with Henrys law (Sander, 1999) assuming a pure CH_4 gas phase. Due to a different design of the sample inlet to the gas chromatograph (GC), the errors of all samples analysed in 2011 are larger. The spatial error of sediment displacement is: SSM method ± 2.5 cm; CTC method ± 1.0 cm.

CTC method: The CH_4 -TAMPs determined by the CTC method show a gradient in the upper 20 cm of the sediment. Starting at the water/sediment interface, CH_4 -TAMP values were continuously increasing and stabilised at about 2.1 mM, at a sediment depth of 20 cm. From a sediment depth of 20 cm and downward, the CH_4 -TAMP calculated by the CTC method agrees with the in situ saturation concentration (2.0 - 2.5 mM CH_4 , Fig. 5.3). We note that sampling was performed at a point in time where the sediment had virtually no overlying water column and therefore the retrieval of the sediment core was expected not to foster degassing due to pressure release.

5.3.3 Performance of the two methods when sampling sediments with active bubble formation (Lake Rotsee)

SSM method: In Lake Rotsee, CH_4 -TAMPs determined by the SSM method were in the range of 3 to 5 mM CH_4 (see Fig. 5.4). The results are in line with results from previous studies at Lake Rotsee that used the same method (Schubert et al., 2010). We note that immediately after core recovery, formation of gas bubbles was observed in the sediment during sampling (see Fig. 5.5). The presence of a free gas phase implies that the CH_4 -TAMP exceeded the in situ saturation concentration (7 °C, approximately 15 to 16 m depth, 5.3 - 5.6 mM CH_4). Thus, although CH_4 supersaturation was obvious, the CH_4 -



Figure 5.5: Visible bubbles (within white circle) within the retrieved sediment core from Lake Rotsee 2013. Such bubbles occur spontaneously and immediately after core retrieval indicating that CH_4 concentrations in the pore water is supersaturated.

TAMPs determined by the SSM method were commonly found to be even lower than in situ saturation concentration of CH_4 . Only in some samples of the 2014 core CH_4 -TAMPs were found to slightly exceed the in situ saturation concentration of CH_4 . We also note that the CH_4 -TAMP values determined using the SSM method show a “scatter” with regard to depth and do not show a clear concentration maximum.

CTC method: CH_4 -TAMPs determined by the CTC method were larger than values determined with SSM method. In Lake Rotsee, down to a sediment depth of 30 cm, CH_4 -TAMPs in the pore water were higher than the CH_4 in situ saturation (up to 40 mM CH_4 , see Fig. 5.4). CH_4 -TAMPs in samples taken at a depth below 40 cm were found to be close to the in situ saturation concentration. The CH_4 -TAMPs being higher than the CH_4 in situ saturation concentration make a clear argument for the presence of CH_4 bubbles in the sediment and hence are in line with the observation of gas bubbles in the sediment core (see Fig. 5.5). CH_4 -TAMPs determined using the CTC method were approximately an order of magnitude higher than those determined by the SSM method. Our maximum CTC CH_4 -TAMP results (20 - 35 mM CH_4) agree with the range of results from dialyzer analysis at Lake Rotsee (20 - 40 mM CH_4 ; Falz et al., 1999). Although the dialyzer results at Lake Rotsee agree with the CTC results overall, we note that the dialyzer method did not yield any CH_4 -TAMP maximum within the sediments and that concentrations were subject to considerable scatter with regard to depth. As mentioned above, such erratic CH_4 -TAMP data may well be result from sampling artefacts, e.g. due to gas exchange with the atmosphere during sampling (Dyck and Da Silva, 1981; Adams, 1994).

CTC samples from 2011 and 2013 repeatedly show a marked CH_4 -TAMP maximum

at a depth of 30 to 40 cm. Their CH_4 -TAMP exceeds the in situ CH_4 saturation concentration by at least an order of magnitude. A slight offset of the peak CH_4 -TAMPs in cores between 2011 and 2013 is likely to be related to the uneven sediment displacement in the liner due to squeezing and to the spatial heterogeneity of microbiological CH_4 production. Given a sedimentation rate of between 0.38 and 0.40 cm/y (sedimentation rate was determined by identifying the ^{137}Cs peak of the Chernobyl accident and assuming a constant sedimentation rate; Pennington et al., 1976), the CH_4 -TAMP peak is found in sediments deposited between 1920 and 1950. In the 2014 core, where sampling ports were set after core retrieval, no clear concentration peak was observed. Nevertheless, down to a level of 40 cm, CH_4 -TAMP was significantly higher than the in situ CH_4 saturation concentration. The total CH_4 excess, defined by saturation concentration and the measured CH_4 -TAMP integrated over the sediment depth, is roughly the same for all three cores (2011, 2013 and 2014). Thus, all cores contain a similar amount of CH_4 -TAMP; however, spatial distribution varies. We conclude that different vertical CH_4 -TAMPs indicate that CH_4 was redistributed within the core due to agitation during drilling in 2014, but was not allowed to escape from the bulk sediment mass.

5.4 Implications

Although the sediments investigated in this study are known to actively emit CH_4 , the CH_4 -TAMPs measured using the SSM method were either lower than the expected CH_4 in situ saturation concentration (Lake Lungern) or were not able to detect the expected CH_4 supersaturation (Lake Rotsee) in the sediment pore water. The difference between CH_4 -TAMPs determined using the SSM and CTC methods increased with higher real CH_4 -TAMP and, particularly, with the presence of bubbles in the sediment. CH_4 -TAMP determined using the SSM method were severely biased toward lower concentrations. A CH_4 loss of up to 90% was inferred. Our study confirmed that the SSM method fails to quantitatively and reliably determine the in situ CH_4 -TAMP of unconsolidated lacustrine sediments. In contrast CH_4 -TAMPs determined by the CTC method were always found to be higher than values measured using the SSM method. The concentrations determined by CTC method fell well within the expected CH_4 concentration range.

It is crucial to determine CH_4 in the pore water of lacustrine sediments in a truly quantitative manner in order to set a robust experimental anchor for studying CH_4 dynamics in lakes and their sediments (Schubert et al., 2010). Our study makes the case that the CTC method may allow the accurate quantification of the real in situ CH_4 -TAMP of sediments, even where CH_4 concentrations exceed the in situ saturation concentration, e.g. in productive sediments known to actively emit CH_4 bubbles. The CTC method is applicable in all sediments that can be sampled with a gravity corer and gives good results as long as methane bubbles stay in the local sediment matrix during core recovery. In addition, the CTC method allows us to depict the real spatial distribution of CH_4 -TAMPs within the lacustrine sediments, e.g. concentration gradients can be reconstructed accurately (Lake Lungern) and zones of enhanced CH_4 production can be identified (Lake Rotsee). Although rather demanding from an experimental point of view, the CTC method represents a significant improvement in the analysis of the CH_4 -TAMP of unconsolidated sediments in lakes and oceans. The sampling technique using gas-tight copper tubes avoids gas loss during sample acquisition, and thus eliminates the most critical sampling

artefact when quantifying gas amounts in sediments. Use of the CTC method for noble gas analysis (Brennwald et al., 2003; Tomonaga et al., 2011a) showed that CTC method could be applied to the quantification of the gas concentrations in highly compacted sediments, e.g. in ocean sediments or sediments being retrieved by deep drilling (Tomonaga et al., 2014, 2015). Furthermore, in principle, the CTC method also makes it possible to determine the real, in situ concentrations of other dissolved gases (e.g. H_2S , NH_3 , CO_2 , N_2 by using a different head space gas) as well as their isotopic composition in the pore space of unconsolidated sediments. This enables the characterisation of the gas/solute budget in the sediment and the gas exchange at the sediment/water interface.

Chapter 6

Noble gases as tracer for the gas dynamics in methane supersaturated lacustrine sediments

Chapt. 6 is ready to be submitted to:

L. Tyroller; Y. Tomonaga; M.S. Brennwald; R. Kipfer. Noble gases as tracer for the gas dynamics in methane supersaturated lacustrine sediments. *Environmental Science and Technology*.⁵

Abstract The commonly observed heterogeneous and erratic emissions of methane from lacustrine sediments are difficult to quantify. The use of noble gases as tracer opens a novel route to analyse and quantify such emissions. This work explores the potential of the combined analysis of methane and noble gas concentrations in the pore water to determine the gas dynamics in the sediments of two lakes with different hydrogeochemical settings. In hypertrophic Lake Rotsee the microbial activity in the sediment pore water results in a virtually continuous gas bubble formation and emission. By determining noble gas concentration gradients and the maximum methane supersaturation the minimum methane emission from the sediment was quantified ($\sim 5 \text{ mmol}\cdot\text{m}^{-2}\cdot\text{d}^{-1}$). The gas evolution in the pore water of the sediments of Lake Lungern are strongly affected by annual lake level variations of up to 20 meter. Noble gas concentrations allow to reveal the past gas dynamics for different lake levels. At “hot spots” of bubble emission microbial methane from deeper sediments was released in response to the decreasing hydrostatic pressure, e.g. lake level drop. Furthermore noble gases were used to identify zones of the sediment that seasonally fall dry. The oxygen supply to the sediment due to redissolved air bubbles, which entered the sediment during dry period, was inferred from the observed noble gas excess in the pore water. This study demonstrates that the combined analysis of noble gas and CH_4 concentrations is a promising tool to trace the dynamics related to gas bubble formation in unconsolidated sediments in lakes and possibly also in wetlands and oceans.

⁵Acknowledgements: We thank Tonya Del Sontro for her introduction to the Simrad-echosounder adjusted for bubble search that was used for the hydroacoustic survey of Lake Lungern. Thanks also to Hilmar Hofmann for borrowing his gas funnels and for providing his expertise. This work was financed by the Swiss National Science Foundation (SNF-project 200020 – 132155).

6.1 Introduction

Methane (CH_4) supersaturation in the sediment pore water often results from anthropogenically induced eutrophication. Eutrophication affects lakes, reservoirs, ponds and rivers on a global scale (Smith, 2003; Downing et al., 2008) and goes along with elevated primary production in the lake water, high sedimentation rates and hypoxic or even anoxic conditions in the sediments. Under such conditions microbial CH_4 can be produced in the sediment column and accumulates in the pore water (Lovley and Klug, 1982; Sobek et al., 2009). If the sum of the partial pressures of gases dissolved in the pore water exceeds the total in situ hydrostatic pressure, bubbles can be formed in the sediment (e.g. Boudreau, 2012). In the following these conditions are referred to as supersaturation. If such bubbles formed in the sediment pore space reach a critical size, they can escape from the sediment. The physical processes related to the formation of a free gas phase in the sediment and to bubble emanation from the sediment are of interest for understanding the importance of gas ebullition with respect to the overall gas budget in the sediment column and as an integral part of the gas budget in the lake. Gas supersaturation in the pore water of lacustrine sediments and subsequent bubble formation can result, for example, from enhanced microbial production, from rising water temperatures or can be triggered by a hydrostatic pressure decrease, i.e. a change in the total in situ hydrostatic pressure. Such pressure unload might be caused by shear stress in the sediments induced by bottom currents, by wind events (i.e. wind pumping, see Precht et al., 2004; Hofmann et al., 2010), by variations in atmospheric pressure (Joyce and Jewell, 2003), or by decreasing water level (Beaulieu et al., 2017; Harrison et al., 2017). The effect of such changes of the water level on the gas dynamics in lacustrine sediments has received little scientific attention so far, although the few available observations make the case that the resulting ebullition might foster the CH_4 emission significantly (Varadharajan and Hemond, 2012; Maeck et al., 2014; Beaulieu et al., 2017; Harrison et al., 2017).

Gas ebullition from the sediment pore water occurs very heterogeneously in time and space and often happens as a single erratic event and over short periods of time. Such irregular gas ebullition events might be missed by conventional sampling strategies which commonly cover only a limited time span. The biogeochemically inert noble gases have the potential to record such events as they integrate the effect of free gas formation and subsequent ebullition over relatively long time scales, e.g. in the case of suppressed diffusive transport in the pore water the time that has passed since pore water entrapment (Tomonaga et al., 2015). Bubbles formed in the sediment pore water are composed of the gases that were present in the surrounding pore water during gas bubble formation (e.g. CH_4 , CO_2 and noble gases), whereas the amount of a respective gas in the formed bubble depends on the partial pressure in the surrounding pore water and on the solubility of the respective dissolved gas. In the case of strong microbial CH_4 production in the sediment a local CH_4 excess in the pore water can cause a formation of bubbles. As a result such bubbles initially mainly contain CH_4 and induce a diffusive transport of other gas species (e.g. noble gases) into the bubble, depending on the respective gas diffusion coefficient and on the difference in partial pressure. Gas exchange of gases in the bubble and gases dissolved in the pore water continues until attaining solubility equilibrium of the free gas phase with the surrounding pore water. Such gas bubble formation in the pore water leaves a characteristic depletion pattern of the hardly soluble noble gases in

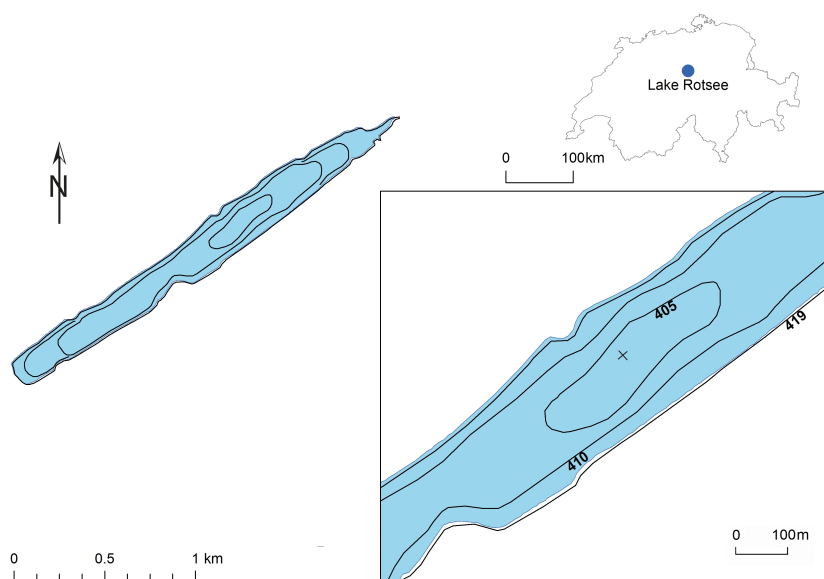


Figure 6.1: Bathymetric map of Lake Rotsee. The height [m.a.s.l.] of the subaqueous contour lines are given beside each line. The sampling site is marked with a cross. Data source: swisstopo DV 5704 000 000, reproduced by permission of swisstopo / JA100119.

the surrounding pore water. Such noble gas depletion can be used to reconstruct past gas bubble (CH_4) emissions, as shown in the case of highly eutrophic Lake Soppen (Brennwald et al., 2005). However, so far the Lake Soppen study is the only application of noble gas concentrations dissolved in sediment pore water to trace past gas bubble (CH_4) emissions.

Recent technical advances in sampling (see Chapt. 5 and Tyroller et al., 2016) now make it possible to quantify reliably the CH_4 concentration in the sediment pore water, even in strongly supersaturated sediments where CH_4 is present both in dissolved and in free gaseous form. The combined analysis of noble gas and CH_4 concentrations is a promising tool to trace the gas dynamics related to gas bubble formation in unconsolidated sediments.

In this chapter the results from noble gas and CH_4 measurements in the uppermost meter of the sediment (commonly the zone of most active CH_4 production and emission) of two lakes (Lake Rotsee and Lake Lungern) are discussed, with the aim to further expand the use of trace gas geochemistry in aquatic systems and to improve the understanding of the gas dynamics in lacustrine sediments. The two investigated lakes were chosen by reason of the different conditions inducing bubble formation in the sediments. At Lake Rotsee CH_4 emissions are primarily driven by the high trophic level of the lake, whereas mesotrophic Lake Lungern is subject to extreme lake level variations which may trigger gas release.

6.2 Study sites

Lake Rotsee (Switzerland) is characterized by frequent algae bloom and considerable CH_4 production in the sediment owing to the extremely high nutrient content in the lake.

The lake is stratified during the warm season (May to November) and in the cold season (January to February). During spring and autumn the lake is completely mixed. The sediments of Lake Rotsee are known to emit CH_4 bubbles (Schubert et al., 2010; Naehrer et al., 2012, 2014; Tyroller et al., 2016). Bubble emission can be observed by eye in the littoral zone. The anthropogenic nutrient input, e.g. the sewage load of the city of Lucerne from 1850 to 1978, had the strongest impact on the eutrophication level of Lake Rotsee, although the lake has been eutrophic throughout the Holocene (Lotter, 1990). Fig. 6.1 shows the location of sediment coring in the center of Lake Rotsee at a water depth of 16 m. The sediment cores, retrieved in three sampling campaigns in 2008, 2011 and 2013, were taken within a radius of 5 m from the position indicated in Fig. 6.1.

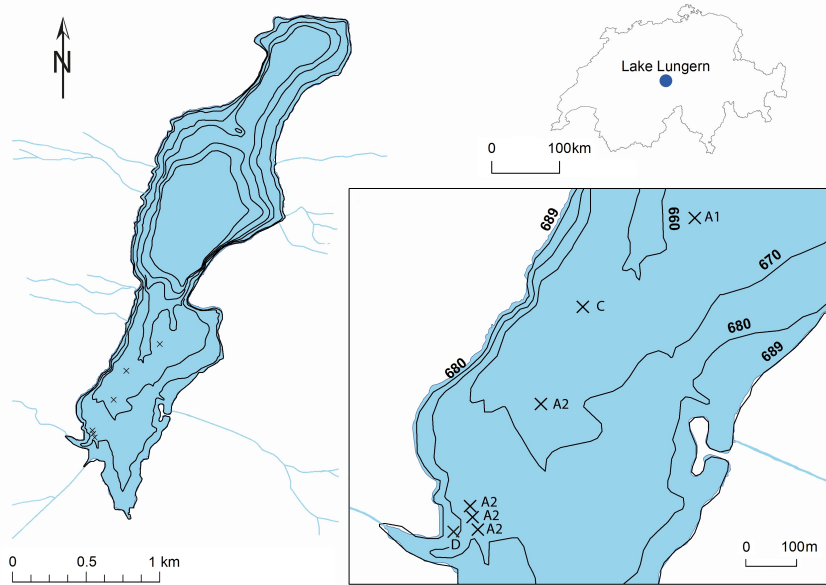


Figure 6.2: Bathymetric map of Lake Lungern and inflowing rivers. The height [m.a.s.l.] of the subaqueous contour lines are given beside each line. The location of each sampling site is marked with a cross: Sites **A** were sampled in the late summer: **A1** where no active bubble emission was observed, **A2** where bubble emission from the sediment was observed by eye and with a side scan sonar. The site **C** was sampled in the wintertime and **D** in spring. Data source: swisstopo DV 5704 000 000, reproduced by permission of swisstopo / JA100119.

Lake Lungern (Canton Obwalden, Switzerland) is a mesotrophic reservoir and is subject to artificially-induced water level variations of up to 20 m as it is used for hydropower production (see Chapt. 5). Most of the littoral sediments originate from crop land that was flooded when the lake was dammed. An earlier study on Lake Lungern suggested that the observed CH_4 bubble emission and the measured high CH_4 concentrations in the deep water during summer stagnation might originate from deep natural gas emissions (i.e. Bossard and Gächter (1981): “fossil methane penetrating the sediment from below”). However, a more recent study found the CH_4 emission from Lake Lungern to be in a similar range to the CH_4 emission from other comparable Swiss reservoirs (Diem et al., 2012). In another study, in July 2006, an echosounder survey was conducted on

Lake Lungern (Ostrovsky, 2009). In this hydroacoustic survey an emission of very small bubbles in the littoral zone (at a water depth of less than 7m) was observed, whereby oxygen concentrations in the water of the lake were significantly supersaturated (Ostrovsky, 2009). In our study echosounding identified active bubble emission in the southern part of the lake. For gas analysis seven sediment cores were taken in the area of these spots of active bubble emission and in the littoral zone of the southern part of the lake (see positions indicated in Fig. 6.2) at different times.

6.3 Methods

Sediment cores were retrieved in liners using a gravity corer (see Chapt. 5). The sediment cores were processed immediately after recovery, whereby the bulk sediment was transferred by squeezing into copper tubes used as sampling containers (see Chapt. 5, Brennwald et al., 2003; Tomonaga et al., 2011a). The length of the copper tubes was chosen such that it could be split into three aliquots by adding and closing airtight additional clamps. The first aliquot was used to determine the geometrical position of the sediment/water interface within the copper tube after the separation of the pore water from the matrix by centrifugation (Tomonaga et al., 2011a). The second aliquot was used to determine noble gas concentrations in the porewater (Brennwald et al., 2003; Tomonaga et al., 2011a) and the third aliquot for the determination of the total CH_4 abundance (Tyroller et al., 2016).

An Isoprime isotope ratio mass spectrometer (IRMS) was used to measure the stable carbon isotope distributions of the CH_4 gas samples obtained in the funnels at Lake Lungern.

A downward-looking Simrad split-beam echosounder (Kongsberg Maritime AS, Norway, EK60, 7° beam angle, 120 kHz transducer), being adjusted for bubble search in aquatic systems by Del Sontro (2011), was used to search for bubbles emitted from the lake sediment and to precisely position the gravity corer at spots of active bubble emission.

6.4 Results and Discussion

6.4.1 Noble gas data from Lake Rotsee

Fig. 6.3 shows the depth profiles of CH_4 concentrations, of Ar isotope ratios and of noble gas concentrations determined in the sediment pore water of Lake Rotsee. Based on the observed trends of the CH_4 and noble gas concentrations with sediment depth, the sediment can conceptually be subdivided in three layers (0 - 25 cm, 25 - 45 cm, below 45 cm):

0 - 25 cm sediment depth: In this layer the determined CH_4 concentrations are close to the local saturation concentration (CH_4 -local; see Fig. 6.3). The noble gases show distinct and systematic elemental fractionation (strongly depleted relative to ASW), whereby the light noble gas concentrations are more depleted than the heavy noble gases ($\Delta\text{Ne} < \Delta\text{Ar} < \Delta\text{Kr} < \Delta\text{Xe}$; Fig. 6.3). Such a depletion pattern has been shown to be characteristic for the stripping of dissolved noble gases by gas bubbles (e.g. CH_4) formed in the sediment

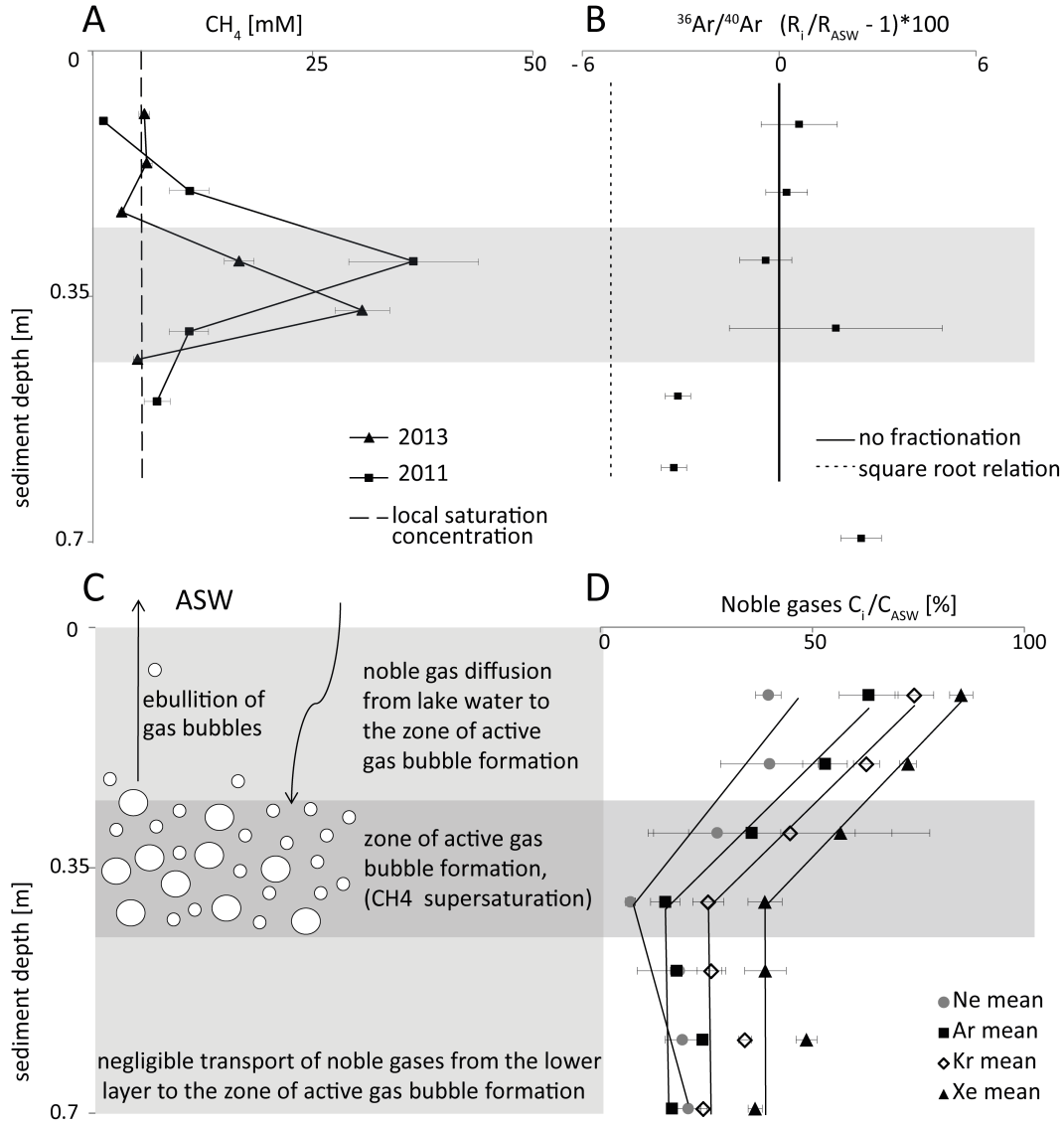


Figure 6.3: **A** CH₄ concentration profiles in Lake Rotsee, determined in sediment cores sampled in 2011 and 2013 (see also Chapt. 5 and Tyroller et al., 2016). We note that air saturated water (ASW) and CH₄-local (intermittent line) was calculated with Henry's law (Sander, 1999), whereby for the latter a pure CH₄ gas phase was assumed. **B** ³⁶Ar/⁴⁰Ar isotope ratio profiles with sediment depth determined in the sediment pore water of Lake Rotsee. The isotope ratios are mean values of the results determined in two sediment cores and normalized to the ³⁶Ar/⁴⁰Ar ratio of ASW (solid line; Beyerle et al., 2000). The dotted line is the fractionation of Ar isotopes according the square root relation (e.g. $(\frac{^{36}\text{Ar}}{^{40}\text{Ar}})_{\text{ASW}} \cdot \sqrt{\frac{^{36}\text{Ar}}{^{40}\text{Ar}}}$, see Tyroller et al., 2014). **C** Chart of the gas dynamics in the different layers of the sediment. **D** Noble gas concentrations in the pore water of Lake Rotsee with sediment depth. Mean values from two sediment cores obtained in 2008 and 2011 at Lake Rotsee at a depth of 16 m. Noble gas concentrations are presented in percent relative to ASW (100%). A linear regression was fitted to the noble gas concentrations in the upper 40 centimetres of the sediment of Lake Rotsee. The grey shaded area indicates the zone of CH₄ supersaturation and hence the zone where CH₄ is present in gaseous phase. The error on the sediment depth is about ~ 0.05 m due to sediment displacement upon sediment squeezing (see Tomonaga et al., 2015).

(Ballentine and Burnard, 2002; Holzner et al., 2004; Brennwald et al., 2005). Noble gas concentrations linearly decrease with increasing sediment depth. The noble gas profile can be interpreted as an indication of a diffusive transport (operating at steady state) of noble gases dissolved in the lake water (ASW) from the sediment/water interface downward to the zone of CH₄ supersaturation and maximum noble gas depletion. The ³⁶Ar/⁴⁰Ar ratios in this layer are not fractionated and agree with the ratio of ASW within the error of measurements. This indicates that the vertical transport of noble gases happens on a time scale large enough for bubbles in the active layer to obtain equilibrium before leaving the sediment. This assumption appears realistic as the sediment in this zone near the sediment/water interface is highly unconsolidated and the diffusive transport of noble gases in the pore water of such sediments is known to be similar to the diffusive transport in free water (Jähne et al., 1987a; Cussler, 2009). As the CH₄ concentrations closely match with the CH₄-local a free CH₄ phase seems not to be present in this zone.

25 - 45 cm sediment depth: The maximum noble gas depletion and CH₄ supersaturation are observed in this layer (grey area in Fig. 6.3). A peak of CH₄ concentrations was observed between 25 - 45 cm sediment depth, with CH₄ concentrations exceeding CH₄-local by one order of magnitude. This CH₄ peak was determined in two independent sampling campaigns (i.e. 2011 and 2013; see Chapt. 5, Tyroller et al., 2016). Furthermore, the strong CH₄ supersaturation indicates that CH₄ is present in dissolved and in gaseous phase. Therefore 25 - 45 cm sediment depth seems to be the depth range where most CH₄ production occurs. This interpretation is also supported by the determined noble gas concentrations in this layer, which are strongly depleted relative to ASW concentration. As mentioned previously such a noble gas depletion pattern (with light noble gases being more depleted than heavy noble gases) indicates that noble gases have been stripped out of the sediment pore water by gas bubbles formed in the sediment. Up to a sediment depth of 45 cm the Ar isotope ratio determined in the pore water (Fig. 6.2, panel B) is not significantly fractionated relative to the Ar isotope ratio of air saturated water (ASW; see Beyerle et al., 2000).

Below 45 cm: In this lower layer CH₄ concentrations were found to be in the range of CH₄-local. The noble gases are strongly depleted relative to ASW, but no trend with increasing sediment depth can be observed (i.e. noble gas concentrations determined at different sediment depths are in a similar range). The ³⁶Ar/⁴⁰Ar ratio at a sediment depth of 45 - 55 cm is lower with regards to ASW ratio, i.e. indicating depletion of light isotopes, which might point to secondary gas exchange of dissolved noble gases with gas bubbles that escaped before reaching an equilibrium with the surrounding pore water (diffusion controlled noble gas stripping; Brennwald et al., 2005). It should be noted that observed elemental and isotopic fractionation in this lower layer (45 - 50 cm) do not add for the quantification of CH₄ emissions from the layer of most active CH₄ formation (25 - 45 cm) as the noble gas concentrations are depleted but constant and therefore there is only negligible transport from the lower layer.

Quantification of the methane emission

The CH₄ emissions from Lake Rotsee were quantified by means of a mass balance approach, combining the results of noble gas and CH₄ analysis.

During 2008 and 2013 very similar profiles of CH₄ and noble gas concentrations were observed in the sediment pore water of Lake Rotsee (see Chapt. 5 and Tyroller et al.,

2016). Therefore noble gas and CH₄ concentrations are assumed to be virtually stable over a time scale of a few years, and the associated CH₄ and noble gas fluxes are assumed to be operating in steady state. Thus the concentration gradient of noble gases observed in the upper sediment layer is interpreted to be the result of the continuous (i.e. steady state) noble gas diffusion from the lake water at the sediment/water interface (ASW concentration) to the zone of maximum CH₄ supersaturation (noble gas depletion relative to ASW concentration). Furthermore it is assumed that gas bubbles containing noble gases are virtually continuously degassing from this zone of CH₄ supersaturation (25 - 45 cm) as a result of virtually continuous CH₄ production. Assuming that the system is operating in steady state, the continuous diffusive transport of noble gases from the sediment/water interface to the zone of active CH₄ bubble formation ($F_{\text{NG}}^{\text{diff-in}}$) is equal to the continuous flux of noble gases stripped out of the sediment ($F_{\text{NG}}^{\text{ebu-out}}$) in response to the gas bubbles leaving the zone of maximum CH₄ concentration in the sediment:

$$F_{\text{NG}}^{\text{diff-in}} = F_{\text{NG}}^{\text{ebu-out}} \quad (6.1)$$

where $F_{\text{NG}}^{\text{diff-in}}$ is the downward noble gas flux from the sediment/water interface to the zone of active CH₄ production at approximately 25 - 45 cm sediment depth and $F_{\text{NG}}^{\text{ebu-out}}$ the upward noble gas flux in response to bubble emission from this zone of active CH₄ production.

The downward noble gas flux $F_{\text{NG}}^{\text{diff-in}}$ was calculated from Eq. 2.5 (i.e. Fick's first law of diffusion) whereby the concentration gradient of the respective noble gas species in the sediment pore water was obtained by linear regression to the respective noble gas profiles (see Fig. 6.3). The molecular diffusivity of the respective noble gas was calculated for the bottom lake water temperature of approximately 279 K (6 °C; see Tab. 2.3 and Jähne et al., 1987a) and adjusted for tortuosity (Maerki et al., 2004) taking into account the sediment porosity (see Eq. 2.5 and 2.6). The distance of diffusive exchange is given by the sediment depth of maximum CH₄ concentrations and noble gas depletion (i.e. the mean sediment depth of the two measured CH₄ peaks: ~ 35 cm, see Fig. 6.3). As CH₄ is continuously produced in the sediment and because it is hardly soluble it is expected to be quantitatively predominant in the gas phase formed in the sediment. It has been shown that there is a positive relationship between the amount of emitted gas bubbles from lacustrine sediments and the partial pressure of CH₄ in the emitted bubbles (Chanton et al., 1989). The strong CH₄ production is expected to lead to a frequent bubble formation in the sediment and stripping of other dissolved gases (e.g. N₂, noble gases) from the pore water, whereby an equilibrium between the concentrations in the pore water and the gas phase is established. This equilibrated free gas phase degasses continuously from the CH₄ production zone. Due to the strong CH₄ production in the sediment of Lake Rotsee the partial pressure of CH₄ in the gas bubbles formed in the sediment is assumed to virtually agree with the total gas pressure in the bubble (P_{tot}) at the respective sediment depth (i.e. the total ambient pressure in the sediment). The partial pressure of the noble gas (P_{NG}) in the gas bubbles was calculated with Henry's law (Eq. 2.1) and the measured pore water concentrations. The flux ratio of CH₄ and noble gas species ($F_{\text{CH}_4}^{\text{ebu-out}}/F_{\text{NG}}^{\text{ebu-out}}$) during steady state agrees with the respective partial pressure ratio of CH₄ and noble gases ($P_{\text{CH}_4}/P_{\text{NG}}$; as according to 1. Fick's law the flux is proportional to the concentration):

$$\frac{F_{\text{CH}_4}^{\text{ebu-out}}}{F_{\text{NG}}^{\text{ebu-out}}} = \frac{P_{\text{CH}_4}}{P_{\text{NG}}} \quad (6.2)$$

By combining Eq. 6.1 and Eq. 6.3 the CH_4 flux via ebullition from the sediment to the overlying water column is calculated (Tab. 6.1) as follows:

$$F_{\text{CH}_4}^{\text{ebu-out}} = \frac{P_{\text{CH}_4}}{P_{\text{NG}}} \cdot F_{\text{NG}}^{\text{diff-in}} \quad (6.3)$$

Tab. 6.1 shows the CH_4 fluxes calculated from the respective concentration gradient observed for each noble gas (Ne, Ar, Kr, Xe; see Fig. 6.3). As a result of the previously made simplifications the CH_4 flux might still be underestimated. In the light of the made assumption, that the noble gas flux is linked to the emitted CH_4 flux, underestimating the noble gas flux to the active zone does result in an underestimation of the emitted CH_4 flux. For example this rough estimate does not account for the transport of noble gases from the deeper sediments to the layer of active bubble formation by molecular diffusion. However, it is noted again that the diffusive transport from below is assumed to be virtually zero as there is virtually no concentration gradient with depth and therefore the respective noble gas fluxes are negligibly low. Bubbles in the sediment pore space have been shown to enhance the gas transport of hardly soluble gases (e.g. noble gases) through the sediment pore water significantly (see Flury et al., 2015). Thus in principle a free gas phase could result in an elevated noble gas flux from the water/sediment interface to the layer of maximum CH_4 emission. However, as free gas phase is only expected at the zone of maximum CH_4 concentrations ($z > 35$ cm, see Chapt. 5, Tyroller et al., 2016) and above this zone the CH_4 concentrations are not significantly over-saturated relative to the local saturation concentration, hence only few free gas bubbles might be formed. Another point which might lead to underestimating the CH_4 flux is incomplete equilibration of CH_4 bubbles with the surrounding pore water before being emitted from the sediment pore space. If a bubble does not reach equilibrium with the gases dissolved in the surrounding pore water the partial pressure ratio between CH_4 and noble gases ($P_{\text{CH}_4}/P_{\text{NG}}$) in such bubbles might be higher. In that case the upward CH_4 flux might exceed the results calculated with the approach presented here. However, bubbles leaving the sediment before equilibration cause a kinetic fractionation of Ar isotopes in the surrounding pore water (whereby $^{36}\text{Ar}/^{40}\text{Ar} < \text{ASW}$). Such an Ar isotope fractionation, in favour of the heavier ^{40}Ar isotope is not observed in the relevant upper layer of the sediment indicating that the emission of not equilibrated bubbles is of minor relevance.

Therefore it is concluded that the CH_4 flux presented here is a minimum flux but represents a good approximation of the real CH_4 flux. The CH_4 flux from the sediment to the overlying water column is expressed as the mean value of the fluxes calculated from the individual concentration gradients of Ne - Xe (mean CH_4 flux_{Ne-Xe} = 3.3 ± 1.1 mmol·m⁻²·d⁻¹, see Tab. 6.1). However, the CH_4 flux calculated based on the Ne concentrations is found to be considerably lower than the flux calculated for the other noble gases, which results from the less pronounced concentration gradient of Ne in comparison to the heavier noble gases Ar - Xe (see Fig. 6.3). The Ne concentrations determined in the upper centimetres of the sediment seem to be more depleted than the concentrations of the other atmospheric noble gases. This might point to the fact that the bubbles formed at a sediment depth of 25 - 45 cm are not completely equilibrated with the surrounding

Table 6.1: CH₄ emissions from the sediment pore water of Lake Rotsee calculated from the concentration gradient of the respective noble gas. The uncertainties were estimated using error propagation.

Noble gas:	CH ₄ ebullition flux [mmol·m ⁻² ·d ⁻¹]:
Ne	1.6 ± 0.4
Ar	4.1 ± 0.7
Kr	3.6 ± 0.6
Xe	3.7 ± 0.7

pore water (see before). It might further be possible that small gas bubbles might also be formed in the upper layer of the sediment and might be emitted more quickly as the sediment is less compacted. Such bubble dynamics in the uppermost sediment column is expected to affect Ne more than the heavier noble gases (i.e. Ar, Kr, Xe). Ne, being a light noble gas, is less soluble in water and hence more sensitive to secondary gas exchange with a free gas phase than the heavier noble gases (Ballentine and Burnard, 2002; Holzner et al., 2004; Brennwald et al., 2005).

The CH₄ fluxes calculated based on concentration gradients of Ar, Kr and Xe, agree with each other within the error: mean CH₄ flux_{Ar-Xe} = 3.8 [mmol·m⁻²·d⁻¹] ± 0.3, (1-sigma deviation, not considering Ne) was calculated not considering the Ne - CH₄ flux. It is noted again that the determined CH₄ fluxes represent minimum values, as, for example, diffusive transport from below and Ne - CH₄ flux are not accounted for.

In the literature the CH₄ flux from the sediment to the lake water are often quoted as total CH₄ flux, which is the sum of the CH₄ flux via diffusion and the CH₄ flux via ebullition (Bastviken et al., 2008). To compare our determined minimum CH₄ flux via ebullition with some available studies, we try to calculate the CH₄ flux via diffusive from the sediment to the lake water from the CH₄ concentrations determined in the pore waters of Lake Rotsee. As the spatial resolution of our CH₄ measurements in the upper centimetre of the sediment column is not high enough to directly determine a CH₄ gradient, we roughly approximate the relevant CH₄ gradient from the CH₄ concentration determined at 10 cm sediment depth. The diffusive flux was estimated to be ~ 1.3 mmol·m⁻²·d⁻¹, about 1/3 of the observed CH₄ flux via ebullition. However, it is noted that this is the minimum diffusive CH₄ flux from the sediments of Lake Rotsee, because the exact distribution of CH₄ between pore water and bubbles in the sediment pore space is unknown.

The total CH₄ flux from Lake Rotsee was calculated adding up the estimated diffusive flux and the mean CH₄ flux_{Ar-Xe} via ebullition, ~ 5.1 mmol·m⁻²·d⁻¹. The total CH₄ flux agrees with the range of CH₄ fluxes through the sediment/water interface in North American lakes (4.5 - 6.1 mmol·m⁻²·d⁻¹, Bastviken et al., 2008). In the Swiss Lake Wohlen higher CH₄ fluxes from the sediments were reported (~ 9.3 mmol·m⁻²·d⁻¹, Del Sontro et al., 2010). In a previous study on Lake Rotsee (Schubert et al., 2012) CH₄ fluxes through

the water/air interface to the atmosphere were determined during peak emissions during the mixing of the water column in wintertime. Although this “atmospheric” CH_4 flux of $\sim 4 \text{ mmol}\cdot\text{m}^{-2}\cdot\text{d}^{-1}$ is not directly comparable to our results, due to the unknown CH_4 consumption within the water column of Lake Rotsee, the two estimates reasonably agree.

As the noble gas distribution within the sediment column of Lake Rotsee virtually remain constant on the time scale of several years we are tempted to interpret our data from three sediment cores to be representative for the entire lake, particularly as its sediments are rather homogeneous in space.

6.4.2 Noble gas data from Lake Lungern

Lake Lungern is characterized by an elevated trophic status and it is subject to extreme water level variations due to its utilization as a hydropower reservoir. This water level variation is seasonal, whereby the water level is high in the summer and low in the wintertime ($\sim 15 - 20$ m below the summer water level).

In summer during a stable high water level an echosounder survey (see e.g. Del Sontro et al., 2010) of the lake bed of Lake Lungern was conducted. During this sonar survey active gas bubble emission was observed in the southern part of the lake in the region of two inflowing rivers (see Fig. 6.2). The zone of inflowing rivers, i.e. river/reservoir (or river/lake) transition, has often be reported to be the zone of most active CH_4 emission (e.g. Del Sontro et al., 2011; Harrison et al., 2017; Beaulieu et al., 2017). Sediment samples from different sites were taken to analyse the gas dynamics related to the observed active CH_4 ebullition in the southern part of Lake Lungern and to study the seasonal variability (in response to seasonal lake level changes).

The characteristics of each sampling point are described in the following:

- **A1/A2** sampled during high water level in summertime, whereby at site A1 sonar did not detect any bubbles, but at site A2 active bubble emission was observed (see Fig. 6.2, 6.4 and 6.5)
- **C** sampled during low water level in wintertime (5 cm overlying water column, see Fig. 6.2 and 6.4 C)
- **D** sampled during rising water level in June 2015 from a site that had been fallen dry during winter (see Fig. 6.2 and 6.4 D)

In the following the results of the individual noble gas analysis at each sampling point are discussed:

A1: As the sonar survey did not yield any sign of active gas bubble emission, sampling site A1 was chosen to be representative for the “background” noble gas concentration in the sediments of the southern part of Lake Lungern. Although in the retrieved sediment core no bubbles were observed by eye, the uppermost 10 cm of the sediment show noble gas concentrations to be depleted relative to ASW. Most likely the depletion results from past secondary gas exchange between noble gases dissolved in the pore water with gas bubbles formed in the sediment and subsequent bubbles emission (see Sect. 6.4.1).

A2: In the southern part of Lake Lungern the sediments are composed of a complex interlayering of sands and fine grained loam (see Fig. 6.5). These different layers are expected to be characterised by a different permeability for gases. During low water level in the winter a partial erosion of the dry sediment was observed. The inflowing rivers carved trenches in the sediment (see Fig. 6.5). In summer during high water level these trenches were well detectable by echo-sounding and an active and continuous bubble emission was observed from the bottom of these trenches (see Fig. 6.5, panel E). These spots of continuous gas emission were detected in several sampling campaigns in different years (2012, 2013). Three sediment cores were taken at such active spots by precisely positioning the gravity corer with the aid of the echosounder (see Fig. 6.5, panel G). In addition, gas bubbles were collected with a funnel, which was also precisely placed over the active site using a side scan sonar.

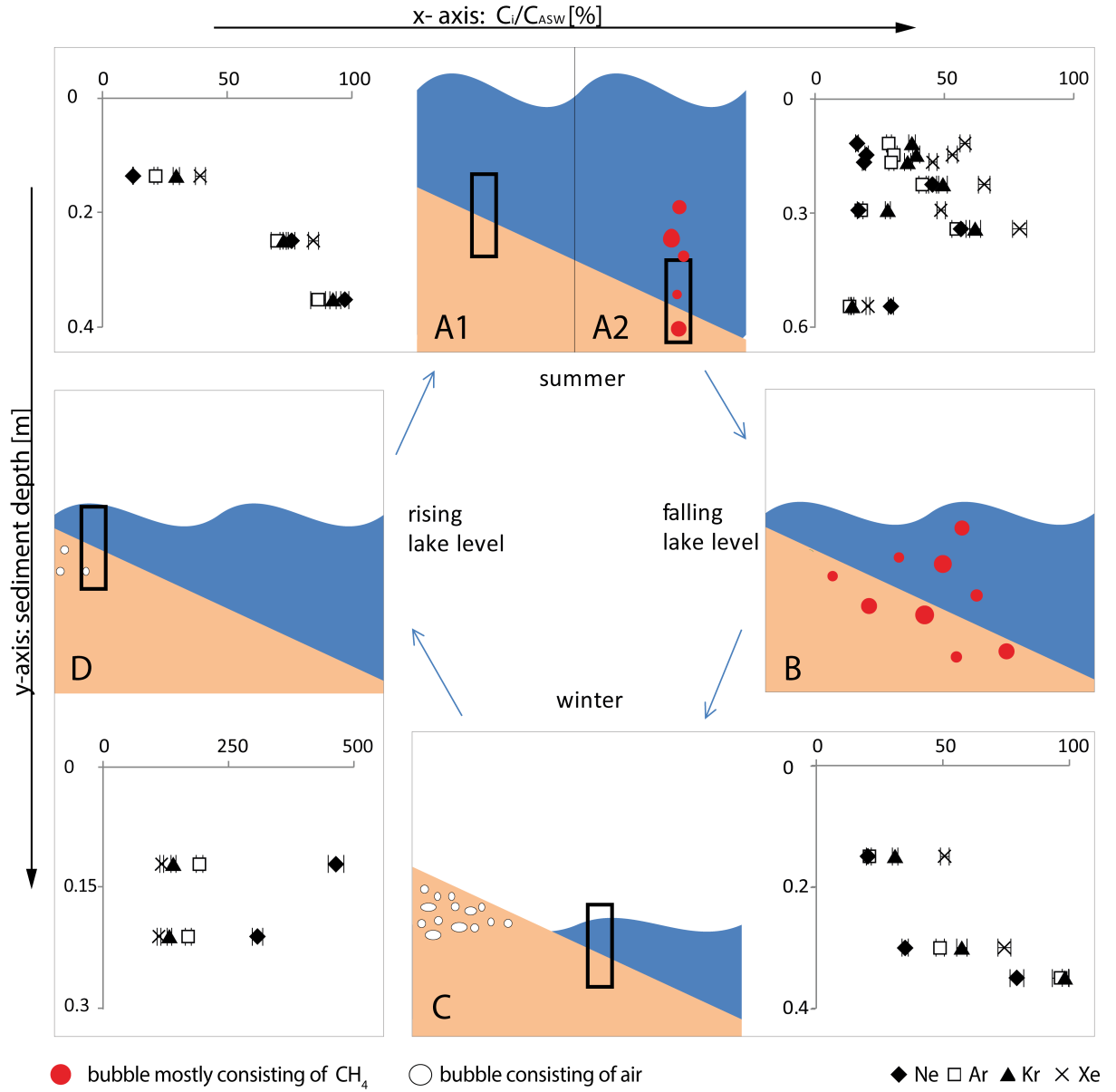


Figure 6.4: Gas dynamics in Lake Lungern. Graphs showing the determined noble gas concentrations versus sediment depth, are combined with a conceptual drawing of the bubble dynamics in Lake Lungern (where the lake water is presented in blue, the sediment in orange and the position of sampled sediment cores are marked as black rectangle): **A1**. During summer the water level is at its highest and virtually stable from June to September. **A2**. At some locations CH_4 is emitted virtually continuously. **B**. During lake level lowering the pressure release in the sediment results in bubble formation and emission. **C**. The lake level is at its lowest in winter and early spring, when part of the sediment is falling dry and is exposed to the atmosphere, i.e. air partly enters the sediment. **D**. With rising water level air gets entrapped in the sediment.

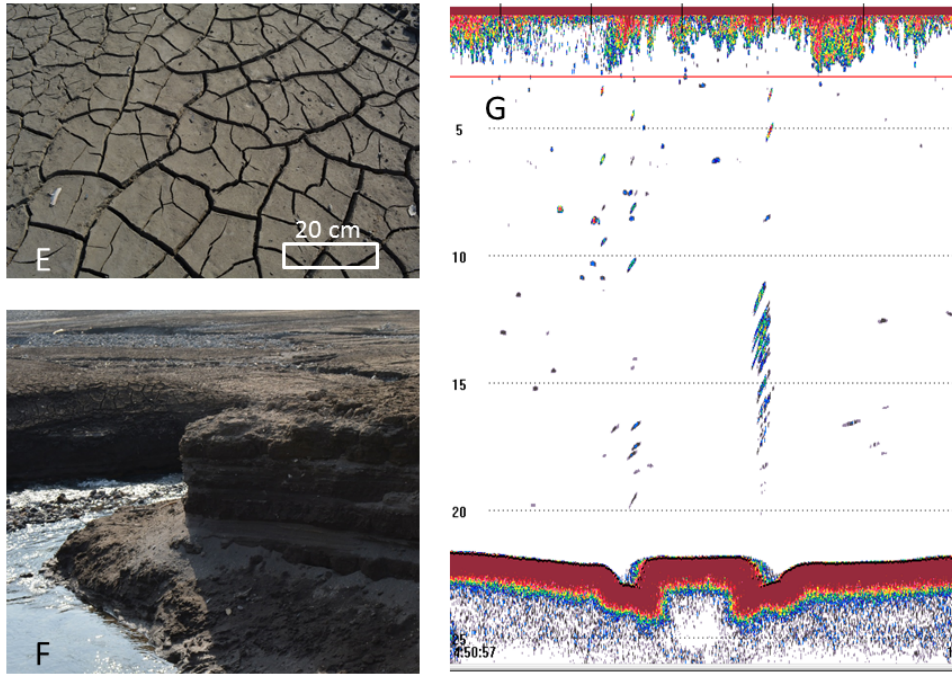


Figure 6.5: **E** Dry sediments of Lake Lungern in winter 2015 during low water level. **F** Inflowing river and sediment layers excavated by the inflowing river during low water level (2015). **G** Side scan sonar image with spots of active bubble emission near site A2 (see Fig. 6.2 and 6.4) in Lake Lungern (2012). Rising bubbles appear as parallel sloped stripes.

Noble gas concentrations in the sediment pore water were found to be strongly depleted relative to the expected ASW concentration throughout all sediment cores. This pronounced depletion indicates that the gas emissions from this spot (A2) are significantly stronger than at the background position (A1). The gas collected in the funnel consisted mainly of CH_4 gas and did not contain measurable amounts of noble gases. The absence of noble gases in the collected bubbles indicates that the gas might derive from a sediment layer where noble gases are strongly depleted as a result of continuous stripping with gas bubbles leaving the sediment. Furthermore the absence of noble gases argues for a biological origin of the CH_4 gas, as elevated He concentrations would be expected in deep terrigenous gas (e.g. Etiope and Klusman, 2002). Indeed the captured CH_4 was found to be isotopically light ($\delta^{13}\text{C} \approx -63 \text{ ‰}$). These results contradict the earlier interpretation suggesting the emitted CH_4 might originate from “fossile methane penetrating the sediment from below” (Bossard and Gächter, 1981).

Accounting for the heterogeneity of the sediment structure (see Fig. 6.5) we hypothesize that the virtually continuous bubble flux emitted from the trenches in the southern part of Lake Lungern (see Fig. 6.5, panel G), consists mainly of microbial CH_4 gas accumulating beneath a hardly permeable sediment layer, e.g. clay layer. If this low permeable layer is “missing”, e.g. it is eroded by the inflowing river, CH_4 can escape along preferential pathways forming the observed virtually continuous gas emission.

C: Similar to A1 no active bubble emission was observed at site C during high water

level in summer. However, the sediments were sampled during wintertime when the lake water level was at its lowest. Due to the low winter temperatures (between + 4 and - 5 °C) the biological activity in the sediment was assumed to be negligible (Duc et al., 2010). However, the CH₄ concentrations in the sediment were found to follow closely the local saturation concentration, i.e. the ambient partial pressure in the sediment (see Chapt. 5, Fig. 5.3 and Tyroller et al., 2016). Such elevated CH₄ concentrations were interpreted as remaining from the production in the warmer season, whereas the formed bubbles had escaped during water level lowering (see Chapt. 5, Fig. 5.3 and Tyroller et al., 2016). Noble gas concentrations were found to be depleted with regard to the ASW concentration up to a sediment depth of 40 cm. This depletion pattern is interpreted to be a result of enhanced CH₄ bubble formation caused by the pressure release during lowering of the lake level. Compared to A1, the noble gas concentrations at site C show a stronger depletion. Such more pronounced depletion of noble gases might result from lake level lowering, as water draw down is expected to enhance the CH₄ emission and noble gas stripping. Even acknowledging that our data set (one core at high and one core at low lake level) is very limited and not really representative for the lake, the results tend to indicate that water level lowering and enhanced gas ebullition from the sediment are linked. A recently published study using passive gas traps to determine CH₄ flux from North American reservoirs found emissions to increase by up to ~ 80 % during lake level lowering (Beaulieu et al., 2017). It is noted that the continuous monitoring of the CH₄ emissions upon lake level draw down with common methods (Beaulieu et al., 2017; Harrison et al., 2017) is time consuming and labour intensive. Thus noble gas analysis in the pore water of lacustrine sediments at different lake level (e.g. before and after reservoir draw down) opens a novel experimental route to study the dynamics of gas ebullition in response to lake level changes.

D: Sediment cores were taken in June 2015 in the littoral zone (< 9 m water depth) in an area that had fallen dry in winter time, i.e. “winter-dry” sediment. Due to its the highly compacted texture only the uppermost 15 centimetres of the sediment column could be sampled by gravity coring. It is further noted that the surplus of air is observed repeatedly at site D and in all respective samples. A surplus of air could indicate a contamination with air, however as “air contamination” is expected at single samples in rather erratic manner, but not systematically in all samples, we are tempted to interpret the observed air excess in the sediments as real signal of the pore water at site D. Further it is noted that the method used here for the determination of noble gases dissolved in sediment pore waters has been shown to be very robust against gas exchange with the atmosphere and thus to be protective against contamination with air (Brennwald et al., 2013b). The pore waters are not only supersaturated with air, but the noble gases also show an elemental fractionation in favour of light noble gas ($\Delta\text{He} > \Delta\text{Ne} > \Delta\text{Ar} > \Delta\text{Kr} > \Delta\text{Xe}$, whereby Δi is the relative deviation from ASW). Such fractionation is characteristic for excess-air resulting from re-dissolution of air bubbles entrapped in water upon a rising hydrostatic pressure (e.g. excess-air formation in groundwater, for reviews see Kipfer et al., 2002; Aeschbach-Hertig and Solomon, 2013, and references therein). The fact that site D had fallen dry in the winter season suggests that the observed noble gas excess might result from air, that entered the sediment pore space. During a rise in the water level this air is entrapped. Subsequently, in consequence of the rising water level the

in situ hydrostatic pressure in the sediment increases (e.g. 0.1 atm per meter overlying water column) and the entrapped air bubbles (partly) redissolve, causing the observed noble gas excess in the surrounding pore water.

Although admitting the given interpretation is rather speculative it seems to be supported by the results from a previous hydroacoustic survey on Lake Lungern in July 2006 (Ostrovsky, 2009). This study report very small bubbles to be emitted from the littoral zone (< 7 m water depth). There the oxygen concentration in the surrounding lake water was found to be extremely oversaturated with oxygen (160 to 170 %). As strong microbial gas production in the sediment pore water is unlikely in such an oxigenic environment, we suggest that the observed bubbles might not consist of CH_4 , but of air escaping from the recently submerged sediment being loaded with excess air during times of rising reservoir level. During the ascent of such small bubbles air exchanges with the surrounding water leaving the observed oxygen excess (see Holzner et al., 2012).

Oxygen as primary electron source is rapidly consumed by micro-organism in the sediment pore water and thus its dynamics cannot easily be determined directly. In reservoirs like Lake Lungern being subject to strong lake level variations, noble gases are an excellent tool to trace the amount of oxygen entering the sediment pore water by the direct injection of air in the sediments as a result of dry falling during low water level. The “winter-dry” sediments of Lake Lungern receive a significant load of oxygen entering the sediment pore water as a component of the entrapped air that partly redissolves during the rising lake level.

Accepted methods allow to convert the noble gas concentrations in different components (e.g. ASW and injected amount of air (A), for details refer to Kipfer et al., 2002; Aeschbach-Hertig and Solomon, 2013). The amount of entrapped air, or excess-air (A [ccSTP/g]), that was injected into the sediment was quantified by applying the closed-equilibrium model (Aeschbach-Hertig et al., 2000) accounting for excess air using the conversion code noble 90 (Aeschbach-Hertig et al., 1999, 2000; Kipfer et al., 2002).

The numerical exercise to convert atmospheric (noble) gas concentrations into different components allows to estimate that between 4 and 25 mg O_2 dissolved per litre of pore water in response to excess air formation. Thus this study makes the case that noble gas analysis in pore water of sediments might facilitate to quantify the amount of O_2 supplied to the sediment pore water as a result of excess air formation in response to seasonal water level variation in a reservoir.

6.5 Conclusions

The noble gas concentrations in the pore waters of Lake Rotsee and Lake Lungern are strongly affected by the formation of gas voids in the pore water and the subsequent emission of the free gas from the sediment in form of bubbles.

In the hypertrophic sediments of Lake Rotsee gas bubble formation is mainly driven by the microbial activity in the sediment pore water and the zone of maximum microbial activity, i.e. the zone of maximum CH_4 production, was determined to lie in between 25 - 45 cm sediment depth. A pronounced concentration gradient of noble gases, from ASW concentrations at the water/sediment interface to a strong depletion of noble gases relative to ASW concentrations in the zone of maximum microbial activity, was observed. The depleted noble gas concentrations in the pore water indicate stripping of dissolved gases by escaping gas bubbles. The gradient of increasing noble gas depletion with sediment depth can be interpreted to reflect the noble gas flux through the pore water and into the gas bubbles formed in the zone of maximum microbial activity. The noble gas gradient and the CH_4 peak were repeatedly determined in different years indicating steady state. This allowed the CH_4 flux from the sediment to the lake water to be calculated. The determined minimum CH_4 flux (diffusion + ebullition) from the sediment ($5.1 \text{ mmol}\cdot\text{m}^{-2}\cdot\text{d}^{-1}$) fall well in the range of available CH_4 fluxes from other lakes ($4.5 - 6.1 \text{ mmol}\cdot\text{m}^{-2}\cdot\text{d}^{-1}$, see Bastviken et al., 2008) and agree with the range of CH_4 emissions measured at the lake surface of Lake Rotsee ($4 \text{ mmol}\cdot\text{m}^{-2}\cdot\text{d}^{-1}$, Schubert et al., 2012).

In Lake Lungern gas bubble formation in the pore water is triggered by the seasonal variation of the lake water level. The gas dynamics being linked to the seasonal and spatial variability in the lake were depicted by analysing noble gases dissolved in the pore water. A virtually continuous bubble flux, mainly CH_4 , was observed to be emitted from disruptions in the sediment floor of Lake Lungern. The absence of noble gases and the light isotope composition indicate in contrast to previous studies (Bossard and Gächter, 1981) the CH_4 to be mainly of local biogenic origin. The decreasing lake level appears to trigger CH_4 bubble emission as a result of release of hydraulic pressure and this pressure release was linked to the observed depletion of noble gas concentrations determined in the sediment of the southern part of Lake Lungern. At coastal sites that had been falling dry during low water level a noble gas excess was determined and interpreted to result from air being entrapped and being redissolved in the pore water when water level is rising again. The initial oxygen concentration being dissolved in the sediment pore water by “dry falling” and by subsequent excess air formation, was found to be larger than the expected oxygen concentration in the open lake water.

Overall the combination of CH_4 and noble gas concentrations was shown to be a promising tool to trace gas dynamics in sediments. For the first time excess-air deriving from lake water level variations was observed in lacustrine sediments. The presence of CH_4 bubbles was found to strongly affect the noble gas composition in the sediment causing a depletion of noble gases.

Chapter 7

Pilot study: Noble gas concentrations in a deep clay sediment layer of Lake Zurich

7.1 Introduction

In the past decade lacustrine and oceanic sediments have been established as noble gas archives for environmental studies (for a review see Brennwald et al., 2013b). Restricted vertical transport of noble gases dissolved in the sediment pore water is a necessary prerequisite for using such noble gases as tracer for past environmental conditions. In previous studies it has been shown that noble gases can be quantitatively trapped in the pore space of some sediments over large periods in time (e.g. Brennwald et al., 2005; Pitre and Pinti, 2010; Tomonaga, 2010) and that in such sediments diffusive transport of noble gases in the pore water is strongly suppressed. This results in a stratigraphically controlled noble gas record in the sediment pore water. Among other parameters the pore radii and pore connectivity were assumed to be decisive for diffusion suppression (see Brennwald et al., 2013b). Thus in clay sediments, commonly characterised by a very low permeability, a low pore interconnectivity and small pore radii, molecular diffusion of noble gases in the pore water is expected to be strongly suppressed or even inhibited (Horseman et al., 1996). To test the extent of diffusion suppression in glacial clay sediments an exploratory study was conducted at a clay layer of Lake Zurich, which inferred from its depositional environment is assumed to date back to before the Glacial-Holocene transition (Boner et al., 1999). Furthermore with this pilot study it was aimed to gain information about de-glaciation and the past environmental conditions during clay deposition in Lake Zurich.

7.2 Study site

Lake Zurich is the fifth biggest pre-alpine lake in Switzerland. Sediment samples were taken from a site approximately 40 m below water surface at a steep slope close to Wädenswil and Stäfa (47°14'09.375"N, 8°41'38.360"E). Previously it has been discovered by seismic profiles that this site had been affected by erosion (Boner et al., 1999; Strasser and Anselmetti, 2008). Therefore this deep clay layer, which in other parts of the lake is

overlain by a 20 m sediment column, is exposed. Assuming standard sedimentation rates, this layer was estimated to be older than the late Glacial-Holocene transition (Boner et al., 1999; Strasser and Anselmetti, 2008).

7.3 Methods

As the targeted clay layer crops out near the sediment/water interface it can be sampled by simple gravity coring. Three short sediment cores of approximately one meter length were retrieved. One sediment core was used to determine the density profile by the GEOTEK Multi-Sensor Core Logger (MSCL), which was used for the non-destructive measurement of the bulk density with a gamma ray sensor. Afterwards this core was cut and photographed. The second sediment core was sampled for noble gas analysis by means of the copper tube centrifugation method (Brennwald et al., 2003; Tomonaga et al., 2011a). Subsequently the noble gas concentrations in the sediment samples were determined by standard protocols of mass spectroscopy for noble gas analysis in water (Beyerle et al., 2000) at the noble gas laboratory at ETH Zurich. The third sediment core was cut and divided into sub-samples which were dried to determine the porosity and were used for the later radioisotope analysis (e.g. gamma-ray spectroscopy for the determination of the α emitter U and Th).

7.4 Results

The sampled sediment cores show a clear division in two sections: a recent muddy sediment layer at the top and an older compacted clay layer below. The upper dark and muddy layer extends to a depth of 15 cm. It is assumed to have been deposited after the landslide that uncovered the old clay layer below. At 15 cm the sediment properties, e.g. density, colour and radio-isotopic composition, change abruptly (see Fig. 7.1). Below 15 cm the sediment consists of compacted clay, which is of light colour, rather homogeneous and not laminated. A previous study at this sampling location found the same distinct and abrupt changes of the sediment properties and interpreted them to mark the transition of recent lacustrine sedimentation to a very different and older regime of clay deposition (Boner et al., 1999).

Noble gas concentrations were determined in the clay layer below 15 cm only. In the upper recent sediment no samples for noble gas analysis could be obtained. However, it can reasonably be assumed that atmospheric noble gas concentrations agree with ASW concentrations, as it is commonly the case in recently deposited unconsolidated sediments with high water content (Brennwald et al., 2013b). The most striking noble gas pattern of the clay layer are the high He concentrations, which strongly exceed ASW concentration (up to one order of magnitude see Fig. 7.1, Graph D). The noble gas pattern (see Fig. 7.1, panel B) and three element plots (see Fig. 7.2, panel F & G) suggest two different noble gas clusters in the clay layer. From 15 to 60 cm the shape of the concentration profiles of the atmospheric noble gases (Ne - Xe) with depth are similar (being highlighted in blue Fig. 7.1 and Fig. 7.3 and subsequently being referred to as the “blue layer”). Below 60 cm the atmospheric noble gases - in contrast to the upper part - are elementally fractionated (this layer is highlighted in grey in Fig. 7.1 and Fig. 7.3 and is subsequently referred to

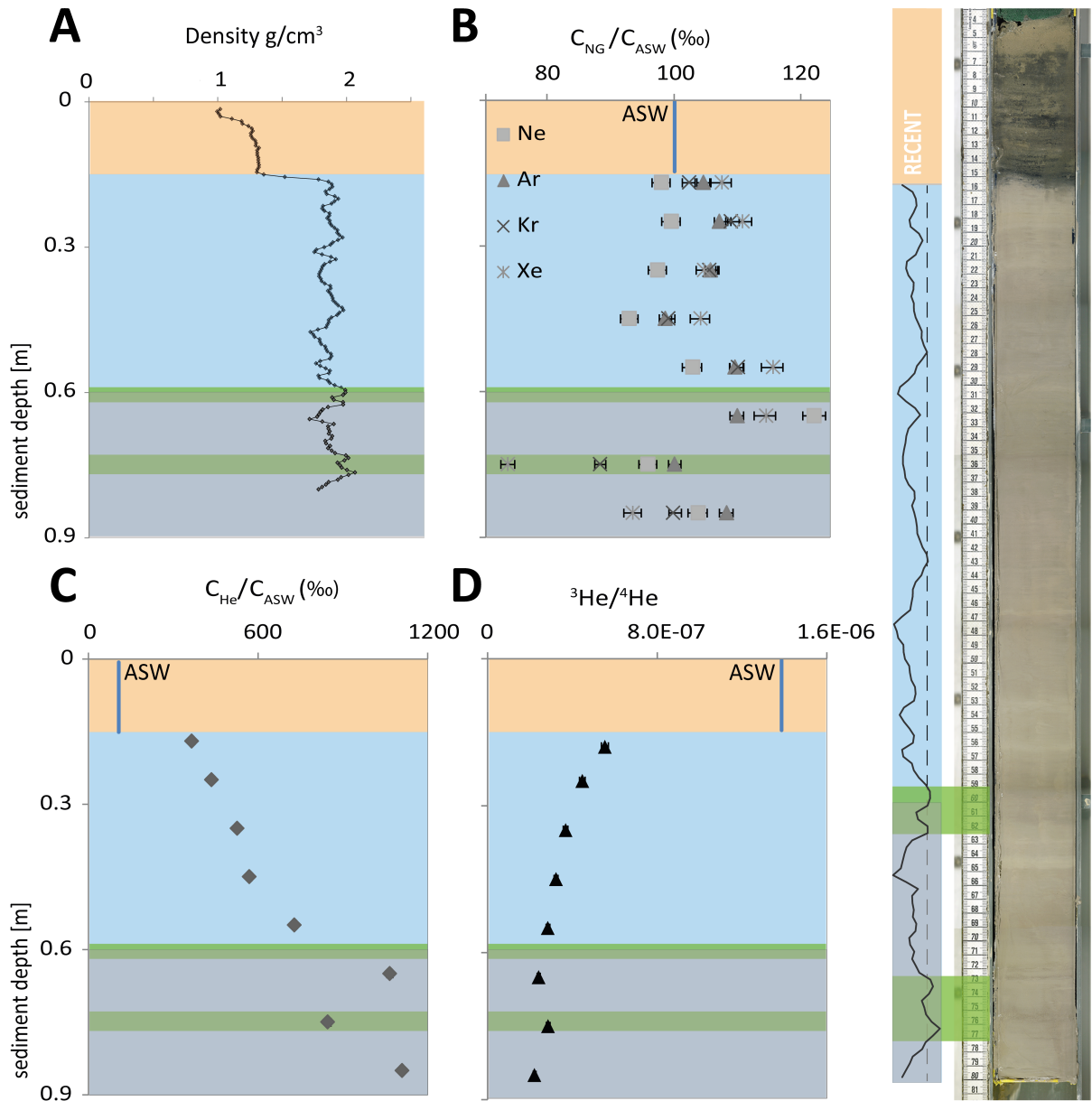


Figure 7.1: **A** The density profile of the sediment core sampled in Lake Zurich in June 2014 plotted against sediment depth. **B** Shows the noble gas concentration of Ne, Ar, Kr and Xe in the sediment pore water relative to the ASW concentration in percent plotted versus sediment depth (100 % is the ASW concentration for 278 K). **C** The He concentration in the sediment pore water (diamonds) relative to the ASW concentration (continuous line) in percent plotted versus sediment depth. **D** $^3\text{He}/^4\text{He}$ ratio (triangle) depth profile, where the continuous line is the $^3\text{He}/^4\text{He}$ ratio in air saturated water. **On the right:** Picture of the cross section of the sediment core and the respective density curve. At a sediment depth between 59 - 63 cm and between 73 - 78 cm peaks in density are observed whereby the density exceeded 2 g/cc (intermittent line). The more recent brownish black sediment (0 - 15 cm) is marked in yellow in the graphs. The older light grey clay (15 - 80 cm) is divided in two layers. The upper layer (15 - 60 cm) is marked in blue, the lower layer (60 - 90 cm) in grey and the density peaks are highlighted in green.

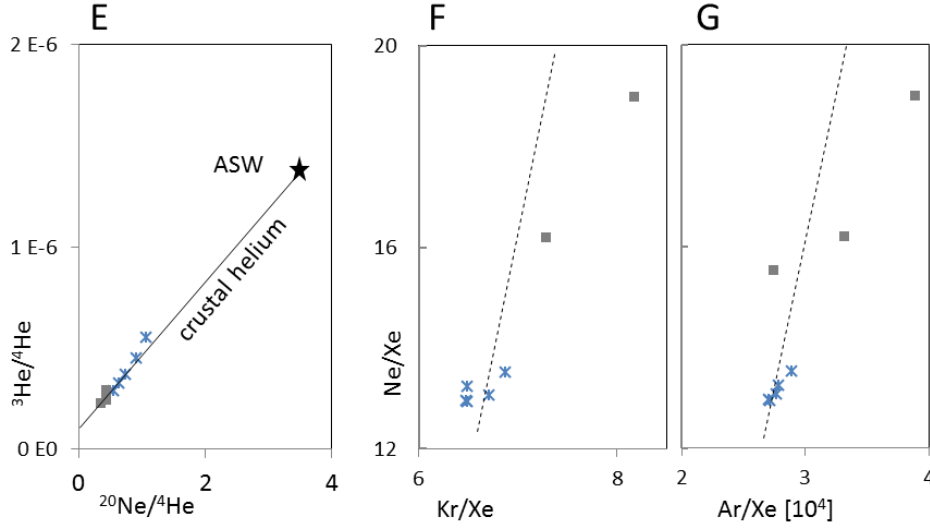


Figure 7.2: **E** The three isotope plot of $^3\text{He}/^4\text{He}$ versus $^{20}\text{Ne}/^4\text{He}$ (the star denotes the ratio of ASW) indicates that the excess He is produced by the radioactive decay of U and Th and by secondary nuclear reactions, e.g. $^6\text{Li}(n,\alpha)^3\text{H}$ to ^3He (e.g. Mamyrin and Tolstikhin, 1984; Tolstikhin et al., 1996). **F & G** Three element plots of atmospheric gases in the clay layer (Ne, Ar, Kr, Xe). The intermittent line gives the element ratios in ASW. The samples from the blue layer are marked with blue crosses, those from the grey layer as grey squares.

as the “grey layer”).

In the **blue layer** (15 - 60 cm) Ne is slightly depleted relative to Ar - Xe, which appear to be in atmospheric equilibrium, i.e. concentrations agree reasonably with ASW. This observation is supported by the three element plots, showing that the noble gas ratios in the sediment pore water agree with the respective ASW ratios. He concentrations increase more or less linearly with sediment depth (e.g. between 35 and 45 cm sediment depth He concentrations are quite constant). The $^3\text{He}/^4\text{He}$ ratios are decreasing with increasing sediment depth. Furthermore a slight fractionation of the Ar isotope ratio (1 - 2%) can be observed between 25 and 45 cm.

In the **grey layer**, (60 to 90 cm) a significant fractionation of the atmospheric noble gases is observed, whereby Xe and Kr are depleted relative to Ar and Ne. The noble gas isotope ratios (grey squares in Fig. 7.2, panel F & G) do not coincide with equilibrium ratios of ASW. Furthermore at ~ 60 cm a jump to significantly higher He concentrations is observed. He concentrations are approximately double the concentrations in the blue layer. The $^3\text{He}/^4\text{He}$ ratios in the grey layer are more or less constant and Ar isotope ratios are not fractionated with regards to ASW. Between 59 - 63 cm and between 73 - 77 cm sediment depth peaks in density can be observed (> 2 g/cc, marked in green in Fig. 7.1). The noble gas concentrations significantly change close to these density peaks. The upper density peak (59 - 63 cm) separates a Ne concentration being depleted by - 10%, from a Ne concentration exceeding significantly ASW ($\sim 30\%$). At the density peak between 73 - 77 cm Xe concentrations jump from being supersaturated (+ 15%) to being depleted (- 30%).

7.5 Discussion

The extent of diffusive transport in the clay layer (blue and grey layer) can only be evaluated qualitatively but not quantitatively determined, as the sedimentation rate, the degree of compaction of the clay layer and the point in time when the clay layer was outcropped by the subaquatic landslide are unknown. However, the observed noble gas pattern argues for attenuation of diffusive transport in the sediment pore water. For example, extrapolation of the trend of $^3\text{He}/^4\text{He}$ ratios to the sediment/water interface does not seem to be consistent with the $^3\text{He}/^4\text{He}$ ratio of the bottom water of Lake Zurich, which is expected to be equal to ASW or higher due to ^3He accumulation resulting from ^3H decay. Furthermore He is supersaturated by factor of 3 at the border between recent sediment and clay only 15 cm below the sediment/water interface. This large He concentrations and discontinuity of the trend of $^3\text{He}/^4\text{He}$ ratios at the sediment/water interface give some evidence that molecular transport seems to be suppressed in the clay layer. However, the linear gradients of the He concentrations and $^3\text{He}/^4\text{He}$ ratios also indicate that there is still upward (molecular) transport which operates at steady state. This upward transport might be strongly reduced in comparison to the transport in free water but is still operational. In fact the observed Ar isotope fractionation in the blue layer again indicates that noble gases might be or might have been affected by diffusive transport.

In the lower part of the clay (grey layer) Ar isotope ratios are not fractionated relative to the ASW ratio, which suggests that heavy noble gases (Ar, Kr, Xe) are quantitatively trapped in the pore water. Such possible noble gas entrapment might be related to the density peaks in the grey layer as there the observed shift in noble gas concentrations can be interpreted to indicate a textural barrier where diffusive transport is significantly reduced. Such behaviour is reported from the sediments from the Baltic Sea (Stockholm Archipelago) where a short increase in sediment density (being associated with a turbiditic deposition) lead to textural changes in the pore space which reduced the molecular transport to such a level that it became virtually “zero” (see Tomonaga et al., 2015)

Based on the noble gas data and the sediment properties of the investigated clay sediment of Lake Zurich there are some valuable arguments to assume that diffusive transport is strongly suppressed. Under such conditions noble gas concentrations can be used to reconstruct the environmental conditions, e.g. temperature of the bottom water, prevailing in the lake during clay deposition (see Chapt. 2). Using the accepted concepts to convert atmospheric noble gas concentrations into environmental conditions prevailing during air/water partitioning, as it is commonly done in meteoric water bodies (see Chapt. 2 and reviews, Aeschbach-Hertig et al., 2000), the respective past temperature in the deep water of Lake Zurich were reconstructed for each sampled sediment depth. In the upper clay layer (blue layer) the reconstructed temperatures, during air/water partitioning (e.g. during time of water column mixing), are in a range of 4.4 to 6.5 °C (see Fig. 7.3), which roughly agrees with the modern bottom water temperatures of Lake Zurich (Peeters et al., 2002b). In contrast, in the deeper clay layer (grey layer) noble gas concentrations of most samples cannot be converted in a statistically acceptable manner into water temperatures (for numerical details see Chapt. 2 and reviews, Aeschbach-Hertig et al., 2000). Only if excess-air is accounted for the concentrations of the sample at 65 cm sediment depth yielded a statistically acceptable temperature by applying the CE - modell (Aeschbach-

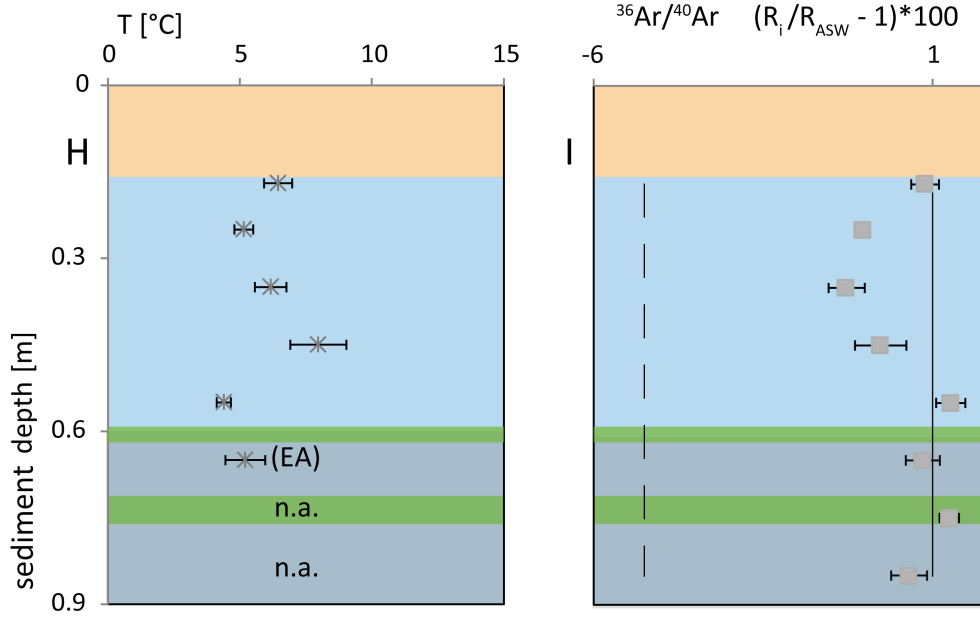


Figure 7.3: **H** Noble gas temperatures fitted with the closed system equilibration (CE) model (Aeschbach-Hertig et al., 2000) for Ne, Ar, Kr and Xe. For the sample at 60 cm excess-air (EA) had to be taken into account to find the temperature. **I** $^{36}\text{Ar}/^{40}\text{Ar}$ isotope ratio profile with sediment depth. The isotope ratios are normalized to the $^{36}\text{Ar}/^{40}\text{Ar}$ ratio of ASW (solid line; Beyerle et al., 2000). The intermittent line shows the maximum fractionation expected upon molecular diffusion in water (Tyroller et al., 2014).

Hertig et al., 2000). The reconstructed temperature of 5.2 °C agreed very well with the range of temperatures reconstructed for the blue layer.

The $^3\text{He}/^4\text{He}$ and $^{20}\text{Ne}/^4\text{He}$ ratios determined in the pore water of the clay layer (grey and blue layer) indicate binary mixing of atmospheric noble gases and a virtually Ne - free He component with a $^3\text{He}/^4\text{He}$ ratio of $\sim 10^{-7}$. The low $^3\text{He}/^4\text{He}$ ratio is indicative for crustal He (produced by radioactive decay of U and Th and secondary induced nuclear reactions, see Fig. 7.2 and e.g. Mamyrin and Tolstikhin, 1984; Tolstikhin et al., 1996). Such isotopic heavy He either derives from in situ production in the sediment or from emanation out of deeper strata. Accepting that diffusion in the glacial clay layer is strongly suppressed it appears reasonable to assume that the He excess, mainly ^4He , primarily originates from in situ production within the clay layer. In that case the time when the pore water was trapped by depositing clay can be approximately scaled from the ^4He concentration of the pore water, the U, Th abundance in sediment matrix, and the density and porosity at the respective sediment depth (e.g. Geyh and Schleicher, 2012, Eq. 2.3). Most of these “U - Th - ^4He ages” in the upper clay (blue layer) fall within a range of 10 to 25 kyr. These “U - Th - ^4He ages” reasonably agree with the age inferred from the depositional environment, dating the sediment back to before the Glacial-Holocene transition (> 10 kyr Boner et al., 1999). In contrast in the lower clay layer (grey layer) “U - Th - ^4He ages” are much larger than the expected age range of deposition of (glacial) clay and therefore it seem unreasonable to interpret the measured He concentration in terms of time. More likely the huge He concentrations indicate that significant amounts of He derive from another source than in situ production and accumulate below the diffusion

barrier (73 - 77 cm). Most likely He generated in deeper strata is diffusing upwards until it reaches less permeable sediment (e.g. 59 - 63 cm and 73 - 77 cm).

Nonetheless in the upper clay layer (blue layer) both the depositional age and “U - Th - ^4He age” - although the age estimates are considerably uncertain - suggest that the observed excess-air at a depth of 65 cm depth in the sediment might be related to glaciation and/or ice dynamics. Glacial melt water is characterized by an excess in atmospheric noble gases (e.g. excess-air) as a result of the dissolution of air trapped in the glacial ice or underneath the ice (Grundl et al., 2013; Hohmann et al., 2002). The entrapment of such air labelled glacial melt water might explain the observed excess air in the upper clay layer. This interpretation that the excess-air signal at 65 cm can be attributed to ice melting is also supported by the observed elemental fractionation of the atmospheric noble gases at that depth. The observed elemental fractionation in favour of light noble gases ($\Delta\text{He} (\text{atmospheric}) > \Delta\text{Ne} > \Delta\text{Ar} > \Delta\text{Kr} > \Delta\text{Xe}$) has been found to be a characteristic of melting ice under the Antarctic ice shield and the injection of this melt water into the Antarctic Weddell Sea (Hohmann et al., 2002). We note that the excess-air signal is observed just in between the density peaks that are assumed to suppress pore water exchange (see before). This observation adds some evidence for effective pore water trapping and thus long conservation of the noble gas concentrations (Tomonaga et al., 2015).

Hence, although caution has to be exercised in drawing a final conclusion, the observation of excess-air in the glacial clay of Lake Zurich might be interpreted to be a result of glacial ice melting. The estimated pore water age (10 - 25 kyr) in the blue layer roughly agrees with the time of the retreat of glacial ice from the basin of Lake Zurich (17 - 18 kyr Lister, 1984). However this interpretation is tentative at best, in the light of the limited number of samples and the considerable uncertainty associated with the U - Th - ^4He method used for pore water dating.

7.6 Conclusions

This study makes the case that diffusive transport in the glacial clay deposits of Lake Zurich seems to be strongly suppressed. The abrupt increase in ^4He abundances at 15 cm sediment depth at the upper onset of the clay layer to concentrations one order of magnitude larger than in the open lake water indicates diffusive pore water exchange to be strongly attenuated. This still tentative findings suggest that lake water and thus noble gases were quantitatively trapped in the pore space during clay deposition. Under such conditions glacial clays are likely to provide an excellent and novel archive for past environmental conditions prevailing in the lake during clay deposition that calls for further investigation. The reconstructed water temperatures from the upper clay layer roughly agree with the expected bottom water temperature in Lake Zurich ($\sim 5^\circ\text{C}$).

A further sharp increase in He and Ne is observed at a sediment depth of 60 cm and is associated with a density peak (59 - 63 cm). This and another density peak (73 - 78 cm) seem to act as transport barrier strongly inhibiting diffusive transport in the pore space similar to the situation in the Stockholm basin in the Baltic Sea (Tomonaga et al., 2015). Between these two density peaks significant amounts of excess-air are observed (e.g. $C_{\text{NG,atm}} > \text{ASW}$). Sedimentological (Boner et al., 1999) and “U - Th - ^4He - age” estimates, indicate clay deposition before the Glacial-Holocene transition. Although caution needs

to be exercised to analyse this data the observed excess of atmospheric gases might be interpreted as input of glacial melt water in the growing lacustrine sediment during the retreat of glacial ice 17 - 18 kyr ago. However, the uncertainty of pore water age puts severe constraints on the given interpretation. But even accepting this limitation, this pilot study argues for the potential of noble gases dissolved in the pore water of glacial clay deposits as a novel archive to reconstruct past environmental conditions in glacial water bodies.

An ongoing SNF project (SNF162447, “Noble gases trapped in the pore fluids of aquatic sediments as environmental tracer”) builds upon the findings of this study and aims to reconstruct the palaeohydrological conditions that prevailed during the de-glaciation and the formation of modern Swiss lakes.

Chapter 8

Conclusions and Outlook

8.1 Conclusions

Noble gases dissolved in the pore water of lacustrine sediments have been shown to be excellent tracers to reconstruct past environmental conditions (Brennwald et al., 2004, 2005; Tomonaga et al., 2011b, 2015; Pitre and Pinti, 2010; Chaduteau et al., 2007a,b). However, there are still open questions regarding the underlying processes and mechanisms that control the noble gas dynamics in unconsolidated sediments, e.g. gas trapping and gas exchange. The laboratory experiments of this thesis yielded surprising answers to the question of how noble gas isotopes fractionate when undergoing molecular diffusion in water. These results provide a robust conceptual basis to apply noble gases as tracer for the (physical) gas dynamics in lacustrine sediments. Expanding on previous work (Brennwald et al., 2005) and to further develop the use of noble gases as tracer for gas exchange in sediment pore water, several field campaigns were conducted. In the field research the aim was to assess the gas dynamics in different lakes that represent extreme cases, e.g. sediments which are strongly supersaturated with CH_4 . To determine robustly such CH_4 supersaturation in the sediment pore water, i.e. to quantify concentrations exceeding the local saturation concentration, a new method was successfully developed and validated in field experiments. The combined analysis of noble gas and methane concentrations yielded new insights regarding the exchange between noble gases dissolved in the pore water and reactive gas bubbles (mainly CH_4) formed in the sediment. Another extreme case that was investigated are sediments where molecular diffusion in the pore water is strongly suppressed.

Molecular diffusion in water is key for the transport of noble gases and other solutes in the sediment pore water. Such diffusive transport through water is commonly assumed to cause a mass dependent fractionation of noble gases and their isotopes that is inversely proportional to the square root of the ratio of their atomic mass, i.e. the square root relation. This assumption lacks a sound physical understanding as it was derived from the kinetic theory of gases and has been challenged by classical molecular dynamics simulations (Bourg and Sposito, 2008). The experiments carried out showed that the fractionation of Ne, Kr and Xe isotopes upon molecular diffusion in water cannot be predicted by the square root relation but were much lower. In contrast, Ar isotopes fractionate in accordance with the square root relation and hence the fractionation of $^{36}\text{Ar}/^{40}\text{Ar}$ ratio can be used to assess diffusive transport in the pore water of unconsolidated sediments

of lakes and oceans. Although the results from the laboratory experiments do not allow the development of a theoretical framework for the quantitative description of the fractionation of noble gas isotopes due to molecular diffusion in water, the results make a robust experimental fundament for studies using the fractionation of the noble gases as a physical tracer to analyse diffusive transport in pore waters. In the light of the results of this thesis, recent *ab initio* calculation on noble gas diffusion in water (de Magalhães et al., 2017) yielded some insights into the molecular processes that constrain the fractionation of noble gas isotopes diffusing through water. Such advanced calculations might provide the physical basis for a full understanding of the isotopic fractionation of (noble) gas isotopes during diffusive exchange in water.

An example of an application of Ar isotope ratios in field is the use in sediments supersaturated with regards to CH₄ gas. If the sum of partial pressures in the pore water of such sediments exceeds the *in situ* hydrostatic pressure bubbles can be formed. Such bubbles initially mainly consist of CH₄ and induce a diffusive transport of other gases dissolved in the surrounding pore water to these bubbles until reaching equilibrium with the surrounding pore water. By means of the Ar isotope ratios determined in the sediment pore water it can be assessed if diffusive transport to the gas bubbles is still going on or if the bubble has attained equilibrium. This thesis builds on the previous finding that noble gas analysis enables to depict the mechanisms underlying gas bubble formation in the sediment and allows to study the bubble emission from the sediment to the open water (see also Brennwald et al., 2005).

Measuring CH₄ concentrations exceeding the local saturation in the sediment pore water is a necessary prerequisite for identifying sediments containing free gas bubbles and for determining the total amount of CH₄ gas present in lacustrine sediment. However, common methods for the quantification of CH₄ concentrations in the sediment pore water are often subject to gas exchange with the atmosphere, i.e. gas loss to the atmosphere, and therefore cannot be used to determine the real CH₄ *in situ* concentrations. These experimental limitations were successfully overcome in this thesis, by developing a new analytical method to quantitatively determine CH₄ concentrations, even in highly productive lacustrine sediments. In two lakes (Lake Rotsee and Lake Lungern) the newly developed method was successfully applied and combined with noble gas analysis to depict the gas and CH₄ dynamics in the respective lake sediments.

The processes constraining gas dynamics in sediments were analysed in targeted experiments assessing the uppermost meter of the sediment column of Lake Rotsee and Lake Lungern. These sediments are characterised by a strong CH₄ accumulation in the pore water fostering the emission of CH₄ bubbles from the sediment to the bottom water of the lake. In Lake Rotsee the layer of maximum CH₄ production was identified and the (minimum) CH₄ flux from the sediments to the lake water was successfully quantified. Lake Lungern is subject to lake level variations, which strongly effects the gas dynamics in the sediment, e.g. by triggering bubble formation in the sediment pore water and subsequent bubble emission to the open lake water. The assumption of fossil CH₄ input to Lake Lungern made in an earlier study was not confirmed, as measured isotopic composition of CH₄ in the gas bubbles emitted from the sediment of Lake Lungern indicate a biological origin of the gas and as no terrigenous gases were detected in these bubbles. When the water level is lowered parts of the sediment of Lake Lungern dry out. In such sediments air can be entrapped when the water level is rising again. Such air bubbles redissolve

with the rising hydrostatic pressure, which leads to a significant noble gas excess in the sediment pore water. Accordingly O_2 also enters the sediment and was quantified by means of the determined noble gas excess in the sediment pore water.

While in some sediments which are gas supersaturated the noble gas transport can be accelerated, e.g. due to stripping with escaping gas bubbles, in some other sediments noble gas transport can be suppressed (e.g. Brennwald et al., 2005; Pitre and Pinti, 2010; Tomonaga, 2010; Tomonaga et al., 2015). For example in the highly compacted clay sediments of Lake Zurich noble gases are expected to be quantitatively trapped in the sediment pore water and to store the noble gas concentrations prevailing during sediment formation. Therefore an atmospheric noble gas excess determined in these glacial clays is hypothesized to originate from some type of glacial melt water input into Lake Zurich. These results showed that in principle noble gas concentrations in glacial clays can be stored over long periods of time, and therefore clays have the potential to be an excellent noble gas archive for past environmental change. This is to be explored in future studies.

8.2 Outlook

The findings of this thesis provide an adequate basis to formulate future research perspectives as it raised new questions that call for assessment.

- **The effect of molecular diffusion through other fluids than water on noble gas isotopes:** The unexpected fractionation behaviour of noble gas isotopes in water are assumed to be the results of solute interaction on the molecular level of a strong polar solvent (water) and a very unpolar solute (noble gas; de Magalhães et al., 2017). Hence the observed fractionation pattern cannot be generalized and used for other solutes and solvents. The isotopic fractionation of gases diffusing through liquids other than water calls for investigation, e.g. noble gas diffusion in oil and/or alcohol etc..
- **The behaviour of the isotopes of reactive gases during molecular diffusion in water:** The isotope ratio of the CH_4 dissolved in meteoric water is frequently used, e.g. to identify the origin of CH_4 (biological or geogenic origin; Bergamaschi et al., 1998). However diffusive transport in water might also alter the isotopic composition. A previous study assessing gas transfer of O_2 , N_2 , CH_4 , and H_2 found a kinetic fractionation that cannot be accurately predicted by a square root dependence on mass (Knox et al., 1992). Similarly to our studies and to de Magalhães et al. (2017), Knox et al. (1992) hypothesised that: "[...] the isotopic difference is an effect not only of the mass but also of the interaction between the water and gas molecules." A broader data set on the effect of diffusive transport in water on the gas isotope ratios of O_2 , N_2 , CH_4 , and H_2 might help to understand the mechanism behind diffusive transport through water and to build a robust basis for future studies using the isotopic fractionation of reactive gases in aquatic environments.
- **Determination of the elemental diffusion coefficients of noble gases:** It is noted again that the diffusion coefficients of Kr and Xe are only rather weakly

constraint and (see Chapt. 4, Tab. 4.3 and Tyroller et al., 2018). The set-up used for the determination of noble gas isotope behaviour undergoing molecular diffusion in water can also be used to determine the elemental diffusion coefficients. To achieve this the uncertainties of the experimental set up need to be significantly reduced. The uncertainties which result from the geometry of the set-up can be reduced by relatively easy measures, such as determining the thickness of the agarose layer in the diffusion cell and the contact area between the gel and test gas more accurately. The uncertainty related to temperature can be reduced by submerging the set-up in a water-bath with controlled temperature.

- **Simulation of diffusive transport of noble gases through clay by quantum mechanics and ab initio molecular dynamics simulation:** The surprising fractionation behaviour of noble gases stimulated additional studies. To test the hypothesis that weak intermolecular interactions are the determining factor behind molecular (noble) gas diffusion through water, novel ab initio molecular dynamics calculations accounting for quantum mechanical and relativistic effects were carried out by de Magalhães et al. (2017). The modelling exercise supports the findings of this thesis, as different diffusive transport regimes were identified for noble gas isotope diffusion through water. The dominant transport mechanism for small particles (He, Ne) is quantum mechanical inter-cavity hopping, whereas mass-independent viscous friction controls the behaviour of large particles (Kr, Xe). Only Ar seems to be strongly affected by molecular collision with surrounding water molecules, and hence appears to be subject to mass-dependent isotope fractionation (de Magalhães et al., 2017). Such novel ab initio molecular dynamics calculations might also be suitable to understand the diffusive transport of noble gases in clay, which is of the utmost interest for understanding the mechanisms underlying diffusion suppression in clay sediments. In a previous study a less sophisticated model was used to simulate the diffusion of He through a two-dimensional microporous media (i.e. clay). Similar to the findings of de Magalhães et al. (2017) it was hypothesized that He diffusion in micro pores may be suppressed by quantum effects (Chen et al., 1994).
- **Laboratory study on the effect of varying hydrostatic pressure in super-saturated gas-rich sediments:** Lake level variations were found to have a strong impact on gas saturated sediments of eutrophic lakes and can easily be traced by noble gas analysis. CH₄ emissions in response to lake level variation have received little scientific attention so far, but seem to be of rising interest as recent publications suggest (Harrison et al., 2017; Beaulieu et al., 2017). The case of Lake Lungern shows that noble gases are an excellent tool to depict the gas dynamics related to water level variations. Noble gases can also be used to quantify the CH₄ emitted as a result of a water level drop. This is advantageous because in principle only two sediment cores need to be sampled, one previous to and one after the water level drop. Furthermore it is suggested to carry out systematic laboratory experiments aimed at understanding the mechanisms of gas bubble formation resulting from a changing hydrostatic pressure and to study how noble gases redistribute between bubble and pore water. Preliminary results from Lake Boadella⁶ (see Fig. 8.1) in-

⁶Sampling was carried out in the framework of a short scientific mission funded by NETLAKE COST Action, ECOST-STSM-ES1201-101013-035532

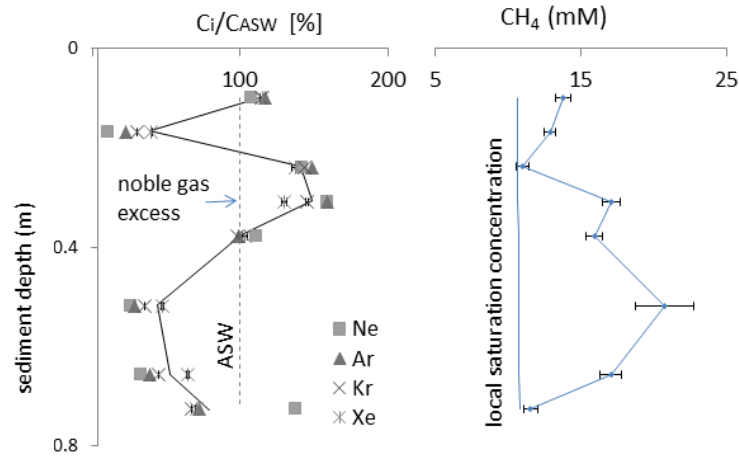


Figure 8.1: Results from a sediment core retrieved from a water depth of 60 m in Lake Boadella (Spain, Catalunya), an eutrophic reservoir (Marcé et al., 2015) which is subject to significant water level variations. Sampling took place during high water level in autumn. On the left: Noble gas concentrations relative to ASW concentrations in percent plotted versus sediment depth. On the right: CH_4 concentrations plotted versus sediment depth. The concentrations of noble gases and methane with sediment depth seem to mirror each other which raises questions connected with the dynamics of gas transport within the sediment body.

indicate that such secondary gas exchange processes might occur in natural systems and reservoirs. In Lake Boadella the observed noble gas excess relative to ASW in the sediment pore water (see Fig. 8.1) might result from such redistribution of noble gases in the sediment column. Under controlled conditions in the laboratory noble gas redistribution between bubble and pore water can be simulated and the processes which alter the noble gas concentrations might be determined more precisely.

These are just a few suggestions for future research. Although this thesis yielded some insights into gas dynamics in lacustrine sediments, the given suggestions, which are far from being complete, show that there are still open questions connected with gas ebullition and secondary gas exchange between gas bubbles and surrounding pore water which call for assessment to fully understand CH_4 emissions from sediments into water bodies.

Bibliography

- Adams, D. D. (1994). *Sediment pore water sampling*. Lewis Publishers, Boca Raton, FL, 2 edition.
- Adams, D. D. (2005). *Diffuse flux of greenhouse gases methane and carbon dioxide at the sediment-water interface of some lakes and reservoirs of the world*, pages 129–153. Springer.
- Adams, D. D. and Van Eck, G. T. M. (1988). Biogeochemical cycling of organic carbon in the sediments of the Grote Rug Reservoir. *Arch. Hydrobio. Ergeb. Limnol.*, 31:319–330.
- Aeschbach-Hertig, W., El-Gamal, H., Wieser, M., and Palcsu, L. (2008). Modeling excess air and degassing in groundwater by equilibrium partitioning with a gas phase. *Water Resour. Res.*, 44.
- Aeschbach-Hertig, W., Peeters, F., Beyerle, U., and Kipfer, R. (1999). Interpretation of dissolved atmospheric noble gases in natural waters. *Water Resour. Res.*, 35(9):2779–2792.
- Aeschbach-Hertig, W., Peeters, F., Beyerle, U., and Kipfer, R. (2000). Palaeotemperature reconstruction from noble gases in ground water taking into account equilibration with entrapped air. *Nature*, 405:1040–1044.
- Aeschbach-Hertig, W. and Solomon, D. (2013). *The Noble Gases as Geochemical Tracers*, chapter Noble Gas Thermometry in Groundwater Hydrology, pages 81–122. Advances in Isotope Geochemistry. Springer, Berlin, Heidelberg.
- Ammann, B. and Lotter, A. F. (1989). Late-Glacial radiocarbon-and palynostratigraphy on the Swiss Plateau. *Boreas*, 18(2):109–126.
- Anderson, A., Abegg, F., Hawkins, J., Duncan, M., and Lyons, A. (1998). Bubble populations and acoustic interaction with the gassy floor of Eckernförde Bay. *Cont. Shelf Res.*, 18(14):1807–1838.
- Bagno, A. (1998). The ab initio neon-water potential-energy surface and its relationship with the hydrophobic hydration shell. *J. Chem. Soc., Faraday Trans.*, 94:2501–2504.
- Ballentine, C. J. and Burnard, P. G. (2002). Production, release and transport of noble gases in the continental crust. In Porcelli, D., Ballentine, C., and Wieler, R., editors, *Noble Gases in Geochemistry and Cosmochemistry*, volume 47 of *Rev. Mineral. Geochem.* Mineralogical Society of America, Geochemical Society.

- Bastviken, D., Cole, J. J., Pace, M. L., and Tranvik, L. J. (2004). Methane emissions from lakes: Dependence of lake characteristics, two regional assessments, and a global estimate. *Global Biogeochem. Cycles*, 18(4).
- Bastviken, D., Cole, J. J., Pace, M. L., and Van de Bogert, M. C. (2008). Fates of methane from different lake habitats: Connecting whole-lake budgets and CH₄ emissions. *J. Geophys. Res.*, 113(G2).
- Bastviken, D., Tranvik, L. J., Downing, J. A., Crill, P. M., and Enrich-Prast, A. (2011). Freshwater methane emissions offset the continental carbon sink. *Science*, 331(6013):50–50.
- Battin, T. J., Luyssaert, S., Kaplan, L. A., Aufdenkampe, A. K., Richter, A., and Tranvik, L. J. (2009). The boundless carbon cycle. *Nat. Geosci.*, 2(9):598–600.
- Beaulieu, J. J., Balz, D. A., Birchfield, M. K., Harrison, J. A., Nietch, C. T., Platz, M. C., Squier, W. C., Waldo, S., Walker, J. T., White, K. M., and Young, J. L. (2017). Effects of an experimental water-level drawdown on methane emissions from a eutrophic reservoir. *Ecosystems*.
- Beaulieu, J. J., Smolenski, R. L., Nietch, C. T., Townsend-Small, A., and Elovitz, M. S. (2014). High methane emissions from a midlatitude reservoir draining an agricultural watershed. *Environ. Sci. Technol.*, 48(19):11100–11108.
- Bergamaschi, P., Brenninkmeijer, C. A. M., Hahn, M., Röckmann, T., Scharffe, D. H., Crutzen, P. J., Elansky, N. F., Belikov, I. B., Trivett, N. B. A., and Worthy, D. E. J. (1998). Isotope analysis based source identification for atmospheric CH₄ and CO sampled across Russia using the Trans-Siberian railroad. *J. Geophys. Res.-Atmos.*, 103(D7):8227–8235.
- Berner, R. A. (1980). *Early diagenesis: a theoretical approach*. Number 1. Princeton University Press.
- Beyerle, U., Aeschbach-Hertig, W., Imboden, D. M., Baur, H., Graf, T., and Kipfer, R. (2000). A mass spectrometric system for the analysis of noble gases and tritium from water samples. *Environ. Sci. Technol.*, 34(10):2042–2050.
- Boerboom, A. and Kleyn, G. (1969). Diffusion coefficients of noble gases in water. *J. Chem. Phys.*, 50(3):1086–1088.
- Boner, M., Gebhardt, A. C., and Pabst, B. (1999). Are late glacial deposits exposed in Lake Zurich? In *Looking into the sediment subsurface of lakes*, Zürich.
- Bossard, P. and Gächter, R. (1981). Methan- und Sauerstoffhaushalt im mesotrophen Lungernsee. *Schweiz. Z. Hydrol.*, 43(2):219–252.
- Boudreau, B. P. (2012). The physics of bubbles in surficial, soft, cohesive sediments. *Mar. Petrol. Geol.*, 38(1):1 – 18.

- Boudreau, B. P., Algar, C., Johnson, B. D., Croudace, I., Reed, A., Furukawa, Y., Dorgan, K. M., Jumars, P. A., Grader, A. S., and Gardiner, B. S. (2005). Bubble growth and rise in soft sediments. *Geology*, 33(6):517–520.
- Bourg, I. and Sposito, G. (2008). Isotopic fractionation of noble gases by diffusion in liquid water: Molecular dynamics simulations and hydrologic applications. *Geochim. Cosmochim. Ac.*, 72:2237–2247.
- Brennwald, M. S., Hofer, M., and Kipfer, R. (2013a). Simultaneous analysis of noble gases, sulfur hexafluoride, and other dissolved gases in water. *Environ. Sci. Technol.*, 47(15):8599–8608.
- Brennwald, M. S., Hofer, M., Peeters, F., Aeschbach-Hertig, W., Strassmann, K., Kipfer, R., and Imboden, D. M. (2003). Analysis of dissolved noble gases in the pore water of lacustrine sediments. *Limnol. Oceanogr.-Methods*, 1:51–62.
- Brennwald, M. S., Kipfer, R., and Imboden, D. M. (2005). Release of gas bubbles from lake sediment traced by noble gas isotopes in the sediment pore water. *Earth Planet. Sci. Lett.*, 235(1-2):31–44.
- Brennwald, M. S., Peeters, F., Imboden, D. M., Giralt, S., Hofer, M., Livingstone, D. M., Klump, S., Strassmann, K., and Kipfer, R. (2004). Atmospheric noble gases in lake sediment pore water as proxies for environmental change. *Geophys. Res. Lett.*, 31(4):L04202.
- Brennwald, M. S., Schmidt, M., Oser, J., and Kipfer, R. (2016). A portable and autonomous mass spectrometric system for on-site environmental gas analysis. *Environ. Sci. Technol.*, 50(24):13455–13463.
- Brennwald, M. S., Vogel, N., Scheidegger, Y., Tomonaga, Y., Livingstone, D. M., and Kipfer, R. (2013b). *The Noble Gases as Geochemical Tracers*, chapter Noble gases as environmental tracers in sediment porewaters and in stalagmite fluid inclusions, pages 123–153. *Advances in Isotope Geochemistry*. Springer, Berlin, Heidelberg.
- Busemann, H., Baur, H., and Wieler, R. (2000). Primordial noble gases in. *Meteorit. Planet. Sci.*, 35:949–973.
- Chaduteau, C., Fourré, E., Jean-Baptiste, P., Dapoigny, A., Baumier, D., and Charlou, J. (2007a). A new method for quantitative analysis of helium isotopes in sediment pore-waters. *Limnol. Oceanogr. Meth.*, 5:425–432.
- Chaduteau, C., Jean-Baptiste, P., Fourré, E., Charlou, J., and Donval, J. (2007b). Helium transport in sediment pore fluids of the Congo-Angola Margin. *Geochem. Geophys. Geosy.*, 10(1).
- Chanton, J. P., Martens, C. S., and Kelley, C. A. (1989). Gas transport from methane-saturated, tidal freshwater and wetland sediments. *Limnol. Oceanogr.*, 34(5):807–819.
- Chen, B., Kim, H., Mahanti, S., Pinnavaia, T., and Cai, Z. (1994). Percolation and diffusion in two-dimensional microporous media: Pillared clays. *J. Chem. Phys.*, 100(5):3872–3880.

- Clever, H. L. (1979). *Krypton, xenon and radon - gas solubilities*, volume 2 of *Solubility data series*. Pergamon Press, Oxford.
- Cole, J. J., Prairie, Y. T., Caraco, N. F., McDowell, W. H., Tranvik, L. J., Striegl, R. G., Duarte, C. M., Kortelainen, P., Downing, J. A., Middelburg, J. J., and Melack, J. (2007). Plumbing the global carbon cycle: Integrating inland waters into the terrestrial carbon budget. *Ecosystems*, 10(1):172–185.
- Colt, J. (2012). *Dissolved Gas Concentration in Water: Computation as Functions of Temperature, Salinity and Pressure*. Elsevier.
- Corella, J. P., Arantegui, A., Loizeau, J.-L., Del Sontro, T., Le Dantec, N., Stark, N., Anselmetti, F., and Girardclos, S. (2014). Sediment dynamics in the subaquatic channel of the Rhone Delta (Lake Geneva, France/Switzerland). *Aquat. Sci.*, 76(1):73–87.
- Craig, H. and Gordon, L. (1965). Deuterium and oxygen 18 variations in the ocean and the marine atmosphere. In Tongiorgi, E., editor, *Stable isotopes in oceanographic studies and paleotemperatures*, pages 9–130, Spoleto. Consiglio Nazionale delle Ricerche, Laboratorio di Geologia Nucleare, Pisa.
- Craig, H. and Weiss, R. F. (1971). Dissolved gas saturation anomalies and excess helium in the ocean. *Earth Planet. Sci. Lett.*, 10(3):289–296.
- Crank, J. (1975). *The mathematics of diffusion*, 2nd ed. Clarendon Press.
- Cussler, E. L. (2009). *Diffusion: Mass transfer in fluid systems*, 3rd ed. Cambridge Univ. Press, Cambridge.
- Daynes, H. (1920). The process of diffusion through a rubber membrane. *P. R. Soc. London*, 97(685):286–307.
- de Magalhães, H. P., Brennwald, M. S., and Kipfer, R. (2017). Diverging effects of isotopic fractionation upon molecular diffusion of noble gases in water: Mechanistic insights through ab initio molecular dynamics simulations. *Environ. Sci.-Proc. Imp.*
- Del Sontro, T., Kunz, M. J., Kempter, T., Wuest, A., Wehrli, B., and Senn, D. B. (2011). Spatial heterogeneity of methane ebullition in a large tropical reservoir. *Environ. Sci. Technol.*, 45(23):9866–9873.
- Del Sontro, T. S. (2011). *Quantifying methane emissions from reservoirs: from Basin-scale to discrete analyses with a focus on ebullition dynamics*. PhD thesis, University of California, Santa Barbara.
- Del Sontro, T. S., McGinnis, D. F., Sobek, S., Ostrovsky, I., and Wehrli, B. (2010). Extreme methane emissions from a Swiss hydropower reservoir: Contribution from bubbling sediments. *Environ. Sci. Technol.*, 44(7):2419–2425.
- Diem, T., Koch, S., Schwarzenbach, S., Wehrli, B., and Schubert, C. (2012). Greenhouse gas emissions (CO₂, CH₄, and N₂O) from several perialpine and alpine hydropower reservoirs by diffusion and loss in turbines. *Aquat. Sci.*, 74(3):619–635.

- Downing, J. A. (2010). Emerging global role of small lakes and ponds: little things mean a lot. *Limnetica*, 29:0009–24.
- Downing, J. A., Cole, J. J., Middelburg, J. J., Striegl, R. G., Duarte, C. M., Kortelainen, P., Prairie, Y. T., and Laube, K. (2008). Sediment organic carbon burial in agriculturally eutrophic impoundments over the last century. *Global Biogeochem. Cy.*, 22(1).
- Duc, N. T., Crill, P., and Bastviken, D. (2010). Implications of temperature and sediment characteristics on methane formation and oxidation in lake sediments. *Biogeochemistry*, 100(1-3):185–196.
- Dyck, W. and Da Silva, F. (1981). The use of ping-pong balls and latex tubing for sampling the helium content of lake sediments. *J. Geochem. Explor.*, 14:41–48.
- Etiope, G. and Klusman, R. W. (2002). Geologic emissions of methane to the atmosphere. *Chemosphere*, 49(8):777–789.
- Falz, K. Z., Holliger, C., Grosskopf, R., Liesack, W., Nozhevnikova, A., Müller, B., Wehrli, B., and Hahn, D. (1999). Vertical distribution of methanogens in the anoxic sediment of Rotsee (Switzerland). *Appl. Environ. Microb.*, 65(6):2402–2408.
- Flato, G., Marotzke, J., Abiodun, B., Braconnot, P., Chou, S. C., Collins, W. J., Cox, P., Driouech, F., Emori, S., Eyring, V., et al. (2013). Evaluation of climate models. in: climate change 2013: the physical science basis. contribution of working group i to the fifth assessment report of the intergovernmental panel on climate change. *Climate Change 2013*, 5:741–866.
- Flury, S., Glud, R. N., Premke, K., and McGinnis, D. F. (2015). Effect of sediment gas voids and ebullition on benthic solute exchange. *Environ. Sci. Technol.*, 49(17):10413–10420.
- Forster, P., Ramaswamy, V., Artaxo, P., Berntsen, T., Betts, R., Fahey, D. W., Haywood, J., Lean, J., Lowe, D. C., Myhre, G., Nganga, J., Prinn, R., Raga, G., Schulz, M., and Van Dorland, R. (2007). *Changes in Atmospheric Constituents and in Radiative Forcing, Contribution of Working Group I to the Fourth Assessment Report of the Intergovernmental Panel on Climate Change*, pages 131–217. Cambridge University Press.
- Geyh, M. A. and Schleicher, H. (2012). *Absolute age determination: physical and chemical dating methods and their application*. Springer Science & Business Media.
- Goldstein, R. H. (2001). Fluid inclusions in sedimentary and diagenetic systems. *Lithos*, 55(1-4):159–193.
- Graham, T. (1833). On the law of the diffusion of gases. *Philosophical Magazine*, 2(9):175–190.
- Grinham, A., Dunbabin, M., Gale, D., and Udy, J. (2011). Quantification of ebullitive and diffusive methane release to atmosphere from a water storage. *Atmos. Environ.*, 45(39):7166–7173.

- Grundl, T., Magnusson, N., Brennwald, M. S., and Kipfer, R. (2013). Mechanisms of subglacial groundwater recharge as derived from noble gas, ^{14}C , and stable isotopic data. *Earth Planet. Sc. Lett.*, 369:78–85.
- Harrison, J. A., Deemer, B. R., Birchfield, M. K., and OMalley, M. T. (2017). Reservoir water-level drawdowns accelerate and amplify methane emission. *Environ. Sci. Technol.*, 51(3):1267–1277.
- Heber, V. S. (2002). *Ancient solar wind noble gases in lunar and meteoritic archives and tests for modern solar wind collection with the GENESIS mission*. PhD thesis, ETH Zürich.
- Hoehler, T. M., Alperin, M. J., Albert, D. B., and Martens, C. S. (1994). Field and laboratory studies of methane oxidation in an anoxic marine sediment: Evidence for a methanogen-sulfate reducer consortium. *Global Biogeochem. Cycles*, 8(4):451–463.
- Hofmann, H., Federwisch, L., and Peeters, F. (2010). Wave-induced release of methane: Littoral zones as source of methane in lakes. *Limnol. Oceanogr.*, 55(5):1990–2000.
- Hohmann, R., Hofer, M., Kipfer, R., Peeters, F., and Imboden, D. M. (1998). Distribution of helium and tritium in Lake Baikal. *J. Geophys. Res.*, 103(C6):12823–12838.
- Hohmann, R., Schlosser, P., Jacobs, S., Ludin, A., and Weppernig, R. (2002). Excess helium and neon in the southeast Pacific: Tracers for glacial meltwater. *J. Geophys. Res.*, 107(C11):3198.
- Holocher, J., Peeters, F., Aeschbach-Hertig, W., Hofer, M., Brennwald, M., Kinzelbach, W., and Kipfer, R. (2002). Experimental investigations on the formation of excess air in quasi-saturated porous media. *Geochim. Cosmochim. Ac.*, 66(23):4103–4117.
- Holzner, C., Tomonaga, Y., Stöckli, A., Denecke, N., and Kipfer, R. (2012). Using noble gases to analyze the efficiency of artificial aeration in Lake Hallwil, Switzerland. *Water Resour. Res.*, 48(9).
- Holzner, C. P., Klump, S., Amaral, H., Brennwald, M. S., and Kipfer, R. (2004). Assessment of methane emission from bubble plumes in the Black Sea by noble gases. In *Goldschmidt Conference*, volume 68 of *Geochim. Cosmochim. Ac. (Supplement)*, page A323, Copenhagen, Denmark. *Geochim. Cosmochim. Ac. (Supplement)*.
- Holzner, C. P., McGinnis, D. F., Schubert, C. J., Kipfer, R., and Imboden, D. M. (2008). Noble gas anomalies related to high-intensity methane gas seeps in the Black Sea. *Earth Planet. Sc. Lett.*, 265(3-4):396–409.
- Horseman, S., Higgs, J., Alexander, J., and Harrington, J. (1996). Water, gas and solute movement through argillaceous media. *Nuclear Energy Agency Rep. CC-96/1. OECD, Paris*.
- Ince, N. H. and Belen, R. (2001). Aqueous phase disinfection with power ultrasound: Process kinetics and effect of solid catalysts. *Environ. Sci. Technol.*, 35(9):1885–1888.

- Jähne, B., Heinz, G., and Dietrich, W. (1987a). Measurement of the diffusion coefficients of sparingly soluble gases in water. *J. Geophys. Res.*, 92(C10):10767–10776.
- Jähne, B., Münnich, K. O., Börsinger, R., Dutzi, A., Huber, W., and Libner, P. (1987b). On the parameters influencing air-water gas exchange. *J. Geophys. Res.-Oceans*, 92(C2):1937–1949.
- Jørgensen, B. B., Weber, A., and Zopfi, J. (2001). Sulfate reduction and anaerobic methane oxidation in Black Sea sediments. *Oceanogr. Res. Pap.*, 48(9):2097–2120.
- Joyce, J. and Jewell, P. W. (2003). Physical controls on methane ebullition from reservoirs and lakes. *Environ. Eng. Geoscience*, 9(2):167–178.
- Kampbell, D., Wilson, J. T., and Vandegrift, S. (1989). Dissolved oxygen and methane in water by a GC headspace equilibration technique. *Int. J. Environ. An. Ch.*, 36(4):249–257.
- Kipfer, R. (1991). *Primordiale Edelgase als Tracer für Fluide aus dem Erdmantel*. PhD thesis.
- Kipfer, R., Aeschbach-Hertig, W., Peeters, F., and Stute, M. (2002). *Noble gases in geochemistry and cosmochemistry*, volume 47, chapter Noble gases in lakes and ground waters, pages 615–700. Mineralogical Society of America, Geochemical Society.
- Kirschke, Stefanie, e. a. (2013). Three decades of global methane sources and sinks. *Nat. Geosci.*, 6(10):813–823.
- Klump, S., Kipfer, R., Cirpka, O. A., Harvey, C. F., Brennwald, M. S., Ashfaq, K. N., Badruzzaman, A. B. M., Hug, S. J., and Imboden, D. M. (2006). Groundwater dynamics and arsenic mobilization in Bangladesh assessed using noble gases and tritium. *Environ. Sci. Technol.*, 40(1):243–250.
- Klump, S. R. (2007). *The formation of excess air in groundwater studied using noble gases as conservative tracers in laboratory and field experiments*. PhD thesis, ETH Zurich.
- Knox, M., Quay, P., and Wilbur, D. (1992). Kinetic isotopic fractionation during air-water gas transfer of O₂, N₂, CH₄, and H₂. *J. Geophys. Res.-Oceans*, 97(C12):20335–20343.
- Lee, J.-Y., Marti, K., Severinghaus, J. P., Kawamura, K., Yoo, H.-S., Lee, J. B., and Kim, J. S. (2006). A redetermination of the isotopic abundances of atmospheric Ar. *Geochim. Cosmochim. Ac.*, 70(17):4507–4512.
- Liikanen, A., Flöjt, L., and Martikainen, P. (2002). Gas dynamics in eutrophic lake sediments affected by oxygen, nitrate, and sulfate. *J. Environ. Qual.*, 31(1):338–349.
- Lippmann, J., Stute, M., Torgersen, T., Moser, D., Hall, J., Lin, L., Borcsik, M., Bellamy, R., and Onstott, T. (2003). Dating ultra-deep mine waters with noble gases and ³⁶Cl, Witwatersrand Basin, South Africa. *Geochim. Cosmochim. Ac.*, 67(23):4597 – 4619.
- Lister, G. (1984). Deglaciation of the Lake Zurich area: A model based on the sedimentological record. *Contrib. Sediment.*, 13:31–58.

- Litt, T., Krastel, S., Sturm, M., Kipfer, R., Örcen, S., Heumann, G., Franz, S., Ülgen, U., and Niessen, F. (2009). Paleovan, international continental scientific drilling program (ICDP): site survey results and perspectives. *Quaternary Sci. Rev.*, 28:1555–1567.
- Lotter, A. (1990). Die Entwicklung terrestrischer und aquatischer Ökosysteme am Rotsee (Zentralschweiz) im Verlauf der letzten 15000 Jahre. *Mitt. Nat.forsch. Ges. Luzern*, 31:81–97.
- Lovley, D. R. and Klug, M. J. (1982). Intermediary metabolism of organic matter in the sediments of a eutrophic lake. *Appl. Environ. Microb.*, 43(3):552–560.
- Ludwig, R. (2001). Water: From clusters to the bulk. *Angew. Chem. Int. Ed.*, 40(10):1808–1827.
- Mächler, L., Brennwald, M. S., and Kipfer, R. (2012). Membrane inlet mass spectrometer for the quasi-continuous on-site analysis of dissolved gases in groundwater. *Environ. Sci. Technol.*, 46(15):8288–8296.
- Maeck, A., Hofmann, H., and Lorke, A. (2014). Pumping methane out of aquatic sediments: Ebullition forcing mechanisms in an impounded river. *Biogeosciences*, 11(11):2925–2938.
- Maerki, M., Wehrli, B., Dinkel, C., and Müller, B. (2004). The influence of tortuosity on molecular diffusion in freshwater sediments of high porosity. *Geochim. Cosmochim. Ac.*, 68(7):1519–1528.
- Mamyrin, B. A. and Tolstikhin, I. N. (1984). *Helium isotopes in nature*, volume 3 of *Developments in Geochemistry*. Elsevier, Amsterdam, Oxford, New York, Tokyo, 1 edition.
- Marcé, R., Armengol, J., and Navarro, E. (2015). Assessing ecological integrity in large reservoirs according to the water framework directive. In *Experiences from Surface Water Quality Monitoring*, pages 201–219. Springer.
- Mark, D., Stuart, F., and De Podesta, M. (2011). New high-precision measurements of the isotopic composition of atmospheric argon. *Geochim. Cosmochim. Ac.*, 75(23):7494–7501.
- Martinez, D. and Anderson, M. A. (2013). Methane production and ebullition in a shallow, artificially aerated, eutrophic temperate lake (Lake Elsinore, CA). *Sci. Total Environ.*, 454:457–465.
- McGinnis, D. F., Greinert, J., Artemov, Y., Beaubien, S., and Wüest, A. (2006). Fate of rising methane bubbles in stratified waters: How much methane reaches the atmosphere? *J. Geophys. Res.: Oceans (1978–2012)*, 111(C9).
- McGinnis, D. F., Kirillin, G., Tang, K. W., Flury, S., Bodmer, P., Engelhardt, C., Casper, P., and Grossart, H.-P. (2015). Enhancing surface methane fluxes from an oligotrophic lake: Exploring the microbubble hypothesis. *Environ. Sci. Technol.*, 49(2):873–880.
- Moore, J. (1999). *Physical chemistry*, 5th ed. Prentice Hall.

- Moss, B., Kosten, S., Meerhof, M., Battarbee, R., Jeppesen, E., Mazzeo, N., Havens, K., Lacerot, G., Liu, Z., De Meester, L., et al. (2011). Allied attack: climate change and eutrophication. *Inland waters*, 1(2):101–105.
- Müller, B., Buis, K., Stierli, R., and Wehrli, B. (1998). High spatial resolution measurements in lake sediments with PVC based liquid membrane ion-selective electrodes. *Limnol. Oceanogr.*, 43(7):1728–1733.
- Naeher, S., Niemann, H., Peterse, F., Smittenberg, R. H., Zigah, P. K., and Schubert, C. J. (2014). Tracing the methane cycle with lipid biomarkers in Lake Rotsee (Switzerland). *Org. Geochem.*, 66:174–181.
- Naeher, S., Smittenberg, R. H., Gilli, A., Kirilova, E. P., Lotter, A. F., and Schubert, C. J. (2012). Impact of recent lake eutrophication on microbial community changes as revealed by high resolution lipid biomarkers in Rotsee (Switzerland). *Org. Geochem.*, 49:86–95.
- Naeher, S., Smittenberg, R. H., Gilli, A., Kirilova, E. P., Lotter, A. F., and Schubert, C. J. (2012). Porosity and accumulation rates of sediments of Lake Rotsee, Switzerland. PANGAEA. In supplement to: Naeher, S et al. (2012).
- Nisbet, E. G., Dlugokencky, E. J., and Bousquet, P. (2014). Methane on the rise - again. *Science*, 343(6170):493–495.
- Ortiz-Llorente, M. and Alvarez-Cobelas, M. (2012). Comparison of biogenic methane emissions from unmanaged estuaries, lakes, oceans, rivers and wetlands. *Atmos. Environ.*, 59:328–337.
- Ostrovsky, I. (2009). Fish and methane bubbles in aquatic ecosystems: Hydroacoustic separation and quantification. *Int. Ver. The.*, 30(6-7):870.
- Ozima, M. and Podosek, F. (2002). *Noble gas geochemistry*. Cambridge University Press, Cambridge.
- Panneer Selvam, B., Natchimuthu, S., Arunachalam, L., and Bastviken, D. (2014). Methane and carbon dioxide emissions from inland waters in India – implications for large scale greenhouse gas balances. *Global Change Biol.*, 20(11):3397–3407.
- Pavese, F., Fellmuth, B., Head, D. I., Hermier, Y., Hill, K. D., and Valkiers, S. (2005). Evidence of a systematic deviation of the isotopic composition of neon from commercial sources compared with its isotopic composition in air. *Anal. Chem.*, 77(15):5076–5080.
- Peeters, F., Beyerle, U., Aeschbach-Hertig, W., Holocher, J., Brennwald, M. S., and Kipfer, R. (2002a). Improving noble gas based paleoclimate reconstruction and ground-water dating using $^{20}\text{Ne}/^{22}\text{Ne}$ ratios. *Geochim. Cosmochim. Ac.*, 67(4):587–600.
- Peeters, F., Livingstone, D. M., Goudsmit, G.-H., Kipfer, R., and Forster, R. (2002b). Modeling 50 years of historical temperature profiles in a large central European lake. *Limnol. Oceanogr.*, 47(1):186–197.

- Pennington, W., Cambray, R., Eakins, J., and Harkness, D. (1976). Radionuclide dating of the recent sediments of Blelham Tarn. *Freshwater Biol.*, 6(4):317–331.
- Perry, C. and Taylor, K. (2009). *Environmental sedimentology*. John Wiley & Sons.
- Pitre, F. and Pinti, D. (2010). Noble gas enrichments in porewater of estuarine sediments and their effect on the estimation of net denitrification rates. *Geochim. Cosmochim. Ac.*, 74:531–539.
- Popp, B. N., Sansone, F. J., Rust, T. M., and Merritt, D. A. (1995). Determination of concentration and carbon isotopic composition of dissolved methane in sediments and nearshore waters. *Anal. Chem.*, 67(2):405–411.
- Precht, E., Franke, U., Polerecky, L., and Huettel, M. (2004). Oxygen dynamics in permeable sediments with wave-driven pore water exchange. *Limnol. Oceanogr.*, 49(3):693–705.
- Richter, F. M., Mendybaev, R. A., Christensen, J. N., Hutcheon, I. D., Williams, R. W., Sturchio, N. C., and Beloso Jr., A. D. (2006). Kinetic isotopic fractionation during diffusion of ionic species in water. *Geochim. Cosmochim. Ac.*, 70(2):277–289.
- Saltzman, E., King, D., Holmen, K., and Leck, C. (1993). Experimental determination of the diffusion coefficient of dimethylsulfide in water. *J. Geophys. Res.-Oceans (1978–2012)*, 98(C9):16481–16486.
- Sander, R. (1999). Compilation of Henry’s law constants for inorganic and organic species of potential importance in environmental chemistry.
- Sarsan, S. (2013). Effect of storage of water in different metal vessels on coliforms. *Int. J. Curr. Microbiol. App. Sci*, 2(11):24–29.
- Sawakuchi, H. O., Bastviken, D., Sawakuchi, A. O., Krusche, A. V., Ballester, M. V., and Richey, J. E. (2014). Methane emissions from Amazonian Rivers and their contribution to the global methane budget. *Global Change Biol.*, 20(9):2829–2840.
- Schlosser, P. (1992). Tritium/³He dating of waters in natural systems. In *Isotopes of noble gases as tracers in environmental studies*.
- Schlosser, P. and Winckler, G. (2002). *Noble gases in geochemistry and cosmochemistry*, volume 47, chapter Noble gases in the ocean and ocean floor. Mineralogical Society of America, Geochemical Society.
- Schubert, C. J., Diem, T., and Eugster, W. (2012). Methane emissions from a small wind shielded lake determined by eddy covariance, flux chambers, anchored funnels, and boundary model calculations: a comparison. *Environ. Sci. Technol.*, 46(8):4515–4522.
- Schubert, C. J., Lucas, F., Durisch-Kaiser, E., Stierli, R., Diem, T., Scheidegger, O., Vazquez, F., and Müller, B. (2010). Oxidation and emission of methane in a monomictic lake (Rotsee, Switzerland). *Aquat. Sci.*, 72(4):455–466.

- Schwarzenbach, R. P., Gschwend, P. M., and Imboden, D. M. (2003). *Environmental Organic Chemistry*. John Wiley & Sons, Inc., New York, 2 edition.
- Smith, V. H. (2003). Eutrophication of freshwater and coastal marine ecosystems a global problem. *Environ. Sci. Pollut R.*, 10(2):126–139.
- Sobek, S., Del Sontro, T., Wongfun, N., and Wehrli, B. (2012). Extreme organic carbon burial fuels intense methane bubbling in a temperate reservoir. *Geophys. Res. Lett.*, 39(1).
- Sobek, S., E. Durisch-Kaiser, R., Zurbrügg, N., Wongfun, M., Wessels, N., N., P., and B., W. (2009). Organic carbon burial efficiency in lake sediments controlled by oxygen exposure time and sediment source. *Limnol. Oceanogr.*, 54(6):2243–2254.
- Sollberger, S., Corella, J. P., Girardclos, S., Randlett, M.-E., Schubert, C., Senn, D., Wehrli, B., and Del Sontro, T. (2014). Spatial heterogeneity of benthic methane dynamics in the subaquatic canyons of the Rhone River Delta (Lake Geneva). *Aquat. Sci.*, 76(1):89–101.
- Solomon, D. K. and Cook, P. G. (2000). ^3H and ^3He . In *Environmental tracers in subsurface hydrology*, pages 397–424. Springer.
- Søndergaard, M., Jeppesen, E., Lauridsen, T. L., Skov, C., Van Nes, E. H., Roijackers, R., Lammens, E., and Portielje, R. (2007). Lake restoration: Successes, failures and long-term effects. *J. Appl. Ecol.*, 44(6):1095–1105.
- Stanley, E. H., Casson, N. J., Christel, S. T., Crawford, J. T., Loken, L. C., and Oliver, S. K. (2016). The ecology of methane in streams and rivers: patterns, controls, and global significance. *Ecol. Monogr.*, 86(2):146–171.
- Stephenson, M., Schwartz, W. J., Melnyk, T. W., and Motycka, M. F. (1994). Measurement of advective water velocity in lake sediment using natural helium gradients. *J. Hydrol.*, 154(1):63–84.
- Strasser, M. and Anselmetti, F. (2008). Mass-movement event stratigraphy in Lake Zurich; a record of varying seismic and environmental impacts. *Beitr. Geol. Schweiz: Geotech.*, 95:23–41.
- Strassmann, K. M., Brennwald, M. S., Peeters, F., and Kipfer, R. (2005). Dissolved noble gases in porewater of lacustrine sediments as palaeolimnological proxies. *Geochim. Cosmochim. Ac.*, 69(7):1665–1674.
- Sun, X., Hu, Y., and Zhu, H. (2013). Ab initio potential energy surface and predicted rotational spectra for the $\text{Ne-H}_2\text{O}$ complex. *The Journal of Chemical Physics*, 138(20):204312.
- Tempest, K. E. and Emerson, S. (2013). Kinetic isotopic fractionation of argon and neon during airwater gas transfer. *Mar. Chem.*, 153(0):39 – 47.

- Tolstikhin, I., Lehmann, B. E., Loosli, H. H., and Gautschi, A. (1996). Helium and argon isotopes in rocks, minerals, and related groundwaters: A case study in northern Switzerland. *Geochim. Cosmochim. Ac.*, 60(9):1497–1514.
- Tomonaga, Y. (2010). *Noble gases as tracers for transport of solutes and fluids in lake and ocean sediments*. PhD thesis, Zurich.
- Tomonaga, Y., Blättler, R., Brennwald, M. S., and Kipfer, R. (2012). Interpreting noble-gas concentrations as proxies for salinity and temperature in the worlds largest soda lake (Lake Van, Turkey). *J. Asian Earth Sci.*, 59:99–107.
- Tomonaga, Y., Brennwald, M. S., and Kipfer, R. (2011a). An improved method for the analysis of dissolved noble gases in the porewater of unconsolidated sediments. *Limnol. Oceanogr.: Methods*, 9(2):42–49.
- Tomonaga, Y., Brennwald, M. S., and Kipfer, R. (2011b). Spatial distribution and flux of terrigenous he dissolved in the sediment pore water of Lake Van (Turkey). *Geochim. Cosmochim. Ac.*, 75(10):2848–2864.
- Tomonaga, Y., Brennwald, M. S., and Kipfer, R. (2015). Attenuation of diffusive noble-gas transport in laminated sediments of the stockholm archipelago. *Limnol. Oceanogr.*, 60(2):497–511.
- Tomonaga, Y., Brennwald, M. S., Livingstone, D. M., Kwiecien, O., Randlett, M.-È., Stockhecke, M., Unwin, K., Anselmetti, F. S., Beer, J., Haug, G. H., et al. (2017). Porewater salinity reveals past lake-level changes in Lake Van, the Earths largest soda lake. *Sci. Rep. – UK*, 7.
- Tomonaga, Y., Brennwald, M. S., Meydan, A. F., and Kipfer, R. (2014). Noble gases in the sediments of Lake Van—solute transport and palaeoenvironmental reconstruction. *Quat. Sci. Rev.*, 104:117–126.
- Tranvik, L. J., Downing, J. A., Cotner, J. B., Loiselle, S. A., Striegl, R. G., Ballatore, T. J., Dillon, P., Finlay, K., Fortino, K., Knoll, L. B., et al. (2009). Lakes and reservoirs as regulators of carbon cycling and climate. *Limnol. Oceanogr.*, 54(6):2298–2314.
- Tsuruta, A., Aalto, T., Backman, L., Hakkarainen, J., Van Der Laan-Luijkx, I. T., Krol, M. C., Spahni, R., Houweling, S., Laine, M., Dlugokencky, E., et al. (2017). Global methane emission estimates for 2000–2012 from CarbonTracker Europe-CH₄ v1.0. *Geosci. Model Dev.*, 10(3):1261–1289.
- Tyroller, L., Brennwald, M. S., Busemann, H., Maden, C., Baur, H., and Kipfer, R. (2018). Negligible fractionation of Kr and Xe isotopes by molecular diffusion in water. *Earth Planet. Sc. Lett.*, 492:73–78.
- Tyroller, L., Brennwald, M. S., Mächler, L., Livingstone, D. M., and Kipfer, R. (2014). Fractionation of Ne and Ar isotopes by molecular diffusion in water. *Geochim. Cosmochim. Ac.*, 136:60–66.

- Tyroller, L., Brennwald, M. S., Ndayisaba, C., Tomonaga, Y., and Kipfer, R. (2013). Linking noble gas and CH₄ concentrations in the sediment porewater of Lake Lungern, Switzerland. *Limnol. Oceanogr.: Methods*, 9:42–49.
- Tyroller, L., Tomonaga, Y., Brennwald, M. S., Ndayisaba, C., Naeher, S., Schubert, C., North, R. P., and Kipfer, R. (2016). Improved method for the quantification of methane concentrations in unconsolidated lake sediments. *Environ. Sci. Technol.*, 50(13):7047–7055.
- Varadharajan, C. and Hemond, H. F. (2012). Time-series analysis of high-resolution ebullition fluxes from a stratified, freshwater lake. *J. Geophys. Res. Biogeosci.*, 117(G2).
- Visser, A., Broers, H., and Bierkens, M. (2007). Dating degassed groundwater with ³H/³He. *Water Resour. Res.*, 43(10):W10434.
- Weiss, R. F. (1971a). The effect of salinity on the solubility of argon in seawater. *Deep-Sea Res.*, 18:225–230.
- Weiss, R. F. (1971b). Solubility of helium and neon in water and seawater. *J. Chem. Eng. Data*, 16(2):235–241.
- Weiss, R. F. and Kyser, T. K. (1978). Solubility of krypton in water and seawater. *J. Chem. Eng. Data*, 23(1):69–72.
- Wise, D. and Houghton, G. (1968). Diffusion coefficients of neon, krypton, xenon, carbon monoxide and nitric oxide in water at 10–60°C. *Chem. Eng. Sci.*, 23(10):1211 – 1216.
- Yang, H., Xie, P., Ni, L., and Flower, R. J. (2011). Underestimation of CH₄ emission from freshwater lakes in China. *Environ. Sci. Technol.*, 45(10):4203–4204.
- Zhou, Z., Ballentine, C. J., Kipfer, R., Schoell, M., and Thibodeaux, S. (2005). Noble gas tracing of groundwater/coalbed methane interaction in the San Juan Basin, USA. *Geochim. Cosmochim. Ac.*, 69(23):5413–5428.
- Zolitschka, B. and Enters, D. (2009). *Lacustrine Sediments*, pages 486–488. Springer Netherlands, Dordrecht.

Curriculum vitae

Lina Tyroller

(*1982 in Munich, Germany)

- 08.01.2018 Dr. sc. ETH Zurich, Switzerland
- 2011 - 2017 Ph.D. student and research assistant at the Department of Environmental Systems Science, Institute of Biogeochemistry and Pollution Dynamics, ETH Zurich, Switzerland
- & in the Environmental Isotope Group, Department of Water Resources and Drinking Water, Eawag - Aquatic Research Institute, Switzerland
- 2009 - 2010 Research assistant, Department of Hydraulic, Maritime and Environmental Engineering, Universitat Politècnica de Catalunya, Spain
- 12.07.2010 Graduate engineer (Dipl.-Ing.), Technische Universität Berlin, Germany
- 2003 - 2010 Undergraduate studies, Environmental Engineering, Technische Universität Berlin, Germany
- 2008 - 2009 Student assistant, Department of Urban Water Management, Technische Universität Berlin, Germany
- 28.06.2002 University - Entrance Diploma, High school in Straubing, Germany